Establishing Data-Derived Emissions Limitations

H. Gregor Rigo
Rigo & Rigo Associates, Inc.
1 Berea Commons, Suite 211
Berea, Ohio 44017

and

Gary Liberson
Environmental Risk Sciences, Inc.
1000 Thomas Jefferson St., NW, Suite 506
Washington, D.C.20007

INTRODUCTION

The emissions limitations found in regulations and permits have traditionally been set using engineering judgment, commercial considerations and public perception of potential harm and achievability. Given the restricted list of pollutants in Section 129 of the Clean Air Act (CAA) and EPA's decision to base municipal waste combustor (MWC) Maximum Achievable Control Technology (MACT) Floor determinations on limitations in enforceable permits, the need for determining these values from test data seems to be past. However, this does not stop local jurisdictions from imposing additional requirements. Local regulatory bodies and concerned citizens frequently want to regulate pollutants that are not addressable using EPA's permit limit procedure; too few permits include limitations on specific emissions. The need to correctly calculate achievable emissions remains. At the very least, it is imperative that correctly calculated limitations be placed in the administrative record supporting a permit so that if a problem occurs, a facility retains the ability to defend itself. Fortunately, emissions limitations can be calculated using statistical techniques that consider both regulatory constraints and source variability. These procedures provide a deterministic, objective link between test results and a lower limit that bounds achievable, data-derived regulatory and permit restrictions.

PHILOSOPHICAL FRAMEWORK

EPA set the MACT floor for MWCs by ranking individual pollutant limitations from existing permits from lowest to highest and selecting the 12 percent that were lowest based on the number of incinerators in a category. This group of permitted limits was then averaged. EPA's approach presumes that the permit limitations were being achieved and that the arithmetic average is routinely achievable. Averaged emissions limitations simply imply that some values are larger than the average and some are smaller. Consider, for example, averaging: 20, 20, 20, 20 and 10 to get 18. For this group, only one would be in compliance with the arithmetic average of the emissions limitations even when all five are operating at their permitted level. This points out an obviously unintended consequence of reading the adjective "average" (meaning "typical") in the CAA as the verb or noun meaning "arithmetic average". To establish an emissions limitation using the data average is clearly wrong.

To address this problem, a number of different approaches have been posited by the EPA and industry. The balance of this paper presents these approaches, along with a couple of additional conceptual approaches that could prove useful when faced with the problem of establishing permit limitations for previously unregulated pollutants.

STATISTICAL CONSIDERATIONS

Average emitted concentrations and variance estimates are derived from test data. Figures 1 and 2 show the theoretical statistical effect of uncertainty on the expected distribution of the sample average compared to the true value. The true distribution may be shifted to the left or right of the calculated average; it may also be flatter or more peaked because of the uncertainty with which the standard deviation is known. We can be reasonably certain, however, that the true mean is within the 95 percent statistical confidence level confidence limit for the average and the population standard deviation (the true variability of the sample) is similarly bounded by the 95 percent statistical confidence level confidence limit for the standard deviation. When these two sources of uncertainty are combined, the emissions limitation is correctly determined by the 95 percent statistical confidence level, percent coverage tolerance limits that contain a specified percentage of future tests at a given statistical confidence level result. The errors are incorporated by K-statistics[1,2].

Inherent Limitations of a Statistical Bound

Regardless of the quality of data and validity of the statistical procedures employed, there is a known chance that a well-operated plant will exceed the average. This is inherent in the statistical procedure. When working at the 95 percent statistical confidence level, there is a 5 percent chance that a valid measurement will be outside the calculated bound. Similarly, when limits are calculated to contain a specified percentage of future measurements, say 99 percent, there is still a one percent chance that a valid measurement will not be included when the plant operates as it did when tested to set the limits!

Consider the implications of these errors to a well-operated MWC with three units being tested for six reference method pollutants every year—a combined total of 18 tests per year must be passed. At the 95 statistical confidence level, one exceedance would be expected virtually every year when statistically perfect emissions limitations are promulgated since 1 out of 20 tests under the same conditions should result in a violation at the 95 percent confidence level. Similarly, if the limits are designed to contain 99 percent of the future test values at the 95 percent statistical confidence level, more than one violation of a set of consistently tight, but perfectly derived, emissions limitations can be expected.

Sources of Error

Characterizing stack emissions involves field sampling and recovery, sample handling, laboratory analysis, data entry, results calculation and interpretation. When three runs make up a performance test[3], the results are never exactly alike due to normal variability (random errors) introduced at each step of the characterization process. Analyzing emissions from different test conditions introduces another source of variability due to changes in the fundamental performance of the system. All the foregoing assumes that the same team and laboratory do all the testing. Different field teams, laboratories and chemical supply houses introduce additional sources of variability during retesting.

From a global perspective, available test data can be said to contain two broad types of error:

- within-test error—this characterizes the differences between the three runs or repeated measurements made close together in time to characterize a single test condition.
- between-test error—this characterizes the differences between the average obtained from a number of different tests taken under different conditions and at different times.

Each error source must be accommodated when emissions limitations are calculated. Just as performance is characterized by the average of the individual test runs, within-test error is characterized by the standard deviation of those same runs. Between-test variability is estimated as the standard deviation of the individual test condition averages for an individual plant. When these are combined, the overall source variability, including the effects of different test teams, laboratories, operating conditions and normal performance changes, are characterized. Combining either the between- or within-test variability from several test series or sources is known as pooling. This is a valid technique for maximizing the information.

Statistical Outliers

Even the best laboratories and field teams sometimes produce aberrant data. When there are enough replicates, a number of statistical tests can be employed to identify unusually large and small values. Leaving such values in the analysis bias the average and inflates the standard deviation. Removing such values leaves a facility exposed to exceedances for normal occurrences. This is an issue that requires careful attention and balance. Those interested in tight regulations will want outliers excluded. Those

interested in not being penalized for chance occurrences will want them included. Agreement on outlier identification and handling should be reached prior to applying any statistical treatment of the data.

Combining (Pooling) Data From Several Tests

Unless the overall variability (both the between- and within-test variability) are properly incorporated, the expected range of future test results cannot be characterized. Facilities that comprise the MACT Pool could routinely fail future tests even when tested under identical conditions if the emissions limitations are not properly set.

Emissions data sets typically contain results for a number of test conditions and units. Determination of the statistics for the pooled standard deviation and the effective number of runs for both the within- and between-test conditions can be accomplished with the same basic equations.

The data from individual test conditions are used to estimate within-test variance. Our review of the data indicates that the within-test standard deviation — estimated for each run using the natural logarithms of the data since the data are lognormally distributed[4] —can be treated as coming from an equal variance population.

Under this assumption, the pooled standard deviation (S_p) and effective number of runs (N_p) which characterize all test conditions (C), not just an individual test series, are defined by the following equations:

$$S_p = \sqrt{\frac{\sum (n-1)s_c^{\,2}}{\sum n - C}} \tag{1}$$

$$N_p = \sum n - C + 1 \tag{2}$$

Estimating the overall test condition standard deviation (S_o) and effective number of runs (N_o) by pooling the between- and within-test condition variability (S_b and S_w, respectively) is more complicated than simply pooling either of these two variability sources alone. Review of the available data indicates we cannot assume that the variances are equal. The pooling is done by using the following equations for combining two standard deviations when they cannot be assumed[5] equal:

$$S_o = \sqrt{\frac{(N_w - 1)S_w^2 + (N_b - 1)S_b^2}{(N_w + N_b - 2)}}, \tag{3}$$

$$N_o = 1 + \frac{(N_B\theta + N_w)^2}{\frac{(N_b\theta)^2}{N_w - 1} + \left(\frac{N_w}{N_b}\right)^2}, \text{ and} \tag{4}$$

$$\theta = \left(\frac{S_w}{S_b}\right)^2 \tag{5}$$

Ranking Test Series Averages

Before selecting best performance, the results of emissions testing have to be ranked. The arithmetic average of three runs complies with regulatory requirements for determining compliance, but it does not consider the precision with which a test result is known. In CETRED[6], EPA added twice the standard deviation to the test series average as an approximation of the value likely to contain the average with 95 percent confidence. Unfortunately, three times the standard deviation should have been added to account for the uncertainty associated with using the sample[7].

A better approach is to rank the facilities using the 95 percent statistical upper confidence limit for the average of lognormally distributed data as suggested by Land[8]. The following equations by Rigo[9] produce the same numeric estimates for the upper confidence limit, but have the advantage of being implementable using standard statistical tables and functions available in modern spreadsheets like Excel®:

$$Plus2 = \overline{X} + 2 \times S \tag{6}$$

$$Plus3 = \overline{X} + 3 \times S \tag{7}$$

$$UCL_{Land} = \mu + \tfrac{1}{2}\sigma^2\left(t_{\nu,\alpha/2}\sigma^2 + \left[\tfrac{1}{2}\sigma^2\left\{\frac{N-1}{\chi^2_{N-1,1-\alpha}} - 1\right\}\right]^2\right)^{1/2} \tag{8}$$

Experience using the various formulations indicates that *Plus3* and UCL_{Land} produce generally similar rankings. *Plus2*, on the other hand, frequently differs materially from either the correct nonparametric limiting value and the upper confidence limit on the mean for lognormally distributed data.

Method Precision—The Accuracy of Reported Numbers

Test results that are below the analytical laboratory detection limit (ADL), and even those below the Reference Method Practical Quantitation Limit (RMPQL), contribute no meaningful information about the operation of a source since these results are either indistinguishable from zero or are too variable (error greater than ±30 percent for methods evaluated in accordance with 40 CFR 63, Method 301 Method Validation). These results must be eliminated from the data in order to calculate stable between- and within-test estimates of variability. When values below the ADL are eliminated, much of the "data" currently being used to establish variability are lost.

Correct Statistical Confidence Level and Interpretation of Data-Derived Limits

In the proposed Hazardous Waste Combustor Rule, there are five data-derived emissions limitations that must be met simultaneously (mercury, lead, semivolatile metals, low-volatile metals and total chlorine). For the statistics of the proposed rule to be at the 95 percent confidence level recommended by OSW for other RCRA applications and by the Office of Air Programs for New Source Performance Standards and Guidelines for Existing Sources (see 40 CFR 60 Appendix A, Method 19, for example), individual data-derived MACT Floor limits must be set at the 99 percent statistical confidence level.

Gastwirth[10] explains that "the probability that the *joint procedure* rejects" (the null hypothesis that a plant is in compliance) is:

$$P(A \cup B) = P(A) + P(B) - P(A \cap B)^{11} \tag{9}$$

The above equation can be extended to cover the situation where 5 test conditions must be simultaneous met at the 95 percent statistical confidence level.

Using the Bonferroni approximation, the significance level for k comparisons to meet the intended $\propto$ level is:

$$\alpha^* = \alpha/k \quad (10)$$

The intended overall statistical significance is achieved by using a statistical significance — α^* — of 0.01, which is the 99 percent statistical confidence level.

Data-derived emissions limitations provide floors below which no one should write or accept a limit in a regulation permit[12]. A data-derived emissions limitation based permit must include either additional margin or a provision that passage of a prompt retest deems the initial test a statistical aberration that is not subject to citizen suits and enforcement actions.

Pitfalls of Pollutant-by-Pollutant Calculations

A pollutant-by-pollutant (also know as HAP-by-HAP) approach to setting emissions limits precludes consideration of confounding and conflicting affects between and among the various proposed limitation. Potentially conflicting parameters must be considered when setting standards for various constituents. When pollutants are controlled by different techniques, it may be appropriate to analyze them separately. However, this decision must be re-verified for conflicts in performance of individual control technologies applied in series. For instance, the design of air pollution control devices [APCDs] to control particulates, semi-volatile metals and low volatile metals is the antithesis of designs needed to minimize the synthesis of dioxins and furans. Larger ESPs and baghouses reduce particulate and particulate related pollutant emissions. Unfortunately, these larger APCDs also increase the amount of time the flue gas is held at elevated temperature before being exhausted to the environment. More dioxins and furans are formed in ESPs and baghouses operating at the same temperature which have larger specific collector areas (SCAs) and lower air-to-cloth ratios (ACRs).

It must be recognized that several pollutants are controlled by the same device. Overlooking this point can quickly lead to the ridiculous conclusion that an individual source must be simultaneously equipped with ESPs (lower dioxins) and FFs (lower metals), but not both! This clear technical impossibility is easily avoided if a common pool of best performing facilities or at least a common set of characteristics for those plants is used.

ALTERNATIVE APPROACHES TO CALCULATING A DATA-DERIVED EMISSIONS LIMITATION

Over the past few years, a number of different methods of calculating data-derived emission limitations have been forwarded. These were originally developed to lend a scientific basis to a historically judgmental problem. Since the passage of the 1990 Clean Air Act Amendments with the requirement to establish Maximum Achievable Control Technology (MACT) floors for historically unregulated sources, the attention paid to this problem has increased. The following brings together the most recent versions of the concepts currently in use.

Combined Statistical—Technical Procedure

The combined statistical—technical procedure used by EPA in the Hazardous Waste Combustion Rule procedure is conceptually simple. All the data for a single pollutant and category are arrayed in ascending order. Additional test averages are included until 6% of the facilities for which complete data

are available are included. This means that several test conditions for some facilities will make it into the pool and some low emitting facilities will be excluded because of incomplete emissions characterization data. All other facilities having similar design and feed characteristics are identified and brought into the facility pool. These additional facilities with similar characteristics to the best performing group are called the expanded universe (EU).

The average emissions from the highest emitting test condition among this group of deemed equivalent facilities are used as a proxy for between-test variability. The data-derived MACT emissions limitations is set equal to the data-derived emissions limitations for that test condition using the pooled within-test variability for all included test conditions. Unfortunately, this specific formulation proffered by EPA did not recognize that the pooled within-test standard deviation is only an estimate of the population standard deviation and used the normal deviate ($\phi^{-1}(0.99)$) instead of the appropriate tolerance interval ($K_{0.055,\,0.99,\,N}$).

Equation (11) was used by EPA to determine data-derived emissions limitations and design values (annual average emissions) from the data used to characterize the pool facilities[13].

$$EL_{EPA} = \exp\left[\mu_3 + \phi^{-1}(0.99)\sigma_3\sqrt{1+\frac{3}{N}}\right] \tag{11}$$

where:

$$\mu_3 = \log(\bar{X}) - \frac{1}{2}\sigma_3^2 \tag{12}$$

$$\sigma_3^2 = \log\left[\frac{S^2}{3[\bar{X}]^2}+1\right] \tag{13}$$

$$\bar{X} = \exp\left(\mu_m + \frac{1}{2}\sigma_0^2\right) \tag{14}$$

$$S^2 = \left(\exp(\sigma_0^2)-1\right)\exp(2\mu+\sigma_0^2) \tag{15}$$

$$\bar{X} = \exp\left\{\log(EL_{EPA}) + \frac{1}{2}\log\left(\frac{1}{3}\exp(\sigma_0^2)+\frac{2}{3}\right) - \phi^{-1}(0.99)\left[\log\left(\frac{1}{3}\exp(\sigma_0^2)+\frac{2}{3}\right)\right]^{1/2}\right\} \tag{16}$$

In the published equation for S^2, σ_o instead of $\sigma_o{}^2$ was incorrectly used in two in places in the equation when compared to the published[14] derivation for S^2.

When $\bar{X}$ is calculated, the mean and standard deviation of the logarithms of the data for the highest emitting condition in the pool facilities are used. A more technically correct approach uses the highest test-condition average in the pool along with the pooled geometric standard deviation to estimate the internally consistent geometric mean for the highest emitting source. Of course, if the geometric standard deviation for the highest emitting source and the pool variance are similar, this refinement is not needed. Given the presence of outliers which can inflate variances, the refinement is prudent and turns out to be necessary in many cases.

As discussed previously, $\phi^{-1}(0.99)$ is a reasonable statistic to use when there is a very large emissions database that produces, say, more than 50 degrees of freedom. When fewer runs are available, the upper two-sided tolerance limit *K*-Statistic for 99 percent coverage, 95 percent statistical confidence level and

N runs should be used instead. Tabulated values can be found in previously referenced books by Natrella, and Hahn and Meeker.

An alternative to the combined statistical—technical procedure used for some pollutants was dubbed a breakpoint analysis. Here the average emitted concentrations, or preferably some related statistic that considers variability, is ranked from smallest to largest. Different equations[15] are used to estimate the slope (*SL*) and inflection (*I*) points:

$$SL = X_{i+1} - X_{i-1} \tag{17}$$

$$I = X_{i+1} + X_{i-1} - 2X_i \tag{18}$$

By plotting *SL* and *I* versus rank on the same graph, the slope of various segments of the line describing the data is visualized. Slope changes are marked by jumps in the value of *I* which mark inflection points in the curve. The breakpoint is marked by the largest value of *I* and the corresponding emitted concentration is X_i. Once X_i is identified, if it does not already explicitly incorporate uncertainty, the relevant concentration is described by previous Equation (11) except that $\overline{X}$ is replaced by X_i and α_o is the appropriate pooled value. Consideration should be given to using the median of the individual series standard deviations in this context.

12% MACT Approach

The 12% MACT approach differs from the HWC Rule approach in that progressively higher emitting test conditions are collected until 12% of the facilities for which data are available, but not less than 5 under Sections 112 and 129 of the CAA, are included. An expanded pool of similar facilities is then established and the data-derived emissions limitation is then calculated using the average of the EU emissions and within-test variability. Adjustments for the effect of below detection limits data using the δ-log approach is recommended by EPA. This approach obviously does not consider between-test variability, even via a proxy. Thus, it ignores good engineering and statistical practice and procedures. It is not considered viable by these authors and is not discussed further.

CETRED Approach

When the Agency began the regulatory process for HWCs, they published CETRED[16]. In that report, most of the particulate and PCDD/F data found in EPA's emissions database were analyzed. The methodology employed was similar to EPA's current 12% MACT approach except that the results of all test conditions for individual facilities were treated as a single characterization. The data-derived emissions limitations were done considering both between- and within-facility variance[17].

Most facilities have been tested several times and under various operating conditions. When the mean of the test series averages is calculated, it generally falls very close to the average developed by simply averaging each data point for all test conditions. This is an expected result since most test series involve the same number of runs and it doesn't matter how an overall average is calculated as long as each data point is included the same number of times.

The standard deviation, however, can and does explode (dramatically increase) when the results for individual test conditions are tightly clustered, but the various run conditions are widely separated. This is because the calculated standard deviation includes both the between- and within-test sources of variance.

In CETRED, the statistical methodology considered both the variability exhibited within each test series and between all test conditions contained in the best performing group using a tolerance limit formulation developed by Vangel. Vangel's method requires that the same number of runs have been conducted in each test. Since the majority of emissions test series use three runs, a statistically incorrect but practically inconsequential error is introduced by using the average number of runs in the formulas even though it is physically impossible to have a fractional number of runs. The emissions limitation is:

$$EL_{CETRED} = \bar{\bar{x}} + k^{*}\sigma_{x} \tag{19}$$

where: $$\bar{X}_i = \frac{\sum X_{ij}}{iC} \tag{20}$$

$$S_1^2 = C\sum \frac{\left(\bar{\bar{x}} - \bar{X}_i\right)^2}{i-1}, \text{ the variance calculated between test series averages} \tag{21}$$

$$S_2^2 = \sum\sum \frac{\left(X_{ij} - \bar{X}_i\right)^2}{i(C-1)}, \text{ the pooled within test series variance} \tag{22}$$

$$Q = \frac{S_1^2}{S_2^2} \tag{23}$$

$$W = \left(1 + (C-1)/Q\right)^{-1/2} \tag{24}$$

$$k^{*} = MAX\left(Kc_{p,1-\sigma,ic}, \left[K_{p,1-\alpha,ij} - K_{p,1-\alpha,c}/\sqrt{C} + \left(K_{p,1-\alpha,C} - K_{p,1-\alpha,iC}\right)W\right] / \left(1 - 1/\sqrt{C}\right)\right) \tag{25}$$

CKRC Approach

EPA previously rejected the CETRED approach because no facility simultaneously met the data-derived emissions limitations when it was applied to hazardous waste combustors (cement kilns, incinerators, light weight aggregate kilns and boilers) in CETRED. An obvious touchstone, a valid calculated result, was failed. The approach, however, can be made workable. ERS[18] proposed a modification which implements the CETRED approach that considers both between-test condition variability and the use of a single group of facilities to establish simultaneously achievable emissions limitations for co-controlled pollutants. The results allow well-operated facilities to simultaneously meet the calculated emissions limitations.

Instead of using the highest emitting source in the EU as a proxy for between-test variability, the CETRED approach can be correctly applied by accounting for both between- and within-test variability and recognizing that the data are lognormally distributed. As done by EPA in CETRED, the Cement Kiln Recycling Coalition [CKRC] centered the distribution on the grand mean (average of the averages). All test conditions for the best performing 12 percent of the units in the hazardous waste burning cement kiln universe were incorporated. Of course, if more than 12 percent display below reference method practical quantitation limits (RMPQL) emissions, then they must all be included. Because some pollutants are co-controlled, a common pool for all pollutants should be defined so that internally consistent and technically compatible emissions limitations can be developed.

In the ERS report, the upper confidence limit for the average particulate emissions from each facility was used to characterize test series emissions. Consistent with EPA's methodology, these sources are ranked from lowest to highest. EPA, however, further subdivides the test results by test condition and only includes those that meet the Agency's criteria rather than all permitted plant operating conditions.

Any permitted operating condition for a facility must remain in the MACT analysis to properly characterize source emissions and not just the part of them which happen to occur under some test condition. That is, it is reasonable to statistically analyze each operating condition separately, but once a facility meets the conditions used to establish a pool facility for one constituent it should remain in for all constituents. All the operating conditions for a pool facility should also be included, unless it can be demonstrated that a specific controllable operating condition resulted in previously unacceptable emissions. All measured emissions are inherent characteristics of the source. You cannot simply declare an emissions set unrepresentative unless there is a specific action the operator can take to preclude such emissions. Put differently, when the pool is selected, EPA should not stop when the required number of facilities are included. They should keep adding facilities until all test conditions for the required number of facilities are included.

The MACT Floor should then be calculated using either the tolerance limit or prediction limit as described by the Office of Solid Waste[19]. The tolerance limit as discussed under the 6% MACT floor is a limit designed to contain a specified proportion of the population (e.g., 99 percent of the future test results from all plants). Prediction limits, on the other hand, are designed to contain the next specified number of sample values from the characterized facility assuming that the statistical characteristics of the plant do not change (e.g., the next performance and trial burns between recertifications).

As a result of inherent physical characteristics of the emission process, emissions data tends to be lognormally distributed[20]. Consequently, any procedure used to derive emission limitations must consider the lognormal characteristics of the emissions. A procedure for developing statistical limits for lognormally distributed data is outlined by Land[21]. Land's procedure was followed and the following equations estimate emissions limitations from lognormally distributed data including consideration of the uncertainty with which the standard deviation is known. Simulation studies comparing EPA's HWC rule formulation to that previously published by Rigo[22], demonstrated that EPA's equations for going from individual run data to 3-run averages is superior and included in the following equations:

$$EL_{CKRC-T} = \exp\left(\mu^3 + K_{N,P,1-\alpha}\sigma_3\left[1 + 3/N\right]^{1/2}\right), \text{ and} \tag{26}$$

$$EL_{CKRC-P} = \exp\left(\mu^3 + t_{N,1-\alpha_k}\sigma_3\left[1 + 3/N\right]^{1/2}\right) \tag{27}$$

Both EL_{CKRC-T} and EL_{CKRC-P} are conceptually equivalent to EPA's EL_{EPA} emissions limitation. The numerical values are different and the choice depends on whether the limit is to contain a percentage of all future tests or the next specified number of tests. The real question is whether the limitations should be based on the percentage of tests that will be in compliance from well-run, EU similar facilities or should the Agency be concerned about the number of statistical failures an individual facility is likely to face between permit renewals. Hahn and Meeker use the analogy of an astronaut who is not concerned about the amount of fuel consumed in an average trip to the moon or the percentage of trips that can be successfully completed with a given amount of fuel. Instead, like plant managers, astronauts are concerned about getting home on the fuel carried on their trip (the fines they will receive or jail time they will serve as a result of the number of times their plants will be tested during that manager's watch).

The $EL_{CKRC\text{-}P}$ is the correct limit to choose if a mechanism for dealing with statistically predictable exceedances is not included in a permit or regulation.

A Modified MWC MACT Approach

The MWC MACT floor was developed by taking the average of the lowest 12 percent of permitted emissions limitations. When establishing limits for previously unregulated pollutants, a conceptually consistent approach is to use the pooled within-test variability for all similarly equipped units in Equation (11) to estimate the 3-run average emissions limitation for each unit. The highest emitting source is selected to estimate the emissions limitation.

When examining the set of data-derived emissions limitations, it is important to understand the meaning of the adjective "average" in the phrase "average emissions limitation." Failure to do so can result in selecting a limit that is only achievable by a single facility — this can happen if one plant has aberrantly low emissions results and the balance are characterized by almost identical emissions profiles—and the arithmetic average is calculated. The arithmetic average will only be above one plant and not inclusive of the 12 percent specified in Sections 112 and 129 of the Clean Air Act. The HAP-by-HAP problem also remains. If a common set of facilities are not used to establish emissions limitations for co-controlled pollutants, the resulting ménage may not be routinely achievable by any facility, much less by the intended number.

Instead of averaging the emissions limits that characterize the best performing 12 percent; the correct approach is to use the highest data-derived emissions limitation for the pool facilities as the relevant limitation. This approach maintains consistency with EPA's previous practice in MWC regulations while making maximum use of the available data and avoiding the illogical result where only one of the facilities used to establish the emissions limitations is likely to meet the value.

COMPARATIVE RESULTS

Table 1 is a listing of 3-run average naphalene data obtained from tests conducted at MWCs. The concentrations are in ng/dsm^3 @ 7% O_2, the units used to quantify dioxins. To convert these values to ppm_{dv} @ 7% O_2, simply multiply by 1.88x10-9, 20,000 ng/dsm^3. Naphalene, for example, is 0.004 ppm_{dv} (3.8 ppb_{dv}) which can be compared to the OSHA PEL[23] of 10 ppm to provide an indication of the magnitude of these emissions.

The emissions limitations calculated by several of the approaches are:

- CKRC (next 5 tests) — 9,195 ng/dsm^3 @ 7% O_2
- CETRED —10,250ng/dsm^3 @ 7% O_2
- Modified MWC (average) — 12,426 ng/dsm^3 @ 7% O_2
- CKRC (99% Coverage) —12,705 ng/dsm^3 @ 7% O_2
- Combined Statistical—Technical Procedures — 13,054 ng/dsm^3 @ 7% O_2
- Breakpoint Analysis — 15,645 ng/dsm^3 @ 7% O_2
- Combined Statistical—Technical Procedures (Unequal variances) — 18,915 ng/dsm^3 @ 7% O_2
- Modified MWC (highest limitation) — 21,824 ng/dsm^3 @ 7% O_2

There are clear differences in the numerical results, a little more than a 2:1 range from lowest to highest. These differences may not seem significant, but the low end is where precautionary principle advocates

target. The high end, plus a prudent margin is where plant managers and people faced with $25,000 per day per violation fines and penalties focus their attention.

While professional judgment is involved, the methods finally selected must conform to the Clean Air Act definitions if a regulated HAP is involved or simply for public understandability. The CKRC and HWC rule approaches seem to be the best because they are scientifically defensible and correctly treat the law's grammatical construction. Setting an arbitrarily low limit is not useful if it doesn't affect plant design or operation. Regardless, the emissions are going to be what they are.

CONCLUSIONS

The problem of correctly using data to establish emissions limitations is not yet fully resolved. Great strides have been made over the past couple of years. Regulators have progressed from the rules of thumb that set emissions limitations 20 percent (or ¼ inch if a graph was being used) above the highest measured value. Now, data-derived limits—based on Congressional direction that existing facilities should all become as clean as the "emission control that is achieved in practice by the best controlled 12 percent of existing sources" and new facilities should be as clean as the best one already out there—are being calculated.

Unfortunately, the failure to recognize that data-derived emissions limitations are derived from data, has produced a number of strained interpretations of the Clean Air Act, Sections 112 and 129 designed to fulfill non-technical objectives. Clean proposals have been made including:

- EPA calculating statistical emissions limits for HWCs in CETRED that recognized source variability, even if the final produce was untenable because co-controlled pollutants were treated as if they were independent instead of being linked.
- EPA using the average of permit limitations in the MWC rule — while we can argue about the propriety of using the arithmetic average, the approach clearly recognizes that there is a necessary gap between the best performance ever measured and limits that can be achieved during routine testing.
- The HWC rule has taken this a step further by using data-derived emissions limitation based on the limit statistically achievable by the dirtiest plant in the clean pool. The clean pool is defined as all facilities with technology similar to the best performing group. This is essentially a proxy for considering between-test and plant variability in addition to within-test variability explicitly handled by the approach. Again, we can argue about the size of the pool (6% or 12%), but the concept of including all like facilities is sound.
- CKRC has extended EPA's original data-derived emissions limitation approach to recognize that the emissions characteristics of facilities for all co-controlled pollutants should be analyzed as a group using proper statistical techniques.
- A variant on the MWC and HWC rule and CKRC approaches that accounts for simultaneous control characteristics while preserving the basic frame-work of the MWC rule approach is suggested.

Each of these approaches produces different numerical results. Applied with intelligence, the results are generally comparable. Regardless, it must be recognized that data-derived emissions limitations have built-in probabilities of finding exceedances when a facility is operating exactly as it did when the limitation was established. Consequently, it is imperative that either margin be added or a violation declared only when a re-test is failed.

Needlessly low limits, however, do not affect a material improvement in the environment. They discourage innovation and waste resources. On the other hand, they do produce revenue from unavoidable fines and jobs from more testing. The method of calculating data-derived emissions limitations should provide an ample margin of safety against falsely finding violations. Public policy should not affect the way data-derived emission limitations are calculated, rather it should affect the margin of safety allowed and the decision to impose more stringent emissions limitations than the MACT floor.

NOMENCLATURE

σ	is the standard deviation of the natural logarithms of the data.; $\sigma^2 = \ln\left(1+\left[s/\ \bar{X}\right]^2\right.$
S	is the standard deviation of the untransformed data; $S^2 = \exp^{(2\mu+\sigma^2)}\left(e^{\sigma^2}-1\right.$
$\bar{X}$	is the arithmetic average of the concentrations; $\bar{X} = \exp^{\left(\mu+\frac{1}{2}\sigma^2\right.}$
σ	is the standard deviation of the log transformed data; $\sigma^2 = \ln\left(1+\left[\frac{S}{\bar{X}}\right]^2\right)$
σ_3	is the standard deviation of the log transformed data associated with three-run averages derived from the pooled σ; see Equation (11)
EL_{EPA}	is the data-derived emissions limitation using EPA's April 19, 1996 HWC procedure
EL_{CETRED}	is the date-derived emissions limitation used by EPA in CETRED
$EL_{CKRC\text{-}T}$	is the data-derived tolerance limit (% coverage)
$EL_{CKRC\text{-}P}$	is the data-derived prediction limit (number of future tests covered)
EL_{MWC}	is the average of the emissions limitations calculated using the pooled variance and each test series average then using the largest result
$\phi^{-1}(.99)$	is the 99th percentile of the normal probability distribution
N	is the effective number of runs used to estimate σ
i	is the number of runs conducted for each test condition
C	is the number of test conditions in each average
k	is the number of future test series to be contained
m	is the number of runs to be averaged in a test series
P	is the percentage of future test series to be contained
$t_{N\text{-}1,\alpha/k}$	is the t-statistic with the Bonferroni multiple approximation so it approximately equals the prediction limit for k future tests
$K_{N,P,1-\alpha}$	is the tolerance limit coefficient designed to include P percent of future occurrences at the 1-α statistical confidence level
X_i	is the concentration for the ith ranked result
X_{i-1}	is the next smaller concentration
X_{i+1}	is the next larger concentration.

REFERENCES AND NOTES

1. N.G. Natrella, National Bureau of Standards Handbook No. 91, Experimental Statistics, USGPO, 1966.
2. Hahn & Meeker, Statistical Intervals, A Guide for Practitioners, McGraw-Hill, 1990.
3. Federal Regulations (40 CFR 60.8(f)) defines the results of a performance test as the arithmetic average of three individual test runs.
4. A more precise statement is that the assumption that the data are normally distributed can usually be rejected, but the assumption that the data were lognormally distributed cannot. It is impossible to prove what the underlying data distribution is; it is possible to demonstrate that an assumed distribution is not applicable.
5. Natrella, op cit., pp. 3-22 and 3-29.
6. USEPA/OSW, Combustion Emissions Technical Resource Document (CETRED), EPA530R-94-014, May 1994.
7. F. Pukelsheim, "The Three Sigma Rule," *The American Statistician*, Vol. 48, No. 2, pp. 88-91, May 1994.
8. C.E. Land, Tables of Confidence Limits for Linear Functions of the Normal Mean and Variance, Selected Tables in Mathematical Statistics, Vol. III, 1975.
9. H.G. Rigo, "Selecting Statistically Meaningful Emission Rates," presented at Air & Waste Management Association's 86th Annual Meeting & Exhibition, Denver, CO, June 13-18, 1993.
10. J.L. Gastwirth, Statistical Reasoning in Law and Public Policy Volume 2 Tort Law, Evidence, and Health, Academic Press, 1988.
11. $\alpha = 0.05/5$; $0.05 = 0.01+0.01+0.01+0.01+0.01-0.01^5$
12. Rigo, op. cit.
13. USEPA, Draft Technical Support Document for HWC MACT Standards, Volume III: Selection of MACT Standards and Technologies, February 1996, pp. C-11, C-12.
14. J. Atchison, J.A.C. Brown, The Lognormal Distribution, Cambridge University Press, 1969, pp. 8, eq 2.7.
15. D.N. deG. Allen, Relaxation Methods, McGraw-Hill, 1954.
16. CETRED, op.cit.
17. M.G. Vangel, "Limits for a One-Way Balanced Random-Effects ANOVA Model," Technometrics, May 1992, V34, N2, pp. 176-185.
18. Environmental Risk Sciences, Inc., Environomics, Rigo & Rigo Associates, Inc., An Analysis of Technical Issues Pertaining to the Determination of MACT Standards for the Waste Recycling Segment of the Cement Industry, May 1995
19. EPA/OSW, Statistical Analysis of Ground Water Monitoring Data at RCRA Facilities, Interim Final Guidance, 1989 and Draft Addendum to Interim Final Guidance, 1992.
20. W.R. Ott, Environmental Statistics Analysis, Lewis Publishers, 1996.
21. Land, op. cit.

22. Rigo, op. cit.

23. U.S. Department of Labor, Air Contaminants—Permissible Exposure Limits, 29 CFR 1910.1000, 1989.

Table 1. Test series average naphthalene concentrations measured at MWCs.

FACILITY	TESTS	ARITHMETIC		LOGARITHMIC		Plus2	Plus3	UPPER CONFIDENCE LIMIT ON THE AVERAGE	TEST SERIES PREDICTION LIMIT FOR THE NEXT TEST	MWC APPROACH WITH CALCULATED LIMITS
		AVG.	STD.	AVG.	STD.					
151	3	340	16	5.828	0.046	372	388	369	446	2,546
24	2	1,741	6	7.462	0.003	1,752	1,758	1,765	1,872	13,047
24	2	1,746	91	7.464	0.052	1,928	2,019	2,635	6,957	13,072
24	3	2,772	47	7.927	0.017	2,865	2,912	2,852	3,048	20,773
175	3	1,016	371	6.880	0.359	1,758	2,129	3,940	16,536	7,288
24	4	1,713	598	7.388	0.416	2,909	3,508	3,979	11,127	12,112
175	3	1,487	444	7.271	0.330	2,375	2,818	4,787	18,266	10,774
175	12	2,356	2,941	7.254	1.020	8,238	11,179	5,864	19,502	10,598
168	9	3,742	3,302	7.977	0.706	10,347	13,649	8,320	19,464	21,824
136	6	2,005	1,116	7.397	0.815	4,238	5,354	8,376	29,833	12,225
175	3	2,114	790	7.611	0.369	3,694	4,483	8,787	38,064	15,133
67	3	5,888	1,224	8.667	0.203	8,336	9,560	9,878	23,442	43,514
168	7	5,511	4,338	8.436	0.584	14,186	18,523	10,207	24,785	34,540
433	3	6,688	1,291	8.796	0.189	9,271	10,562	10,633	23,834	49,516
136	4	1,602	1,020	7.213	0.677	3,642	4,662	11,379	51,657	10,166
91	3	5,974	1,386	8.675	0.250	8,747	10,133	12,368	35,440	43,886
24	3	4,141	1,318	8.303	0.324	6,777	8,095	12,934	48,378	30,234
166	4	10,468	2,402	9.233	0.257	15,272	17,674	15,645	30,023	76,662
85	3	441	324	5.874	0.655	1,090	1,414	27,070	221,319	2,665
24	2	2,807	385	7.935	0.138	3,577	3,962	33,401	289,563	20,935
168	9	7,963	12,222	8.471	1.013	32,407	44,629	36,365	101,991	35,790
24	2	2,017	320	7.603	0.160	2,658	2,978	54,777	583,494	15,019
24	2	1,756	295	7.464	0.169	2,346	2,641	69,932	802,491	13,068
91	3	8,866	4,381	8.976	0.478	17,629	22,010	85,017	499,153	59,259
24	3	30,264	11,862	10.271	0.364	53,987	65,849	121,494	518,520	216,450
4	3	29,446	12,453	10.243	0.436	54,351	66,803	207,987	1,096,749	210,558
91	3	25,636	13,920	10.056	0.531	53,476	67,396	421,886	2,793,124	174,573
83	5	629,971	257,853	13.294	0.376	1,145,676	1,403,529	1,035,528	2,165,717	4,447,403

Figure 1. Effect of location uncertainty on a normal distribution.

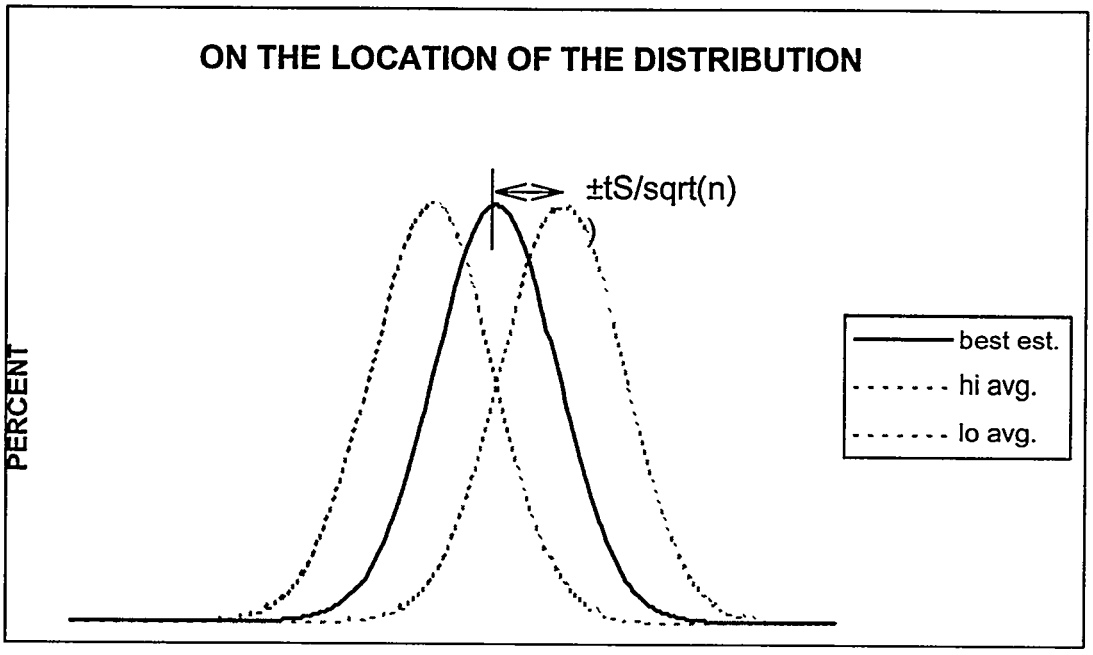

Figure 2. Effect of spread (standard deviation) uncertainty on a normal distribution.

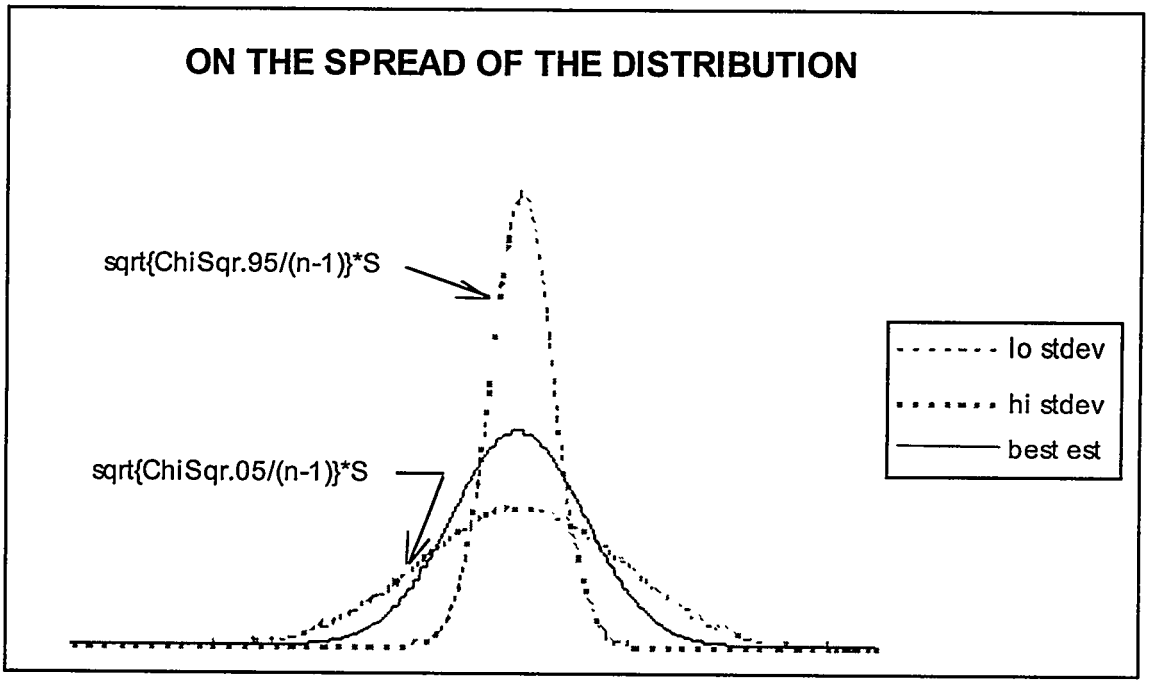

Figure 3. The difference between normal deviates and tolerance limits.

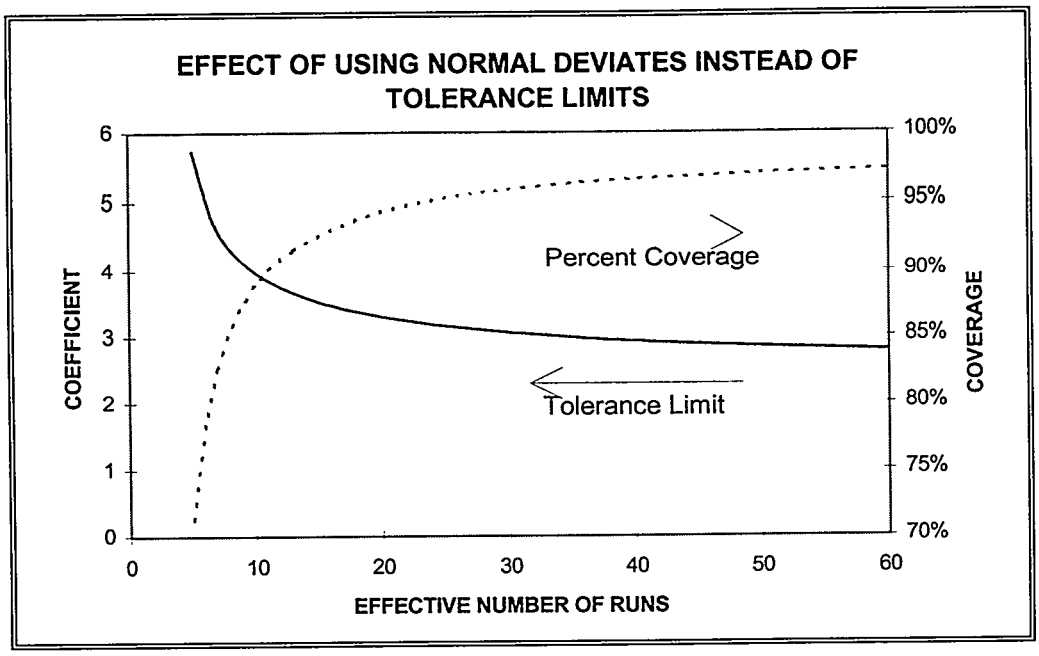

Figure 4. Conceptualization of the difference between the sources of variance.

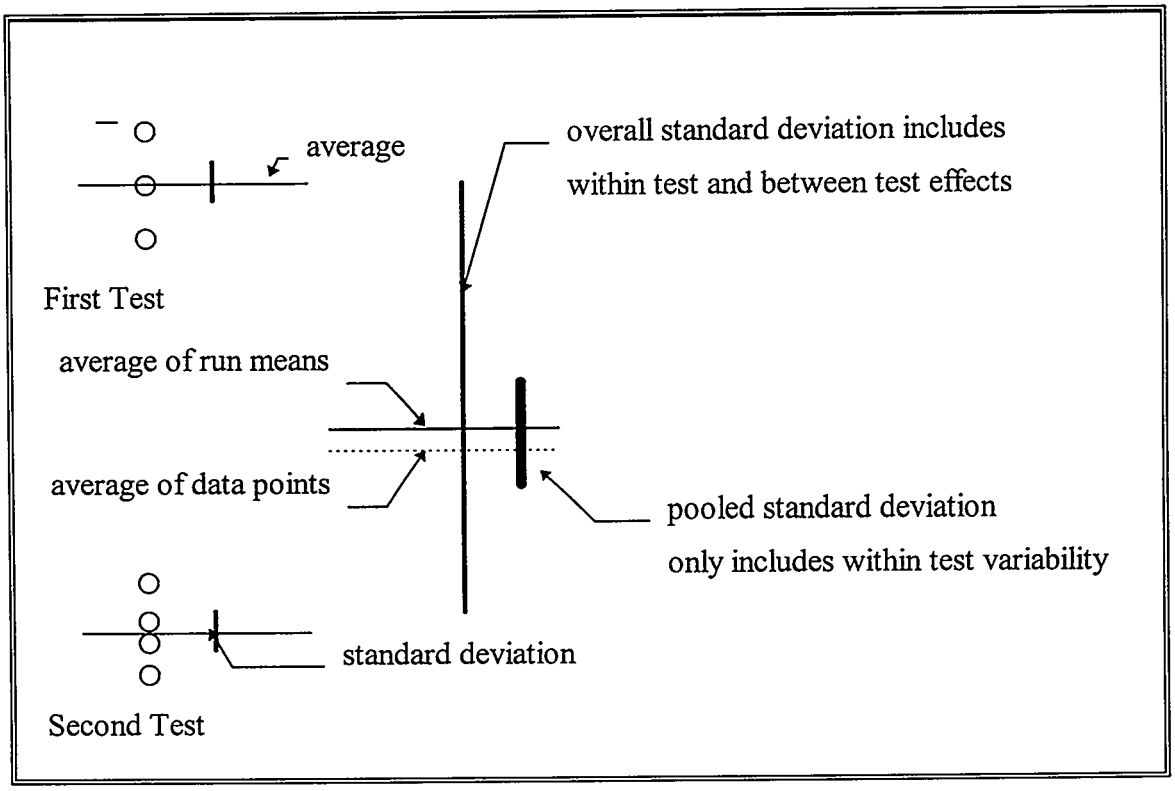

TECHNICAL SESSION II

Ash Utilization

Gas Generation at a Municipal Waste Combustor Ash Monofill - Franklin, New Hampshire

Craig N. Musselman
CMA Engineers, Inc.
35 Bow Street
Portsmouth, New Hampshire 03801

William A. Straub
CMA Engineers, Inc.
35 Bow Street
Portsmouth, New Hampshire 03801

Jeremy N. Bidwell
Rex Technical Services
61 Hoskins Road
Bloomfield, CT 06002

Joyce E. Carpenter
Environmental Risk Limited
120 Mountain Avenue
Bloomfield, Connecticut 06002

James R. Presher
Concord Regional Solid Waste/Resource Recovery Cooperative
6B South Main Street
Penacook, New Hampshire 03303

INTRODUCTION

The characterization of landfill gas generated at municipal solid waste landfills has received significant attention in the United States in recent years. Generation of gas at municipal waste combustor (MWC) ash monofills is, however, generally assumed to be negligible and there is little, if any, published information available concerning such gases. As ash landfills move towards closure in the future, and as progress continues in utilizing certain components of MWC ash residue in construction applications, it is important to identify the mechanisms by which gases may be generated in MWC ash so that appropriate design and material management decisions can be made.

This information is based upon the analysis of gas samples from leachate collection system cleanout pipes at one lined MWC ash landfill. The data were gathered because site operating staff had posed questions as to the contents of the gaseous emissions. The gas characteristics indicated the effects of exothermic chemical reactions in the landfilled ash which affected gas composition in ways which were unexpected, and not widely known.

PROJECT BACKGROUND

The lined MWC ash landfill in Franklin, New Hampshire is owned by the 27 member municipalities of the Concord, NH Regional Solid Waste/Resource Recovery Cooperative ("the Cooperative"). The landfill was initially constructed in 1988, and has operated continuously since 1989.

The landfill accepts combined bottom ash, fly ash and dry lime scrubber product from the 500 ton per day waste to energy (or Municipal Waste Combustor) facility in Concord, New Hampshire owned and operated by a subsidiary of Wheelabrator Technologies, Inc. The MWC facility processes about 177,000 tons per year of municipal solid waste and generates about 68,000 wet tons per year of combined ash. Bottom ash is discharged from the combustion units into wet ash troughs, from which the bottom ash is removed by means of drag chain conveyors. The facility's air pollution control system consists of pneumatic injection of hydrated lime directly into the exhaust gas ductwork for control of acid gas emissions, with fabric filters for control of particulates. The fly ash and dry lime scrubber product is treated with the proprietary WES-PHix process, and combined with the bottom ash on the bottom ash drag chain conveyor. The WES-PHix process involves the addition of phosphoric acid (H_3PO_4) to the fly ash to promote the formation of lead phosphates, in order to limit the solubility of lead in the ash.

The lined MWC ash landfill in Franklin, New Hampshire consists of a double lined landfill with a primary leachate collection system consisting of HDPE piping above the primary (or uppermost) liner. The leachate collection pipes discharge to leachate tanks at the low side of the site, from which leachate is pumped to a remote sewer connection. The leachate tanks are vented to the atmosphere.

Since the primary leachate collection pipes beneath the landfilled ash flow only partially full, air/gas can flow through the pipes with intake at the leachate collection tanks at the low side of the site. Air flows through the primary leachate collection pipes and discharges through the leachate system cleanout pipes located on the high side of the site, through a "chimney" type effect.

The landfill is designed to reach a final maximum depth of about 120 feet. In 1996, residue grades were about 45 feet above the landfill liners. In order to facilitate future leachate collection needs at higher

elevations, two leachate collection pipes had been extended vertically through the fill. One of these two pipes had been perforated every several feet and wrapped with geotextile fabric. During a storm event, ash deposited in the perforated vertical pipe had clogged the bottom 1.5 feet where the pipe connected to the leachate collection pipe. This clogged pipe had a water surface within the pipe, thus closing off convective air access to the leachate collection system. A cross section of this vertical pipe is presented as Figure 1. In this condition, this one vertical pipe inadvertently functioned as a typical landfill gas well. This clogged vertical pipe is noted as the "Phase 1 Vent".

An initial evaluation of the gas was made by Cooperative staff using a handheld explosivity meter ("LEL meter"), on the various cleanouts and leachate collection pipe outlets (or "vents"). The meter's alarm was tripped at two of the outlets for elevated H_2S concentration, and the alarm for lower explosive limit ("LEL") exceedance was tripped for the Phase 1 Vent. This information led the Cooperative to decide to sample and analyze the gaseous emissions.

Ash Characteristics

There are a number of factors pertaining to the specific ash handled at the Franklin site and the operating scheme at the landfill which may affect the generation of gas. These characteristics and the potential impacts of each are listed and discussed below.

- Ash Combustible Content - A comprehensive ash sampling and analysis program conducted in 1990 and 1991 indicated that the bottom ash at that time had a combustible content averaging 6.4% as measured by Loss on Ignition tests (3). This combustible content may be considered moderate to high by US standards. This may have affected non-methane organic compound concentrations.

- Lime Content - The direct dry lime injection system requires the addition of lime at 2 to 4 times the stoichiometric requirement for acid gas control. This rate is higher than at most plants with more stoichiometrically efficient spray dryer absorption systems. The ash at Franklin may have greater alkalinity and unreacted lime than is typical of other ash monofills. The primary leachate, however, has had a pH of 7 or below for the past seven years.

- Phosphoric Acid Addition - Small amounts of phosphoric acid are added to the fly ash/scrubber product using the proprietary "WES-PHix" process. The addition of phosphoric acid has been considered in terms of its potential to have an effect on gas generation. Any effect is presumed minimal due to the neutralization of phosphoric acid by the lime.

- Landfill Operating Scheme - The Franklin ash landfill is operated aggressively as a "dry tomb" type of facility in comparison to most US landfills. The limited amount of time (2-3 years), during which the landfilled ash has been subjected to percolation of water may have an effect on chemical reactions taking place in the landfill.

Other than those factors described above, the ash generated by the Concord, New Hampshire waste to energy facility is considered to be typical of most US facilities based on the type of facility, operation and ash characterization data available.

Landfill Piping Configuration

The specific layout of the various vents is depicted schematically on Figure 2. The nomenclature for

each gas sampling point, and the specific circumstances of each location are presented in Table 1 below.

Gas Temperature and Flows

The landfill interior temperature was measured by lowering a weighted thermocouple into the Phase 1 and Phase 2 vents. Phase 2 pipes were not clogged, but were open to air/gas flow from the leachate collection system below. Ambient air temperature at the time of sampling was 39°F.

The Phase 2 vent could be measured only 9 feet down the pipe due to the presence of a bend. The temperature was 91°F. Gas in this vent was diluted by atmospheric air from the leachate collection system below.

The temperature of undiluted gas in the clogged Phase 1 vent ranged from 132°F to 156°F. The temperature profile with depth is indicated on Figure 3. These temperatures were unexpectedly high and were higher than would typically be expected in an MSW landfill. Optimum temperatures for thermophilic anaerobic digestion of MSW range from 120°to 135°F (4). It is postulated that the elevated temperatures are likely due to a variety of exothermic, primarily inorganic chemical reactions taking place in the landfilled ash.

Measured gas flows are as indicated on the piping schematic presented as Figure 2. A chimney effect is apparent as pipes open to the atmosphere at lower elevations indicated flow into the piping system and the vents connected to the piping system which outlet at higher elevations emitted gas at flows of 20 and 28 cubic feet per minute (CFM). Gas flows at the Phase I vent were estimated to be 30 to 60 CFM. This flowrate is similar in magnitude to the rate which might be experienced at steady state conditions in an active MSW landfill gas well. The zone of influence within the landfill mass of the Phase 1 vent is unknown.

MWC Landfill Gas Characteristics

The vents which had exhaust flow to the atmosphere were sampled and analyzed for atmospheric gases, non-methane organic compounds (NMOCs) and sulfur compounds. Samples were gathered using evacuated SUMMA passivated (polished) canisters with samples withdrawn over a 60 minute duration, per Method TO14. Atmospheric gases were analyzed by GC/FID/TCD using ASTM Method D-3416. NMOCs were analyzed by gas chromatograph/pyrolysis CO_2 using Method TO12 (total NMOC), and by gas chromatography/mass spectroscopy for the full Method TO14 target compound list. Sulfur containing compounds were quantified through ASTM Method 5504.

The summary of the atmospheric gas analyses is presented in Table 2. The oxygen content in the Phase 2 Vent and the Phase 1 Upper Cleanout, both of which were open to atmospheric air in the leachate collection pipes beneath the landfill, were near typical atmospheric levels. The oxygen content in the Phase I Vent, which was clogged and functioning in a way similar to a gas well, was markedly depressed, but not absent. Methane was present in the Phase I Vent at a concentration of 780 ppm. This is low compared to the levels present in gases from MSW landfills (typically 500,000 ppmv, or 50%), and at a level well below the lower explosive limit (LEL) for methane of 50,000 ppmv. If methanogenic bacterial activity was at a high level, the O_2 concentration in the Phase 1 Vent would have been expected to approach zero, and the CO_2 concentration would have been much greater.

Hydrogen was detected in the gas in the Phase 1 Vent. The hydrogen concentration in both Phase 1 Vent samples was measured to be 5.1%, which is in excess of the 4.0% LEL for hydrogen. The presence of

hydrogen at these concentrations is likely the cause of the explosiveness alarm in the initial gas screening described earlier. The hydrogen is postulated to be generated by oxidation reduction reactions of aluminum and other reactive metals, and/or other chemical reactions, taking place within the landfill mass, as discussed later herein.

Hydrogen sulfide concentrations were elevated in the Phase 2 Vent and in the Phase 1 upper cleanout, as indicated in Table 3. H_2S is typically a by-product of the anaerobic decomposition of organic matter. The H_2S concentrations are likely indicative of microbial activity within the landfill mass.

The NMOC concentrations are presented in Table 3. The NMOC concentrations were present at the low end of the range of concentrations reported in the literature (4) for NMOC concentrations in MSW landfill gas. Leachate from the landfill site rarely has detectable concentrations of volatile organic compounds with the exception of periodic low concentrations of acetone.

The concentrations of specific organic compounds were reported for two samples from the Phase 1 Vent and for one sample from the Phase 2 Vent. The results are presented in Table 4. The reported concentrations are all lower than presently applicable health and safety related standards and are generally less than those anticipated in MSW landfill gas (5).

Following the completion of the sampling and analysis described herein, the clog in the Phase 1 vent was removed hydraulically. Later LEL meter testing indicates that the Phase 1 and Phase 2 vents subsequently have similar characteristics.

Discussion of Results and Implications

Generation of Hydrogen Gas. The measured hydrogen gas may be generated by chemical reactions of elemental aluminum and other elemental metals in the presence of water. Typical oxidation reduction reactions may be as follows (6,7):

$$2\ Al^0 + 3H_2O = Al_2O_3 + H_2$$
$$Al^0 + 2\ H_2O = AlOOH + 1.5\ H_2$$
$$Al^0 + 3\ H_2O = Al(OH)_3 + 1.5\ H_2$$

The aluminum reactions are facilitated in the presence of either strong acids or strong bases, which may etch the surface of the aluminum, exposing more elemental aluminum to the reaction. In typical uses of aluminum subject to atmospheric exposure, an adherent protective film of aluminum oxide forms on the surface of the aluminum in pH conditions in the range of 4 to 9 (8). This protective surface film precludes further corrosion of the underlying aluminum. However, in the presence of strong acids or bases, this film may be destroyed and the hydrogen gas generating corrosion reactions can continue. When the protective film is destroyed (or the aluminum is "depassivated"), the exposed elemental aluminum reacts vigorously in the presence of moisture until all exposed aluminum is reacted. The protective oxide film reforms within seconds of exposure of elemental aluminum (15), which limits the length of time that aluminum corrosion continues to occur in atmospheric exposure.

In the landfill, the conditions under which corrosion occurs are more complicated. The aluminum is present both in bulk form and in fine particles, and the chemical conditions which affect corrosion vary locally throughout the landfill mass. Aluminum corrosion can be facilitated by the presence of chloride ions (17), which are present in abundance in MWC ash. The chloride ions affect the aluminum through

pitting, exposing additional elemental aluminum to the corrosion reaction. The chemistry of aluminum is complex, and the reactions taking place in the heterogeneous landfilled residue are not well understood.

Aluminum is present in significant quantities in the ash. Bottom ash from the Concord, New Hampshire MWC facility has a range of aluminum content of 3.4 to 6.4% by weight. Aluminum is also typically present in fly ash in significant concentrations. It is anticipated that a significant percentage of the aluminum present in the ash exists in the elemental form having the potential for the hydrogen generating oxidation reduction reactions.

Hydrogen gas may also be generated by similar reactions with other elemental metals. The oxidation of elemental aluminum, zinc, chromium, iron, copper and other elemental metals can proceed in the proper environmental conditions, releasing electrons. The electrons, in the presence of water and, again, in the proper environmental conditions, can result in the generation of H_2 gas. The aluminum reaction is highlighted herein because of the redox potential of the aluminum reaction, the significant quantity of aluminum in the ash, and the likely presence of elemental aluminum in greater quantities than is likely for the other elemental metals. Oxidation reduction reactions of many elemental metals probably contribute to varying extents to the H_2 gas generation.

Hydrogen is also generated as a byproduct in certain organic decomposition reactions (i.e., in the later stages of anaerobic, non-methanogenic decomposition in an MSW landfill (4)), and can be generated as a byproduct in a variety of other chemical reactions.

It is considered unlikely that the addition of phosphoric acid plays a significant role in hydrogen gas generation at the landfill site. Although the Material Data Sheet supplied by the phosphoric acid supplier warns of the hydrogen gas generation potential when in contact with aluminum, this is due to the acidic nature of the phosphoric acid. The H_3PO_4 acid is neutralized at the MWC facility upon mixing with the highly alkaline scrubber product.

The unusually high alkalinity of the fly ash at the Franklin, New Hampshire landfill in all likelihood results in greater hydrogen gas generation than would be the case for an ash with less available lime. Hydrogen gas at other sites should still be anticipated to be present, although likely at a slower generation rate.

The hydrogen gas generating reactions of aluminum have been known for many years, and have been used in the manufacture of lightweight concrete with a cellular structure (13, 14). Aluminum powder is added to cement and sand. In the presence of lime or other alkali, hydrogen bubbles are formed throughout the concrete, creating a more porous structure. The practice is more prevalent in Europe than in North America.

Anecdotal information is available regarding experience with the generation of hydrogen gas from MWC ash. Fly ash utilized as an aggregate substitute in asphalt cement in Germany developed gas bubbles during paving (11). The gas was analyzed and found to be primarily hydrogen. The generation of hydrogen gas and methane from fly ash and scrubber residue has been documented in laboratory studies in Germany (11, 12). Explosions in a fly ash system in Denmark were attributed to hydrogen gas (15, 16). Explosive conditions were subsequently prevented through ventilation of ash conditioning equipment.

The presence of hydrogen gas at levels above the LEL is not believed to be a major risk factor with respect to landfill operations. Landfill gas from MSW landfills often exhibits methane concentrations above the LEL and below the upper explosiveness limit, at concentrations where explosions could occur in certain circumstances. This risk is managed by proper gas handling in passive or active gas collection systems at closed landfills and by appropriate monitoring of gas concentrations at the site periphery to assure that subsurface migration to nearby structures does not occur. If the generation of hydrogen gas is confirmed at other ash landfill sites, similar design and operation precautions would likely be appropriate for ash landfills as well. Appropriate precautions should be taken when excavating into ash in confined spaces, or when drilling into old landfilled ash.

The potential for generation of hydrogen gas should be considered when evaluating ash utilization alternatives. Until further information is developed, the utilization of unencapsulated ash in close proximity to confined spaces such as structures may be inadvisable. Some researchers (11) have suggested that the aging of ash prior to utilization might be effective in reducing the potential for hydrogen gas release after utilization. The length of time required and the effectiveness of any reduction in subsequent gas generation are not yet known.

- **Ash Temperature**

The elevated temperature determined within the landfill mass is most likely due to a variety of exothermic chemical reactions. Preliminary, theoretical thermodynamic calculations indicate that neither the exothermic aluminum reactions described herein nor the lime hydration reactions would be expected, alone, to generate sufficient heat to bring the landfilled mass to the 156°F maximum temperatures measured. Other exothermic chemical reactions also undoubtedly play a role.

In the peer review process, for this paper, a reviewer commented that high temperatures and carbon monoxide concentrations greater than 100 ppm are generally indicative of combustion conditions in MSW landfills. Some manner of combustion may have been occurring in the ash at the Franklin site. However, the depressed level of CO_2, which is generated in most combustion processes and is generally stable once formed, and the presence of hydrogen gas, which would likely not be present in the midst of combustion, appear to indicate that combustion is not a major factor in the formation of the gases sampled.

From a design standpoint, the elevated ash temperature is not significantly problematic. Temperatures in the ranges measured do not negatively affect most flexible membrane liners and geotextile materials typically used in landfill construction. The design of leachate collection pipes is somewhat temperature dependent in that the calculation of the pipe wall material's modulus of elasticity requires temperature input, depending upon the type of pipe used. Until valid information is developed from other sites indicating the prevalence of much lower ash temperatures, the use of 160°F as the temperature input in leachate collection pipe strength calculations, where required, may be advisable.

- **Provisions for Gas Management in Ash Landfill Closure Designs**

It is apparent from the information reported upon herein that gas management provisions need to be incorporated in the design for closure of an MWC ash landfill. Design procedures similar to those utilized for the closure of smaller MSW landfills with passive gas venting systems may be appropriate. The installation of a suitable gas migration layer beneath impervious capping materials, and passive vents through impervious capping layers, should be, and typically are, incorporated in closure designs.

Further information is needed regarding the movement of gas within landfilled ash to determine whether passive gas wells within the ash are needed or are otherwise of benefit.

- **Additional Information Needs**

Information is needed from other ash landfills to confirm the temperature of ash at depth, and to assess hydrogen gas generation rates and concentrations. Both the temperature and the hydrogen gas generation rates may be lower at other sites where less lime is available for hydration reactions. It should be noted that the hydrogen gas concentrations measured at any site are less a function of generation rate than they are a function of the site's tendency to accumulate gases. The data reported upon herein provides no information regarding the nature of gas pressure and concentration gradients within an ash monofill.

The effect of aging the ash prior to utilization with regards to the subsequent generation of hydrogen gas also deserves investigation.

CONCLUSIONS

The following conclusions can be drawn from the information reported upon herein:

1. MWC ash disposed in an ash monofill may generate gas with NMOC concentrations on the low end of the typical range for NMOCs in MSW landfill gas.

2. Gas flowrates generated in an ash monofill may be significant from a closure design perspective.

3. Hydrogen gas may be generated within the ash mass at an ash monofill from reactions of elemental aluminum and/or from other sources. Hydrogen gas concentrations may exceed the lower explosive limit.

4. Ash temperatures within an MWC ash monofill may be on the order of 156°F, due to reactions of elemental aluminum, lime hydration reactions and other exothermic chemical reactions. The potential for elevated temperatures should be considered in the design of landfill components.

5. Anaerobic non-methanogenic and methanogenic decomposition of waste does not appear to be a significant factor in the generation of gas at an ash monofill, despite the presence of an uncombusted fraction in the ash.

6. Lower ash temperatures and decreased rates of generation of hydrogen gas may be experienced at other ash landfills having less lime available for hydration reactions than was present in the ash at the Franklin, New Hampshire site. However, elevated temperatures and some hydrogen gas generation should be anticipated until experience indicates otherwise.

7. Passive gas vents, and effective gas migration layers beneath impervious caps, should be incorporated in designs for closure of ash monofills.

8. Appropriate precautions should be taken when excavating into ash in confined spaces, or when drilling into old landfilled ash.

9. The potential for generation of hydrogen gas should be considered in ash utilization programs.

Until further information is developed otherwise, the utilization of unencapsulated ash in close proximity to enclosed spaces (i.e., structures) may be inadvisable. The potential benefit of aging of ash on reducing subsequent hydrogen gas generation in utilization merits investigation.

REFERENCES

1. *"Vent Testing Program, Concord Regional Solid Waste/Resource Recovery Cooperative, Secure Residue Landfill, Franklin, New Hampshire"*; Environmental Risk Limited, May, 1996.
2. *"Report on Landfill Gas Testing, Franklin, NH Secure Residue Landfill"*; CMA Engineers, Inc.; June, 1996.
3. Eighmy, TT; Gress, D.; Zhang, X.; Tarr, S; and Whitehead, I; *"Bottom Ash Utilization Evaluation for the Concord, New Hampshire Waste-to-Energy Facility"*; Environmental Research Group, University of New Hampshire; May, 1992.
4. *"Air Emissions from Municipal Solid Waste Landfills - Background Information for Proposed Standards and Guidelines"*; United States Environmental Protection Agency; Research Triangle Park, NC; March, 1991.
5. Carpenter, JE and Bidwell, JN; *"Air Emissions at a Municipal Solid Waste Landfill"*; Environmental Risk Limited; Bloomfield, CT; in the Proceedings of the 17th Biennial Waste Processing Conference, American Society of Mechanical Engineers; 1996.
6. Wefers, K. and Bell, GM; *"Oxides and Hydroxides of Aluminum, Technical Paper No. 19"*; Alcoa Research Laboratories, 1972.
7. Wefers, K. and Misra, C.; *"Oxides and Hydroxides of Aluminum, Alcoa Technical Paper No. 19, Revised"*; Alcoa Laboratories, 1987.
8. Paul, S.; Mitra, P.K.; and Sirkar, S.C.; *"Passivity Breakdown and PZC of Aluminum Chloride Water System"*; in Corrosion, Journal of the National Association of Corrosion Engineers; March, 1993.
9. *"Corrosion, Volume 1, Metal/Environment Reactions"*, Edited by Shreir, L.L.; Newnes Butterworth Publishers; 1976.
10. Metikos-Hukovic, M. and Babic, R.; *"Inhibition of the Hydrogen Evolution Reaction on Aluminum Covered by 'Spontaneous' Oxide"*; in Journal of Applied Electrochemistry, Volume 24; 1994.
11. Eighmy, TT; University of New Hampshire; Personal Communication; 1996.
12. Oberste-Padtberg, R.; Seweden, K.; *"Zur Freisetzung von Wusserstoff aus Mörteln mit MVA-Reststoffen"*; Wasser, Luft and Boden 6:61-62; 1990.
13. Neville, A. M.; *"Properties of Concrete, 3rd Edition"*; Pittman Publishing, Inc.; Marshfield, MA; 1981.
14. Neufeld, R.D.; Vallejo, L.E.; Hu, W.; Latona, M.; Carson, C.; and Kelly, C.; *"Properties of High Fly Ash Content Cellular Concrete"*; in American Society of Civil Engineers Journal of Energy Engineering; April, 1994.
15. *"An International Perspective on Characterization and Management of Residues from Municipal Solid Waste Incineration, Volume 1"*; the International Ash Working Group; July, 1995.
16. Hjelmar, O.; *"Stofudraskniny fra flyveaskefra affaldsforbraendingsanlaeg."* Repport til Miljøstyrelsen. VKI, Hørsholm, Denmark, 1993.
17. Surgi, M. R.; Memorandum Re: *"Thermodynamics and Potential Reactions Causing Elevated Temperatures in Ash Monofills"*; Analytical and Environmental Services, Inc., Glencoe, IL; May 31, 1996 (unpublished preliminary calculations).

Table 1. Gas Sampling Locations.

Sampling Point	Type of Pipe	Depth of Ash	Age of Ash
Phase 1 Vent	Perforated, Clogged at Depth (Similar in Function to Gas Well)	42 feet	0-4 years
Phase 2 Vent	Solid Wall, Open to Leachate System Below (Diluted by air flow from below)	46 feet	1-2 years
Phase 1 Upper Cleanouts	Solid Wall, Open to Leachate System Below (Diluted by air flow from below)	54 feet	4-8 years

Table 2. Summary of Atmospheric Gas Analyses.

Location	Oxygen (%)	Nitrogen (%)	Carbon Monoxide (ppm)	Methane (ppm)	Carbon Dioxide (%)	Hydrogen (%)
Phase 1 Vent						
first (can 3)	3.5	91	110	780	.008	5.1
second (can 4)	3.6	91	110	780	.008	5.1
Phase 2 Vent						
first (can 1)	21	79	<20	<20	.038	.087
second (can 2)	21	79	<20	<20	.038	.092
Phase 1 Primary upper cleanout						
first (can 5)	21	79	<20	30	.051	<.024
second (can 6)	21	79	<20	30	.050	<.024

Table 3. Summary of NMOC and Sulfur Gas Analyses.

Location	Non-methane Organic Compounds (ppm)	Hydrogen Sulfide (ppm)	Total Reduced Sulfur (ppm)
Phase 1 Vent			
first (can/bag 3)	38	<0.004	0.290
second (can/bag 4)	40	<0.004	0.270
Phase 2 Vent			
first (can/bag 1)	3.3	11.0	11.0
second (can/bag 2)	4.4	15.0	15.0
Phase 1 Primary upper cleanout	0.45	11.0	11.0
first (can/bag 5)	0.48		
second (can/bag 6)			

Table 4. Summary of Organic Compound Analyses (All reported in ppb).

Compound	Phase 1 Vent Can 3	Phase 1 Vent Can 4	Phase 2 Vent	Typical Concentrations in MSW Landfill Gas [4]	TLV[2]-TWA	STEL[3]
Chloromethane	75	110	29	900	50,000	100,000
Methylene Chloride	130	<40	30	19,700	50,000	
Benzene	96	97	<16	3,520	10,000	300*
Toluene	100	93	<16	51,600	50,000	
Acetone	9,900	9,500	1,400	3,360	750,000	1,000,000
Tetrachlorethane	<48	<40	<24	7,040	25,000	100,000
2-Butanone (MEK)	840	720	170	2,800	200,000	300,000
Hexane	1,300	1,200	<65	3,010	50,000	
Ethanol	6,400	5,700	4,200	3,410	1,000,000	
Heptane	690	640	<65	N/A	400,000	500,000
Total Organic Compounds	29,661	22,310	6,179	200,000	N/A	N/A

1 - ACGIH: American Conference of Governmental Industrial Hygienists
2 - TLV-TWA: "Threshold Limit Value - Time Weighted Average" (8 hour work day/40 hour work week, without adverse effect)
3 - STEL: "Threshold Limit Value - Short Term Exposure Limit" (maximum 15 minute exposure)
4 - See Reference 4, USEPA

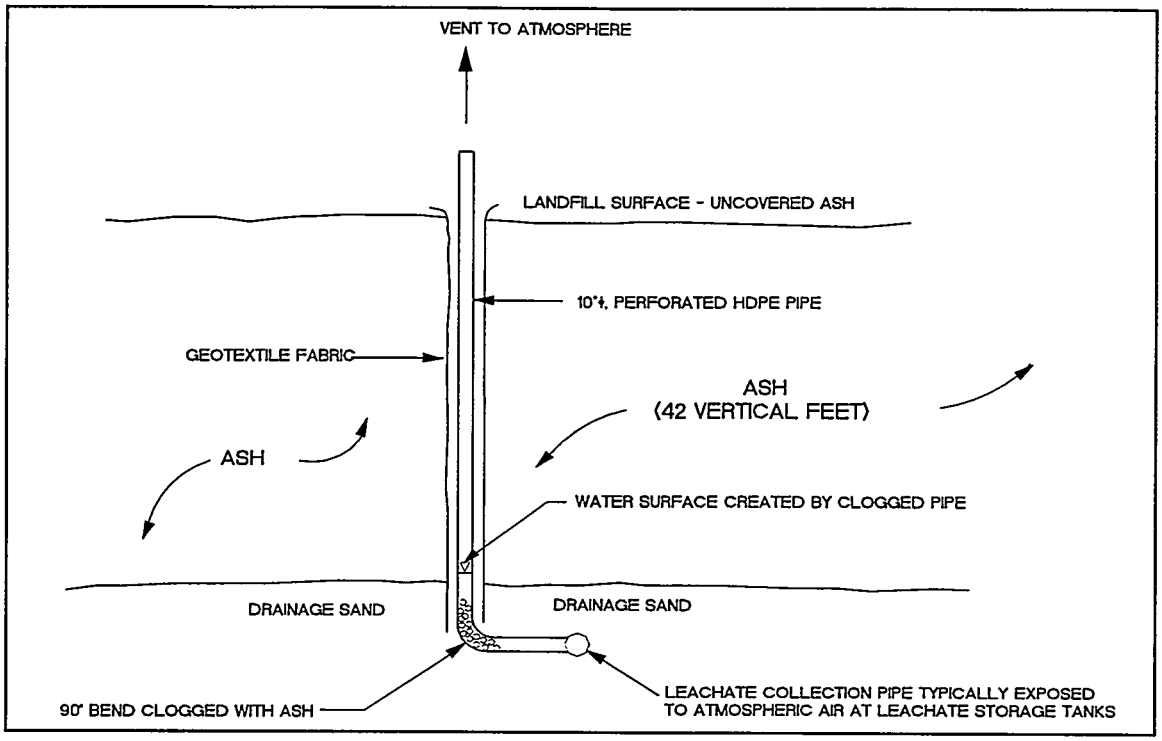

Figure 1. Phase 1 Vent - Cross Section.

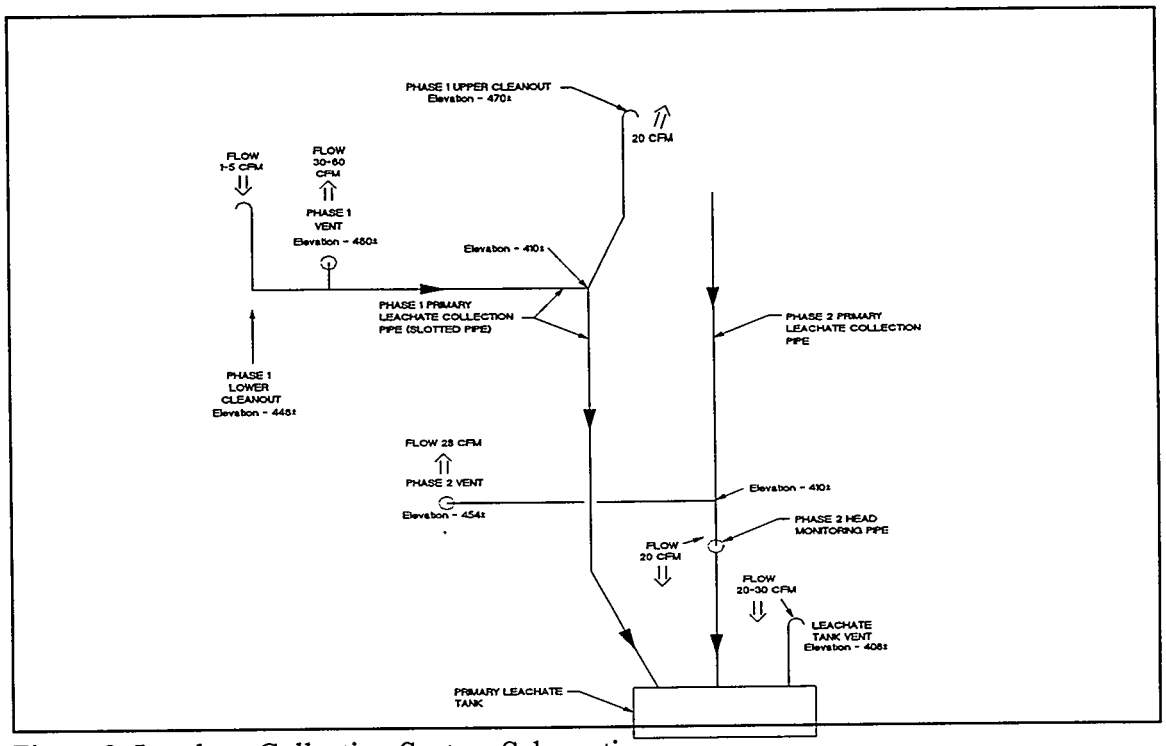

Figure 2. Leachate Collection System Schematic.

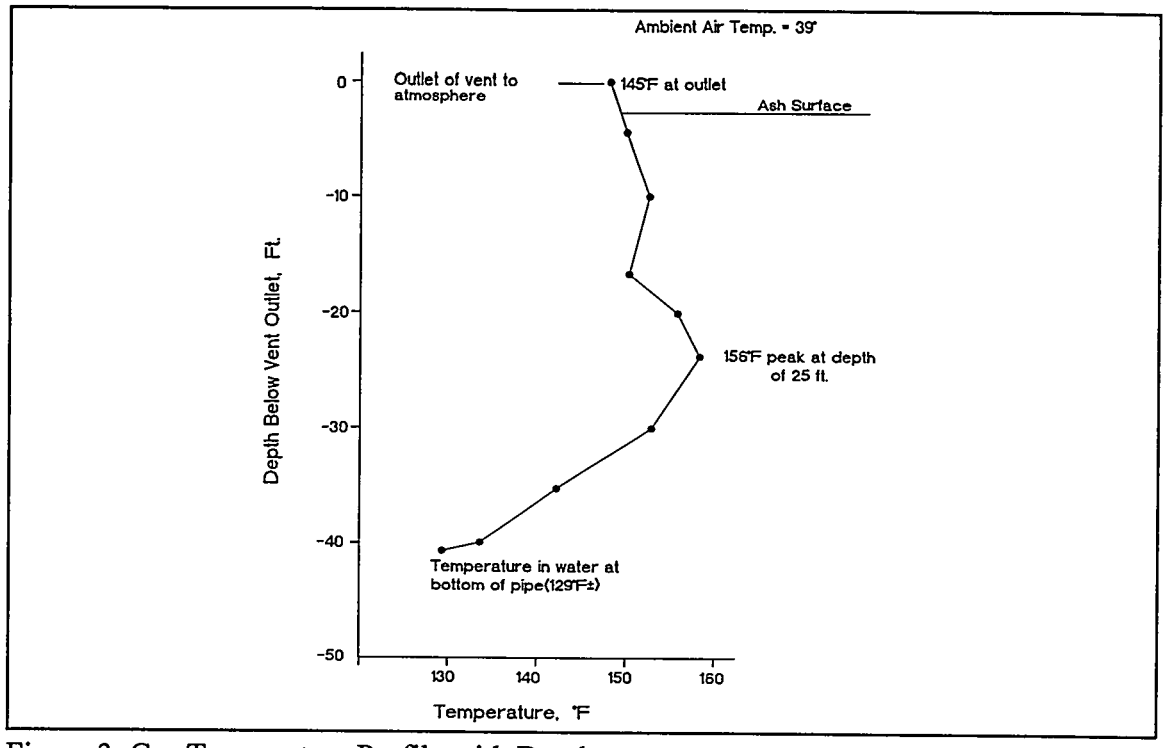

Figure 3. Gas Temperature Profile with Depth.

Ambient Air Monitoring of the Beneficial Use of Municipal Waste Combustor (MWC) Ash as Daily Landfill Cover

Brian H. Magee
Ogden Environmental and Energy Services, Inc.
239 Littleton Rd., Suite 1B
Westford, MA 01886

Amy C. Miller
Ogden Environmental and Energy Services, Inc.
239 Littleton Rd., Suite 1B
Westford, MA 01886

Jeffrey L. Hahn
Ogden Projects, Inc.
40 Lane Road
Fairfield, NJ 07007

Colin M. Jones
City and County of Honolulu
91-174 Hanua Street
Kapolei, HI 96707

INTRODUCTION

This paper summarizes Human Health Risk Assessments of the proposed use of combined ash from the H-Power municipal waste combustor (MWC) in two beneficial uses: (1) Landfill Daily Cover for the Waimanalo Gulch Sanitary Landfill in Ewa, O'ahu, Hawai'i, which is operated by Waste Management of Hawaii, Inc.for the City and County of Honolulu and (2) Landfill Final Cover, a component in the final cover of the Waipahu landfill, in Waipahu, O'ahu, Hawai'i.

The human health risk assessment represents one phase of a larger project involving the investigation of several potential uses of H-Power MWC ash as alternatives to the current practice of disposal in a lined monofill located at the Waimanalo Gulch Sanitary Landfill. The ash consists of approximately 70% bottom ash and 30% fly ash from the MWC, hereafter referred to as H-Power combined ash.

At this time, three alternative uses of H-Power combined ash have been identified: The first option consists of using H-Power combined ash as a component in the final cover in the closure of the Waipahu Landfill; the second option consists of using H-Power combined ash as daily cover at the Waimanalo Gulch Sanitary Landfill; and, the third option consists of mixing H-Power combined ash into aggregate to be used in roadway paving material.

Investigations into these proposed ash uses are detailed in a September 1994 report which presents the rationale for and results of tests conducted to support alternative ash use as landfill cover (daily cover and final cover) and as roadway aggregate.[1] The tests conducted for this Phase I investigation included biological, chemical, and engineering tests (*e.g.*, botanical growth potential, metals content, sieve analyses, strength analyses, permeability, and others). The results of the Phase I investigation indicate that H-Power combined ash is suitable for these alternative beneficial uses.

During June 1995, subsequent to completion of the Phase I investigation, ambient total suspended particulate (dust) concentrations were measured at Waimanalo Gulch Sanitary Landfill during disposal of municipal solid waste (MSW) as well as disposal of H-Power combined ash into the lined monofill. The purpose of collecting these preliminary data was to estimate an emission factor for the combined ash. These data, together with the chemical data collected during Phase I, were used as the basis of human health risk assessments conducted for both landfill cover options (final cover and daily cover).

The human health risk assessment of the use of H-Power combined ash in the closure of the Waipahu Landfill was conducted by Ogden, and a report was submitted to the State of Hawai'i Department of Health (DOH).[2] Preliminary review by the DOH indicated that they approve of the methodology and procedures used therein.

Following this, Ogden prepared a preliminary human health risk assessment of the use of H-Power combined ash as alternate daily cover at the Waimanalo Gulch Sanitary Landfill. Based on chemical analytical data for ash samples collected during the Phase I investigation and other testing, noncarcinogenic and carcinogenic health effects were evaluated for ten constituents. Potential exposures to ash, ash-derived dust, and ash leachate were evaluated for key potential receptors, including landfill workers, adults and children who may visit the landfill (to dispose of household waste), and adults and children who live in nearby residential neighborhoods.

Several activities associated with the proposed use of H-Power combined ash as daily cover theoretically have the potential to create fugitive dust and, therefore, were evaluated in the risk assessment. They include:

- pushing and compacting fresh MSW on the previous day's ash cover;
- pushing and compacting fresh MSW on MSW;
- pushing and compacting fresh combined ash on MSW to create the daily cover; and,
- mining of combined ash.

The ambient air data collected in June 1995 (downwind of combined ash disposal in a lined monofill and MSW disposal in the lined landfill) were used as surrogate data for the dust concentrations associated with these specific activities. However, each of these activities has a different potential for dust generation and, at the time of the preliminary risk assessment, each was expected to produce different downwind dust concentrations. The 1995 dust data were used because activity-specific dust concentrations had not yet been measured. Analytical data generated from ash samples collected during the Phase I investigation and other testing were used to evaluate potential direct exposures to H-Power combined ash (ingestion and dermal contact), to predict leachate concentrations, and as mentioned, to estimate metals concentrations in dust. The results of this preliminary risk assessment were presented in a report to the Hawai'i and indicated that the proposed use of H-Power combined ash for daily cover would pose no significant noncarcinogenic or carcinogenic human health risk.[3]

The preliminary risk assessment for ash use as daily cover identified the lack of available air data associated with specific landfill activities. To address this data gap, approval was sought and obtained from the DOH to conduct a one-week demonstration program involving use of H-Power combined ash as alternate daily cover at the Waimanalo Gulch Sanitary Landfill. This demonstration program was conducted with the cooperation of the City and County of Honolulu, Waste Management of Hawaii, Inc., and the DOH.

These results were incorporated into the final human health risk assessment of the use of H-Power combined ash as alternate daily cover for the Waimanalo Gulch Sanitary Landfill. The revised risk estimates for the daily cover risk assessment are reported in this paper.

AMBIENT AIR MONITORING PROGRAM

During the one-week demonstration program, conducted during July 1996, concentrations of dust, metals, and crystalline silica were measured. Specifically, total and respirable dust, total and respirable metals (including arsenic, barium, chromium, cadmium, lead, nickel, selenium, and silver), respirable crystalline silica, hexavalent chromium, and total mercury (particulate and elemental vapor) were measured. Personal sampling was conducted in equipment cabs and on outdoor employees, and ambient sampling was conducted in numerous locations upwind and downwind of specific landfill activities. Overall, more than 100 personal and area samples were collected using personal sampling pumps, and more than 400 analyses were performed.

Ambient air samples were collected during dumping of ash into stockpiles (for use as daily cover), pushing and compacting of MSW on the previous day's ash cover, pushing and compacting of MSW on fresh MSW (current day's waste), and creating the daily cover at day's end. Data collected during the overnight period when the ash cover was exposed to the elements was evaluated separately. In addition to these daily

activities, air samples were also collected during the excavation of H-Power combined ash previously disposed in the landfill's ash monofill and subsequent loading onto dump trucks (referred to as ash mining).

At certain stations, all-day samples were collected. Locations included: OSHA U (upwind), OSHA D (downwind), CAT (in cab of caterpillar tractor), COMP (in cab of compactor), and SPOT (either on spotter or in spotter area). At other stations, designated ambient stations, samples were collected during four specific time periods defined as shifts 1-4 (S1-S4). These shifts corresponded to early morning, mid-day, late afternoon, and overnight. Ambient locations included: Ambient U (upwind), Ambient D1, Ambient D1A, Ambient D2, and Ambient D2A. In addition, a station designated ASH DUMP was established near to and directly downwind of the daily piles of H-Power combined ash that were dumped during the day for use as daily cover at day's end. Finally, on one day, a demonstration of ash mining in the ash monofill area was monitored. Station ASH MINE DUMP was established directly downwind of the operation, and station ASH MINE LOADER was on the window of the front end loader which loaded ash into dump trucks.

The analytical results from the demonstration program indicate total dust concentrations ranged from 50 to 1,400 $\mu g/m^3$, and respirable dust ranged from 30 to 840 $\mu g/m^3$ (see Tables 1 and 2). The ratio of respirable dust to total dust was calculated for each sample location where both were detected. The average ratio of respirable to total dust was 0.38 from 10 samples collected inside equipment cabs, and 0.24 from 30 outdoor ambient samples.

Arsenic, cadmium, chromium (total and hexavalent), mercury, lead, selenium, and silver were not detected in any of the total or respirable dust samples tested. Barium was detected in one total dust sample (at the detection limit of 0.0002 mg/m^3) but was not detected in any respirable dust samples. Similarly, nickel was detected in two total dust samples (at the detection limit of 0.0002 mg/m^3) but was not detected in any respirable dust samples.

Meteorological Observations

An on-site meteorological station was installed on the top of the hill at monitoring station D2A. Wind direction and wind speed data were collected for 15 minute average time periods. Windroses were developed for each monitoring period of interest so that it could be determined if a station was up-, down-, or cross-wind from a potential source during each specific time period.

The wind roses indicate that regional wind direction was generally from the north, northeast, and east directions during the monitoring period. Thus, the OSHA Upwind and Ambient Upwind stations were generally upwind of the working face at all times. The OSHA Upwind station was generally upwind of the ash piles at all times. The OSHA Compactor, Caterpillar operator, Spotter, and Downwind stations were generally downwind of the ash piles and the working face at all times. The Ambient D1/D1A stations were generally downwind of the ash piles and the working face at all times. Lastly, the Ambient D2/D2A stations were generally down- to cross-wind of the ash piles and the working face.

A simple evaluation of the OSHA eight hour samples indicates that a source other than the working face of the landfill or the ash piles is the likely source of the dust. For instance, on July 10, the total dust was highest in the upwind location and lowest directly on the working face. Respirable dust was also higher in upwind than downwind locations.

Similarly, on July 11, total dust was highest in the upwind location and lowest on the spotter. Respirable

dust was similar in upwind and downwind locations. Also, on July 12, total dust was similar in the upwind location and the spotter location. Respirable dust was greater in the upwind location than in downwind and spotter locations.

A similar evaluation of the ambient monitoring results also strongly suggests that the H-Power combined ash was not the source of the dust. Stations D1/D1A are clearly downwind of the ambient upwind location, and the latter is generally upwind of the ash piles and the working face. There is a trend of the upwind location having higher dust measurements. Out of 8 respirable dust values, 5 were higher in ambient upwind samples than in D1/D1A samples, with the average ratio being 9-fold. Out of 13 total dust measurements, 8 were higher in ambient upwind samples compared to D1/D1A samples with the average ratio being 2-fold. This again suggests that the source of the dust is not the ash piles or the working face.

Comparison of Results During Different Activities

If the ash were a source of dust, the time when most ash-derived fugitive dust would be created would have been during the S1 period when the compactor was operating atop ash and the S3 period when the compactor was creating the day's cover with ash. Measured dust during the S3 period was not elevated. In all samples from ambient downwind locations, no respirable dust or total dust was detected with detection limits of ~0.2 mg/m3. These data indicate that the spreading and compacting of H-Power combined ash to construct a daily cover does not create a significant amount of dust.

In addition, measured dust during the S1 period when the compactor was running over ash was not elevated compared to the S2 period when the compactor was generally running on fresh MSW. (On some days, the ash was not completely covered by the start of the S2 period, but it is still true that the compactor was on ash a greater fraction of the period during S1 than during S2.) Out of 28 samples (respirable dust and total dust) that had a detected value in at least one of the time periods (S1 and S2), only 7 were higher in S1 than in S2. For most of the samples (21/28), the values during S2 were higher than during S1. For this analysis, 1/2 the detection limit was used as a surrogate value for nondetects. In fact, in 17 of the 28 data pairs, dust was not even detected during the S1 period. These data indicate that the running of a heavy compactor over a landfill face covered with H-Power combined ash does not create a significant amount of dust.

The Ashdump sampling station was downwind of the OSHA Upwind station and downwind of the ash piles. The OSHA Upwind station was upwind of the ash piles. In every case (7/10, 7/12, and 7/14), the 8-hour OSHA Upwind sample was higher in respirable dust and total dust than the ashdump sample (by a factor of ~ 5 fold). This suggests that the ash pile itself was not the source of the dust monitored in the Ashdump samples.

Ashmining was also shown not to produce significant dust. No dust was detected at the ambient station placed downwind of the operation. Respirable dust was detected in the cab of the loader as would be expected. Small dust clouds were also visually observed when the loader dumped ash into the trucks.

A comparison of sampling locations where dust was detected with meteorological data concurrently collected during the demonstration program strongly suggests that the H-Power combined ash is not the source of dust concentrations observed. Lastly, it was observed during the demonstration project that running heavy equipment in and atop H-Power combined ash did not generate elevated dust levels, and therefore, typical landfill activities were grouped together and collectively evaluated as "daily activities".

HAZARD IDENTIFICATION

H-Power combined ash samples have been analyzed for several inorganic parameters as well as dioxin/furan congeners. TCLP metals data are available for combined ash samples collected between approximately 1989 and 1996. In addition, total metals analyses have included aluminum, arsenic, barium, cadmium, calcium, chromium, copper, iron, lead, mercury, nickel, potassium, selenium, silver, and zinc. From this list of constituents, aluminum, calcium, copper, iron, potassium, and zinc were eliminated from evaluation in the risk assessment because they have very low toxicity and/or are essential human nutrients. The remaining constituents were evaluated in the risk assessment.

The final list of chemicals of potential concern (CPC) includes the following metals: arsenic, barium, cadmium, chromium, lead, mercury, nickel, selenium, and silver (see Table 3). Furthermore, with the exception of nickel, these are the metals required to be tested by the Resource Conservation and Recovery Act (RCRA). Nickel was included because it is often defined as a chemical of concern for risk assessments of combustors. In addition to these metals, dioxin/furan congeners were also included in this risk assessment because they have historically been the focus of risk assessments of MWC facilities.

TOXICITY ASSESSMENT

Cancer slope factors, Reference Doses, and Reference Concentrations for all CPCs were obtained from standard EPA sources.[4,5] However, there is currently no EPA-verified Reference Dose for lead. Risk assessments for lead commonly use models of varying complexity that predict blood lead levels, which are then compared to benchmark levels of blood lead. The benchmarks have been determined by regulatory agencies to present no significant risk of harm. Because the U.S. EPA model can only predict blood lead levels in children, the Hawai'i Department of Health requested that the California DTSC model be used for this risk assessment.

The major components of the DTSC model were used as presented in DTSC guidance.[6] Specifically, the intake-blood lead slope factors (termed "constants" in the DTSC model) were not modified. However, several of the soil-specific default exposure parameters were modified as allowed by DTSC guidance, so that they were applicable to the assessment of human health risks posed by lead in *ash* versus residential soil. In addition, site-specific information on background lead exposures from air, water, and food was incorporated.

A review of the recent literature revealed that the lowest current regulatory blood lead limit for adults was 25 µg/dL.[7-13] This value was used as the benchmark for risk assessment of adult worker exposures in this analysis. The benchmark for young children and adult females of childbearing age was defined as 10 ug/dL.

EXPOSURE ASSESSMENT

The exposure assessment is presented separately for the Landfill Daily Cover Project (Waimanalo Gulch Sanitary Landfill) and the Landfill Final Cover Project (Waipahu Landfill).

Landfill Daily Cover (Waimanalo Gulch Sanitary Landfill)

It is proposed that H-Power combined ash be used for daily cover of the working face at the Waimanalo Gulch Sanitary Landfill. It is assumed that the daily cover would involve the placement and compacting of H-Power combined ash to a depth of approximately 6 inches over the working face of the landfill. This is assumed to require an 18 inch thickness of uncompacted ash. The risk assessment assumes that the dimensions of working face are approximately 55.5 m by 20.7 m, or 1,149 square meters (12,350 square feet). This was based on actual measurement of the working face during the July 1996 demonstration project.

The risk assessment assumes the amount of H-Power combined ash required for daily cover at the landfill is 686 cubic yards per day. H-Power currently produces approximately 300 cubic yards of combined ash per day. Since H-Power ash has been landfilled at the Waimanalo Gulch Sanitary Landfill for many years, the remaining amount needed for daily cover during the demonstration project, 354 cubic yards, was mined from the previously landfilled H-Power ash. For conservative purposes, it is assumed that the daily cover is 100% H-Power combined ash, supplied by current H-Power operations as well as by mining of the previously landfilled ash.

Ash was mined during the demonstration project from July 9 - July 13. Mined amounts ranged from 360 tons/day to 900 tons/day, with the average amount mined per day being 504 tons. No ash was mined on July 14. Deliveries of unprocessed combined ash during the demonstration project averaged 332 tons/day, which corresponds to approximately 332 cubic yards per day.

It is proposed that the ash will be processed before using it for daily cover of the working face at the Waimanalo Gulch Sanitary Landfill. Ferrous and nonferrous metals will be removed and the water content of the ash will be adjusted to a moisture content of approximately 25%. The estimated volume of processed ash produced per day is 176 cubic yards (214 tons/day /1.215 tons/cubic yard). Thus, the daily requirement for processed combined ash exceeds the production rate for a working face of 12,350 square feet. In the future, it is proposed that the remaining need for daily cover be mined from the previously landfilled ash. Also, the working face is often as small as 6,000 square feet. Daily production of H-Power combined ash would be sufficient to provide daily cover for this size working face, and no ash mining would be required.

The use of H-Power ash as daily cover assumes the following activities: In the morning (0700-1000 hours), workers push and compact municipal solid waste (MSW) over the previous day's ash cover. This ash has been exposed to the air for 14 hours and may have a lower moisture content than fresh H-Power ash. During the mid-day (1000-1500 hours), workers push and compact MSW over MSW deposited earlier the same day (*i.e.*, by this time, the previous day's ash cover has been covered with the current day's MSW, on top of which additional MSW is placed). During this time period, the workers are not running equipment atop of H-Power ash. During the late afternoon (1500-1700 hours), the workers are pushing and compacting ash over the fresh MSW to create the day's cover. This ash is fresh ash, which has a high moisture content. Then, this cover is exposed to the elements during the evening and night (1700-0700 hours). In addition to the daily operations described above, mining of H-Power ash previously disposed at the Waimanalo Gulch Sanitary Landfill is conservatively assumed to take place throughout every workday (0700 - 1700 hours).

Landfill Final Cover (Waipahu Landfill)

It is proposed that H-Power combined ash be used as the bottom layer of the final cover in the closure of

the Waipahu Landfill. This risk assessment assumes that the landfill area to be covered is 43 acres. It is assumed that the closure as proposed would involve the placement and compacting of 24 inches of H-Power combined ash and then 18 inches of local soil. The total amount of H-Power combined ash required to cover 43 acres to a depth of 24 inches is 138,746 cubic yards.

It is proposed that the H-Power combined ash be used as it is produced and processed. Each day's production of ash would be transported to the Waipahu Landfill, placed, compacted, and covered with local soil. The risk assessment addresses potential exposures that might occur during the period when the ash is proposed to be placed, compacted and covered at Waipahu Landfill and during the post-closure period.

The Waipahu Landfill is located adjacent to West Loch of Pearl Harbor with a small residential area to the northwest of the landfill. Accordingly, the risk assessment evaluates potential exposures that might occur in these areas. In addition, there is another residential area towards the southwest of the facility. Exposures in this area are also evaluated. In addition, risks posed by contact with surface water, sediment, and fish in West Loch are quantitated.

The risk assessment evaluated three potential scenarios regarding the manner in which the H-Power ash would be used as part of the landfill closure. In the first, it is assumed that the H-Power ash is delivered to Waipahu Landfill during the week and diverted to Waimanalo Gulch over the weekend. Deliveries only occur during the daylight hours. During the week, ash is stored at the H-Power Plant in covered trailers overnight and delivered to the landfill each morning. At the end of each day, it is assumed that the ash is spread, compacted, and covered with soil. This scenario is referred to as "Closure-No Stockpile" throughout the risk assessment.

In the second scenario, it is assumed that all of the combined ash is delivered to the Waipahu Landfill. Again, however, deliveries only occur during daylight hours (10 hours/day). Overnight during the week, it is assumed that ash is stored in covered trailers at the H-Power plant. During the weekend, the ash is continued to be delivered throughout the day on Saturday and Sunday, thus creating a temporary stockpile at the site that is spread, compacted, and covered with Mililani soil on Monday of each week. At the end of each day, it is assumed that the ash is spread, compacted, and covered with soil. This scenario is referred to as "Closure-Stockpile" throughout the risk assessment.

In the third scenario, it is assumed that the amount of ash delivered daily is spread and compacted, but it is not covered with Mililani soil at the end of the day. It is assumed that the day's ash delivery dries somewhat and can become entrained into the air as fugitive dust overnight before it is covered with soil on the next day. This scenario is referred to as "Closure-Uncovered" throughout the risk assessment.

After closure, it is possible that the Waipahu Landfill will be converted to a soccer field, a softball field, or a picnic area. There is no possibility that the ash can cause airborne dust or surface water run-off, however, because the ash will be covered with 18 inches of native soils. The landfill will also be vegetated. Accordingly, a Post-Closure scenario was defined in which the ash was disrupted so that there was a mechanism by which ash-derived dust and surface water run-off could be created.

For this scenario, it is assumed that dirt bikers have disrupted the integrity of the vegetated cover. It is assumed that this disruption has resulted in 10% of the landfill area (17,402 square meters) becoming unvegetated and thus subject to surface run off. It is also assumed that 2% of the landfill area (3,480 square

meters) has been compromised to the extent that H-Power combined ash is exposed at the surface and subject to dust generation in addition to surface run off. This scenario is referred to as "Post Closure" throughout the risk assessment.

Identification of Receptors

Potential human receptors were identified for on-site and offsite scenarios on the basis of land use information (see Table 5). For the landfill daily cover risk assessment, receptors were identified on-site and offsite at the nearest inhabited location to the south of the site. For the landfill final cover risk assessment, potential human receptors were identified for each closure and post closure scenario. Receptors were identified on-site, off-site at the nearest inhabited locations to the north and south of the site (in the direction of both Trade and Kona Winds), and at locations where relevant activities such as fishing or swimming could occur.

Exposure Point Concentrations

Total metal concentrations in H-Power combined ash are used as exposure point concentrations for the ash, itself (see Table 3). Data from TCLP analyses are used as estimates of chemical concentrations in ash leachate (see Table 3).

On-site and off site receptors may be exposed to chemicals of potential concern in ash via inhalation of fugitive dust generated by placement, grading, and compacting of ash, as well as fugitive dust generated by wind erosion of uncovered ash placed in piles or placed in a layer over a portion of the area of either landfill. The on-site concentrations of fugitive dust generated by various ash use activities were directly measured during the two monitoring events in 1995 and 1996.

To estimate the off-site concentrations of dust generated by these activities, measured on-site concentrations were used to estimate respirable dust emission rates. These emission rates and local meteorological data were used as input parameters for EPA-recommended air dispersion models to estimate off-site dust concentrations. The modeled concentrations of dust in ambient air offsite were combined with chemical concentrations detected in ash to evaluate potential human exposures via inhalation.

This approach is health-protective in that it assumes that all dust is ash-derived and that all of the chemicals detected in ash are transported to dust. As noted above, the dust measured during the daily cover demonstration project was not correlated with ash handling and use. Instead, the dust observed during the project was correlated with truck traffic on dusty roads and rock crushing activities at the adjacent quarry. However, the measured dust concentrations can be used as worst case estimates of the dust generated by ash handling and use.

On-Site Dust Concentrations. During the six day demonstration project during which air monitoring was performed, twelve day-long total suspended particulate samples were taken inside of the caterpillar tractor and the MSW compactor. The average TSP value was 0.278 mg/m^3. The average ratio of TSP to PM_{10} for samples taken inside of equipment was 0.38. Accordingly, the PM_{10} concentration for the landfill workers working inside the cabs of heavy equipment was derived as 0.105 mg/m^3.

One landfill worker, the spotter, worked outdoors throughout the entire work day. Five day-long samples of total suspended particulates were taken. The average TSP value was 0.558 mg/m^3. The average ratio of TSP to PM_{10} for samples outside was 0.24. Accordingly, the PM_{10} concentration for the landfill workers

working outside was derived as 0.134 mg/m^3.

To be health-protective, the respirable particulate (PM_{10}) concentration for the spotter was used for all on-site workers during daily operations. This concentration overestimates the exposures for workers who are working inside of earth moving equipment.

During the ash mining operation, one sample was taken for respirable dust on the window of the front end loader, but no samples were taken for total suspended particulates. Accordingly, the respirable dust value of 0.300 mg/m^3 was used for this potential receptor.

Samples collected during the 1996 demonstration project were used to derive the average outdoor TSP concentration. The average TSP concentration for all outdoor samples was higher than the average TSP concentration for all outdoor *downwind* samples. Of the total dataset of outdoor samples, those samples collected in upwind locations (e.g. at or near the adjacent quarry's rock crushing operations) were excluded. Thirty nine samples were taken outdoors in downwind areas where visitors might be exposed to on-site dust. The average TSP value was 0.268 mg/m^3. The average ratio of TSP to PM_{10} for samples outside was 0.24. Accordingly, the PM_{10} concentration for the on-site landfill visitors (landfill daily cover) or trespassers (landfill final cover) was derived as 0.064 mg/m^3.

Off-Site Dust Concentrations. PM_{10} emission rates were estimated from measured concentration data using a simple Box Model[14] and site-specific data for source length and mean wind speed (5.14 m/sec). The PM_{10} concentration in the box was assumed to be uniformly mixed by human activities on the landfill. Mixing height was assumed to be 2 m.

The SCREEN3 model (Version 95181)[15] was used to estimate offsite ambient PM10 concentrations for the various scenarios. SCREEN3 is a USEPA-preferred model and is recommended by USEPA for a screening-level air dispersion modeling . The SCREEN3 model determines 1-hour chemical concentrations. Eight-hour and annual average PM10 concentrations are calculated by multiplying factors of 0.7 and 0.08, respectively.

Wind data are site-specific with the stability of D and wind speed of 5.14 m/s. Source areas were modeled as ground-level area sources with site-specific areas. A receptor height of 1.0 m was assumed. Site locations were considered as rural areas, and they were modeled using the simple terrain approach because the terrain heights of nearby human receptors are lower than the emission sources.

RISK CHARACTERIZATION

Table 4 presents the results of the lead risk assessment for all receptors and scenarios for both the Landfill Daily Cover risk assessment (Waimanalo Gulch Sanitary Landfill) and the Landfill Final Cover risk assessment (Waipahu Landfill). In all cases, the 99th percentile blood lead concentration is less than the applicable blood lead health benchmark. In all cases, the majority of blood lead was associated with the assumed ingestion and dermal contact with ash. Only a small fraction was associated with inhalation of dust. For instance, for the Landfill Daily Cover risk assessment, inhalation of lead from ash-derived dust in air by on-site workers contributes 0.49 µg/dL, 7% of the total blood lead concentration. Inhalation of lead

from ash-derived dust in air by ash mining workers contributes 1.1 µg/dL, 15% of the total blood lead concentration. Inhalation of lead in ash-derived dust contributes less than 1% of the total blood lead concentration for the on-site adult visitor receptor. Inhalation of lead in ash-derived dust contributes less than 0.1% of the total blood lead concentration for the on-site child visitor receptor.

The same is true for the Landfill Final Cover risk assessment. Inhalation of lead from ash-derived dust in air contributes 0.20 µg/dL, 4% of the total blood lead concentration for construction workers. For the trespasser closure scenarios (assuming no stockpile, stockpile present, and uncovered ash), inhalation of lead in ash-derived dust contributes less than 1% of the total blood lead concentration for each receptor.

For other receptors and scenarios, such as the West Loch recreator (Closure-Stockpile, Closure-Uncovered, and Post-Closure scenarios), exposures to lead in background air, food, and water contribute essentially all of the 99th percentile blood lead concentrations. Surface water, sediment, and fish consumption exposures are associated with less than 1% of the total blood lead concentration for each receptor.

Table 5 presents the results of the noncarcinogenic risk assessment for all receptors and scenarios for both the Landfill Daily Cover risk assessment (Waimanalo Gulch Sanitary Landfill) and the Landfill Final Cover risk assessment (Waipahu Landfill). In all cases, the hazard indices are less than 1.0. These results indicate that proposed use of ash for daily cover at the landfill poses no unacceptable incremental increase in noncarcinogenic health risks.

Estimated Lifetime Cancer Risks (ELCRs) are also shown in Table 5. For all receptors and scenarios, the estimated cancer risk is within or below U.S. EPA's acceptable risk range of 10^{-4} to 10^{-6} and OSHA's criteria of 1×10^{-3} for setting occupational standards. Note that inhalation risks for all receptors were calculated based on the assumption that 100% of dust is ash-derived (*i.e.*, 100% of metals concentrations detected in ash were assumed to be present in dust), and that worker risks were estimated assuming that exposure occurs without regard to personal protective equipment and personal hygiene practices required under the applicable OSHA standards for arsenic, cadmium, and lead.

SUMMARY AND CONCLUSIONS

Human health risk assessments were performed for two proposed beneficial uses of H-Power combined ash: Landfill Daily Cover (Waimanalo Gulch Sanitary Landfill) and Landfill Final Cover (Waipahu Landfill). In all cases, with all receptors and ash use scenarios, estimated blood lead concentrations were less than 25 μg/dL for adult male workers and 10 μg/dL for nonworkers assumed to be young children or female adults of child-bearing age. Estimated hazard indices were all less than 1.0, and estimated excess lifetime cancer risks were within or below U.S. EPA's acceptable risk range of 10^{-4} to 10^{-6} and OSHA's criteria of 1×10^{-3} for setting occupational standards.

Ambient and personal monitoring was performed during a demonstration project of landfill daily cover. Although no metals were detected in total or respirable dust and total dust was not found to be correlated with ash handling and use, measured dust concentrations were assumed to represent worst case estimates of ash-generated dust levels. The risk assessment assumed that dust was totally ash-derived, and ash-derived metal concentrations were derived from the total metals content of H-Power combined ash. Even with this very health-protective assumption, the risk assessment results were found to be dominated by the assumptions that potential receptors would directly ingest and dermally contact H-Power combined ash.

While such assumptions are commonly made by risk assessors, it should be noted that construction workers or landfill workers must adhere to strict requirements concerning personal hygiene practices and the use of personal protective equipment required under the applicable OSHA standards for arsenic, cadmium, and lead. Thus, assuming that workers will violate Federal law is a very health-protective approach to human health risk assessment.

REFERENCES

1. Utilization of Ash from Municipal Solid Waste Combustion. Final Report. Phase I, NREL/TP-430-7382, National Renewable Energy Laboratory, Golden, CO, September, 1994.

2. Risk Assessment of the Beneficial Use of H-Power Combined Ash in the Final Cover for the Waipahu Landfill Closure, Ogden Environmental and Energy Services, Inc., Westford, MA, March, 1996.

3. Risk Assessment of the Beneficial Use of H-Power Combined Ash in the Daily Cover of the Waimanalo Gulch Sanitary Landfill, Ogden Environmental and Energy Services, Inc., Westford, MA, April, 1996.

4. Health Effects Assessment Summary Tables, FY-1995 Annual, EPA/540/R-95/036, U.S. EPA, Office of Solid Waste and Emergency Response, Washington, D.C. May, 1995.

5. Integrated Risk Information System, U.S. EPA, On-Line Database, 1996.

6. Assessment of Health Risks from Inorganic Lead in Soil, California Department of Toxic Substance Control, 1993.

7. Case Studies in Environmental Medicine, Lead Toxicity, Agency for Toxic Substances and Disease Registry, 1992.

8. Toxicological Profile for Lead, PB93-182475, Agency for Toxic Substances and Disease Registry, National Technical Information Service, Atlanta, GA. April, 1993.

9. Preventing Lead Poisoning in Young Children, A Statement by the Centers for Disease Control, Centers for Disease Control, October, 1991.

10. Healthy People 2000: National Health Promotion and Disease Prevention Objectives, PHS 91-50212, Department of Health and Human Services, Centers for Disease Control, 1991.

11. H.W. Henxe, B. Filipak and U. Keil, "The association of blood lead and blood pressure in population surveys," Epidemiology, 4: 173-179 (1993).

12. J.L. Pirkle, J. Schwartz, J.R. Landis, et al., "The relationship between blood lead levels and blood pressure and its cardiovascular risk implications," Am. J. Epidemiology, 121: 246-258 (1985).

13. W. Victery, H.A. Tyroler, R. Volpe, et al., "Summary of discussion sessions: symposium on lead-blood pressure relationships," Env. Health Perspectives, 78: 139-155 (1988).

14. A.C. Stern, Fundamentals of Air Pollution, Academic Press, Inc., 1987.

15. Screening Procedures for Estimating the Air Quality Impact of Stationary Sources, Revised, EPA/454/R-92-019, U.S. EPA, October, 1992.

TABLE 1
TOTAL DUST CONCENTRATIONS

OSHA STATIONS	Day 1 7/10/96 (mg/m3)	Day 2 7/11/96 (mg/m3)	Day 3 7/12/96 (mg/m3)	Day 4 7/13/96 (mg/m3)	Day 5 7/14/96 (mg/m3)	Day 6 7/15/96 (mg/m3)
OSHA U	0.73	1.0	0.43	1.3	0.36	0.21
OSHA D	0.31	0.54	0.32	0.45	0.94	0.20
CAT	0.11	0.22	0.19	0.17	0.25	0.60
COMP	<0.02	0.41	0.27	0.62	0.20	0.28
SPOT	0.48	0.59*	0.07	1.4	0.63	0.21
AMBIENT STATIONS						
U S1	0.2	0.42	0.36	0.1	<0.08	<0.1
U S2	0.65	0.44	0.76	0.27	0.05	0.09
U S3		0.4	<0.2	<0.1		
U S4	<0.02	<0.02	0.06	<0.02	<0.02	<0.02
D1 S1	<0.09		0.3		<0.07	
D1 S2	0.62		0.3		0.12	
D1 S3						
D1 S4			<0.02		<0.02	
D1A S1		0.34		0.33		0.2
DIA S2		0.22		0.39		
DIA S3		<0.2		<0.2		
DIA S4		<0.02		<0.02		0.03
D2 S1	<0.09		<0.07		<0.07	
D2 S2	0.23		0.30		0.17	
D2 S3			<0.2			
D2 S4	<0.02				<0.02	
D2A S1		0.42		<0.02		<0.1
D2A S2		<0.03		0.16		<0.03
D2A S3		<0.2		<0.2		
D2A S4		<0.02		<0.02		<0.02
ASH DUMP		0.83		0.44		0.05
ASH MINING						
ASH MINE DUMP			<0.08			
ASH MINE LOADER						

NOTES:

*Cassette found on the ground and reconnected to sampling apparatus.

TABLE 2
RESPIRABLE DUST CONCENTRATIONS

OSHA STATIONS	Day 1 7/10/96 (mg/m3)	Day 2 7/11/96 (mg/m3)	Day 3 7/12/96 (mg/m3)	Day 4 7/13/96 (mg/m3)	Day 5 7/14/96 (mg/m3)	Day 6 7/15/96 (mg/m3)
OSHA U	0.19	0.23	0.09	0.25	0.03	0.08
OSHA D	0.05	0.27*	0.11	0.09	0.08	0.09
CAT	0.03	0.07	<0.02	0.09	0.05*	0.24
COMP	0.04	0.14	0.13	0.25	0.13	0.07
SPOT	0.09	0.18	0.17*	0.15	0.18	0.06
AMBIENT STATIONS						
U S1	0.4	<0.08	<0.09	<0.09		<0.2
U S2	0.03	0.03	0.05	0.1	<0.04	
U S3		<0.2	<0.3	0.3		
U S4	<0.02	<0.02	<0.02	0.6	<0.02	<0.02
D1 S1	<0.1		<0.08		<0.08	
D1 S2	0.1		0.04		0.05	
D1 S3			<0.2			
D1 S4	<0.02		<0.02		<0.02	
D1A S1		<0.08		0.84		<0.2
DIA S2		0.05		0.07		
DIA S3		<0.2		<0.2		
DIA S4		<0.02		<0.02		<0.02
D2 S1	<0.1		0.2		<0.08	
D2 S2	<0.03		<0.04		0.09	
D2 S3			<0.2			
D2 S4	<0.02		<0.02		<0.02	
D2A S1		<0.07		<0.08		
D2A S2		<0.04		0.1		
D2A S3		<0.2		<0.2		
D2A S4		<0.02		<0.02		<0.02
ASH DUMPING		0.04		0.02		<0.03
ASH MINING						
ASH MINE DUMP			<0.09			
ASH MINE LOADER			0.3			

NOTES:

*Laboratory report indicated sample was contaminated with tap water; results may be biased high.

TABLE 3
DATA SUMMARY FOR H-POWER COMBINED ASH

Chemical	Concentration in Ash (Dry Weight, mg/kg)[1,2]	Concentration in TCLP Leachate (mg/L)[2,3]
Arsenic	49	0.67
Barium	410	1.6
Cadmium	29	0.31
Chromium	69	0.064
Lead	2500	1.0
Mercury	11	0.0045
Nickel	75	not analyzed
Selenium	0.91	0.19
Silver	7.1	0.088
TCDD-Toxic Equivalents[4]	0.00043	not analyzed

[1] Combined ash samples with metal pieces removed, samples collected during 3/20/95-12/18/95.
[2]Upper 95% confidence interval of the mean concentration using H statistic per U.S. EPA guidance assuming lognormal distribution.
[3]Combined ash samples with metal pieces removed, samples collected from 12/89-8/95.
[4]Mean of two samples in which total congener profile was measured.

TABLE 4
ESTIMATED BLOOD LEAD CONCENTRATIONS

LANDFILL DAILY COVER

Receptor	95th %ile (ug/dl)	99th %ile (ug/dl)
On-Site Worker pushing/compacting MSW/Daily Cover	5.3	6.7
On-Site Worker - ash mining	5.8	7.3
On-Site Visitor - young child	2.7	3.4
On-Site Visitor - female of childbearing age	1.4	1.8
Off-Site Resident - young child	1.5	1.9

LANDFILL FINAL COVER

Receptor	95th %ile (ug/dl)	99th %ile (ug/dl)
On-Site Construction Worker	4.0	5.0
On-Site Trespasser (young child)		
Closure No Stockpile	2.1	2.7
Closure with Stockpile	2.7	3.4
Closure Uncovered	2.7	3.4
Off-Site Resident (young child)		
Closure No Stockpile	1.5	1.9
Closure with Stockpile	1.5	1.9
Closure Uncovered	1.5	1.9
Post Closure	1.5	1.9
Recreator (fishing/swimming)		
Closure with Stockpile	1.5	1.9
Closure Uncovered	1.5	1.9
Post Closure	1.5	1.9
Recreator (child dirt biking)		
Post Closure	2.7	3.4

TABLE 5
ESTIMATED NONCARCINOGENIC AND CARCINOGENIC HEALTH RISKS

LANDFILL DAILY COVER

Receptor	Hazard Index	Cancer Risk
On-Site Worker pushing/compacting MSW/Daily Cover	0.4	3×10^{-5}
On-Site Worker - ash mining	0.6	5×10^{-5}
On-Site Visitor - young child	0.2	4×10^{-6}
On-Site Visitor - female of childbearing age	0.05	4×10^{-6}
Off-Site Resident - young child	0.001	2×10^{-8}

LANDFILL FINAL COVER

Receptor	Hazard Index	Cancer Risk
On-Site Construction Worker		
Closure No Stockpile	0.2	2×10^{-6}
Closure with Stockpile	0.2	2×10^{-6}
Closure Uncovered	0.2	2×10^{-6}
On-Site Trespasser (young child)		
Closure No Stockpile	0.08	9×10^{-7}
Closure with Stockpile	0.3	1×10^{-6}
Closure Uncovered	0.3	2×10^{-6}
Off-Site Resident (young child)		
Closure No Stockpile	0.001	2×10^{-8}
Closure with Stockpile	0.008	2×10^{-8}
Closure Uncovered	0.001	2×10^{-8}
Post Closure	0.0008	2×10^{-8}
Recreator (fishing/swimming)		
Closure with Stockpile	0.001	7×10^{-8}
Closure Uncovered	0.004	2×10^{-7}
Post Closure	0.07	9×10^{-7}
Recreator (child dirt biking)		
Post Closure	0.2	1×10^{-6}

Fundamental Mechanisms of Phosphate Stabilization of Divalent Metals in MSW Combustion Scrubber Residues

T. Taylor Eighmy
Environmental Research Group
A115 Kingsbury Hall
University of New Hampshire
Durham, NH 03824

Bradley J. Crannell
Environmental Research Group
A115 Kingsbury Hall
University of New Hampshire
Durham, NH 03824

Leslie G. Butler
Chemistry Department
Louisiana State University
Baton Rouge, LA 70803

Frank K. Cartledge
Chemistry Department
Louisiana State University
Baton Rouge, LA 70803

Earl Emery
Chemistry Department
Louisiana State University
Baton Rouge, LA 70803

Daniel Oblas
Center for Advanced Materials
University of Massachusetts Lowell
1 University Avenue
Lowell, MA 01854

James E. Krzanowski
Mechanical Engineering Department
134 Kingsbury Hall
University of New Hampshire
Durham, NH 03824

J. Dykstra Eusden Jr.
Geology Department
Carnegie Hall
Bates College
Lewiston, ME 04240

Elizabeth L. Shaw
Analytical Shared Experimental Facility
Center for Material Science and Engineering
Room 13-4137
Massachusetts Institute of Technology
77 Massachusetts Avenue
Cambridge, MA 02139

Carl A. Francis
Harvard University Mineralogical Museum
24 Oxford Street
Cambridge, MA 02138

INTRODUCTION

Chemical stabilization of waste materials offers the potential to reduce the leachability of heavy metals in the waste. The principal objective during stabilization is to form new mineral phases with reduced solubilities and increased geochemical stability in a leaching environment. One stabilization agent of recent interest, particularly for Pb^{2+}, is PO_4^{3-}.[1,2,3,4,5]

A patented soluble phosphate treatment process, marketed by Wheelabrator Environmental Systems as the WES-PHix process, is used in 23 MSW combustion or ash processing facilities in the United States. It is also used at 7 wire recycling facilities. The process is licensed to Kurita Water Industries Ltd. of Japan where it is marketed as the ASHNITE process. It is used in over 80 MSW combustion or ash processing facilities in Japan.

Phosphate combines with over 30 elements to form about 300 naturally-occurring minerals.[6,7] Metal phosphates are ubiquitous secondary minerals in the oxidized zones of lead ore deposits and as assemblages around ore bodies.[7] They also occur in soils, sediments, and phosphatic beds.[7] As such, they are stable with respect to pH, Eh, and mineral diagenesis. Isomorphic substitutions are very common for both divalent cations (e.g. Pb^{2+} for Ca^{2+}) and oxyanions (e.g. AsO_4^{3-} for PO_4^{3-}) in these minerals.[7]

Past research efforts have shown that phosphate minerals are likely controlling solids for Ca^{2+}, Cd^{2+}, Cu^{2+}, Pb^{2+} and Zn^{2+} in natural soil systems.[8,9,10,11,12,13] The use of PO_4^{3-} to immobilize metals has been advocated for industrial wastewaters[14,15] and lead-contaminated soils.[13,16,17,18,19,20] Both phosphate-containing minerals and soluble phosphate have been advocated as sources of PO_4^{3-}.

In the case of phosphate-containing minerals as a PO_4^{3-} source, the ongoing work by Traina's group[4,16,17,18,19,20] has explored apatites (e.g. calcium hydroxyapatite, $Ca_5(PO_4)_3OH$) or waste phosphate rock as a source of PO_4^{3-} to precipitate Pb^{2+} from solution or in contaminated soils as lead hydroxypyromorphite ($Pb_5(PO_4)_3OH$); a more thermodynamically stable isostructural analogue to calcium hydroxyapatite.[4]

In the case of soluble phosphate as a PO_4^{3-} source, chemical stabilization mechanisms can involve a continuum from surface sorption processes to existing or newly formed particulate surfaces in a waste material, through the formation of new surface precipitates, to the formation of discrete heterogeneous or homogeneous precipitates.[21] Spectroscopic and geochemical modeling techniques exist to help distinguish between sorption and the various forms of precipitation (e.g. surface, heterogeneous, homogeneous).[22,23,24,25]

When soluble phosphate is used to stabilize metals in waste materials containing appreciable concentrations of Ca^{2+}, it is useful to understand Ca^{2+} and PO_4^{3-} crystallization and precipitation chemistry as this reaction sequence is likely to dominate the system. When Ca^{2+} and PO_4^{3-} are titrated in solution, a variety of phases form.[26,27] In a simple system, the reaction sequence generally involves $Ca_9(PO_4)_6$ (non-stoichiometric amorphous calcium phosphate), $CaHPO_4 \cdot 2H_2O$ (brushite); $CaHPO_4$ (monetite); $Ca_8H_2(PO_4)_6 \cdot 5H_2O$ (octacalcium phosphate), β-$Ca_3(PO_4)_2$ (whitlockite); and ultimately $Ca_5(PO_4)_3OH$ (calcium hydroxyapatite); the most geochemically stable calcium phosphate.[28] The sequence is influenced by ion activity products (IAPs), pH, ionic strength, reaction kinetics, the presence of precursor substrates or "seed", and the presence of inhibitors like Mg^{2+}.[26,27,29]

This reaction sequence is useful in interpreting likely immobilization mechanisms in Ca^{2+}- containing waste materials treated with PO_4^{3-}. There is evidence for relatively fast sorption processes onto calcium hydroxyapatite at low metals concentration for Cd^{2+}, Cu^{2+}, Pb^{2+}, and Zn^{2+}.[15,30,31,32] At higher metals concentration, evidence of surface precipitation on the calcium hydroxyapatite is observed; more so for Pb^{2+} and less so for Cd^{2+} and Zn^{2+}.[5,33] In systems where Pb^{2+} is present in high concentrations in solution, evidence is given that less stable calcium hydroxyapatite will dissolve and preprecipitate as more stable lead hydroxypyromorphite.[4,5,16,17,18,19,20] In systems where all components are initially soluble, it is simple to precipitate lead hydroxypyromorphite[7,10] or ternary metal apatites where Pb^{2+}, Cd^{2+}, Cu^{2+}, and Zn^{2+} isostructurally substitute for Ca^{2+} and form solid solutions like $(Ca, Pb, Zn)_5(PO_4)_3OH$.[34,35]

Dry scrubber residue is a particulate material from the use of dry lime powder (CaO) or dried slaked lime powder ($Ca(OH)_2$) in the scrubbing of flue gas from combustion of municipal solid waste. This is the second largest residual stream for modern waste to energy facilities.[36] The residue contains high concentrations of acid gas scrubber products (e.g. $CaCl_2$, $CaSO_4$), unreacted scrubber material (CaO or $Ca(OH)_2$), condensed semivolatile elements (e.g. Cl^-, Pb^{2+}), condensed volatile elements (e.g. Na^+, K^+, Hg^{2+}, Zn^{2+} and Cd^{2+}), aluminosilicate fly ash particles, and char.[37] The fine-grained residue is highly soluble and very alkaline, making it sometimes difficult to treat or dispose.[36]

The approach taken by our group to understand stabilization mechanisms and identify reaction products formed during treatment of scrubber residues is shown in Figure 1. A variety of spectroscopic and geochemical modeling procedures are used as each provides specific and complementary information and because some suffer from small databases relative to the more exotic mineral phases found in granular waste materials.

This study was designed to determine the mechanisms and reaction products of chemical stabilization of dry scrubber residues treated with soluble orthophosphate. The data gleaned from various spectroscopic analyses, leaching procedures, and geochemical modeling show that precipitation/solid solution formation rather than sorption is the immobilization mechanism and that apatite minerals and solid solutions are the principal solubility-controlling reaction products. As in nature, these minerals are geochemically stable and very insoluble.

These results hold promise for the industry. Knowledge about the basic mechanisms of immobilization allows for further optimization of the process. Successful identification of reaction products using both spectroscopic and geochemical modeling techniques provides confidence for the use of geochemical models as predictive tools for refining treatment formulations, examining long term disposal behavior, and developing management strategies. Research is also ongoing by our group on soluble phosphate treatment mechanisms in MSW bottom ash, MSW ash vitrification dusts, smelter dusts, electric arc furnace dusts, and mine tailings.

METHODS

Combustor Description

A 1,500 ton per day mass burn facility was sampled. It consists of two parallel units comprised of reciprocating grates, water wall boilers, scrubber venturis, and $Ca(OH)_2$ scrubbers with fabric filters. Activated carbon is used as a mercury sorbent; it is injected with the lime. It was operational during sampling.

Sampling occurred over the period from January 3rd to January 7th, 1995. Dry scrubber residue was collected by plant personnel. A grab sample (1 kg) was collected every 10 minutes to make a 4 hour daily composite from one of the scrubber transfer conveyors. The five daily composites were made into a weekly composite using a clean, lab-scale cement mixer.

Processing

For the purposes of this study, an experimental laboratory-scale treatment formulation was selected to ensure that stabilization reaction mechanisms and reaction products could be detected. A standard industrial grade H_3PO_4 acid solution was used. The treatment formulation involved using a dose of 1.2 moles H_3PO_4 per kg of residue. Process mixing water at a liquid to solid (L/S) ratio of 0.4 was used to facilitate mixing. The residues were mixed for 10 minutes in a Hobart mixer and then air dried. The mixing regime is similar to full scale treatment systems. The treated working sample was subsampled for subsequent analyses; the subsample was stored under vacuum desiccation until use.

Total Composition

The dry scrubber residues were quantified for over 47 elements using neutron activation analysis (NAA) for all elements except Pb, Cu, P, S, C and O. Procedures are provided elsewhere.[38,39,40] X-ray fluorescence (XRF) was used for Pb, Cu, S, and P analyses. X-ray photoelectron spectroscopy (XPS) was used to quantify C and O (see below).

STEM-XRM

STEM-XRM was used to examine discrete particle morphology and determine elemental composition and possible mineral formula in discrete particles of the treated and unleached as well as the treated and leached fractions. STEM examinations were conducted on a Hitachi H-600 TEM operated at 100 kV accelerating voltage.

SIMS

SIMS was used to elucidate the stabilization mechanism. The method was used to depth profile selected atomic masses ($^{40}Ca^+$, $^{208}Pb^+$, $^{31}P^+$, $^{35}Cl^+$, $^{28}Si^+$) so as to examine concentration as a function of particle depth (particle exterior to interior). This would provide evidence of possible surface adsorption or surface precipitation or evidence of new discrete phase precipitation.[24]

A Fisons/VG SIMSLAB I (upgraded) quadrapole filter type mass analyzer was used to conduct positive ion (+m/z) depth profiling using an O_2^+ ion beam source. Profiles were conducted at high vacuum (10^{-9} torr). Indium foil was used for sample mounting to minimize charging. Generally, the ion source was operated at 10 keV and 20 nA. Target biases were usually 5-15V. The profiles were done at 200x with the extractor operated at 1,500 V. Estimated sputtering rates were roughly 1 to 10 Å per second. Profiles for $^{208}Pb^+$, $^{31}P^+$, $^{40}Ca^+$, $^{28}Si^+$, $^{35}Cl^+$, and $^{113}In^+$ were usually conducted for 45 minutes to 1 hour.

XRPD

XRPD was used to identify crystalline mineral phases in the residues. A Rigaku-Geigerflex goniometer was used along with a copper X-ray source (45 kV, 35 mA, 1500 W). A divergence slit of 1°, a scattering slit of 1°, a receiving slit (crystal) of 0.8°, and a receiving slit (monochromator) of 0.6° were used. Details on search-match procedures are provided elsewhere[38].

MAS-NMR

MAS NMR was used to monitor the ^{31}P isotropic chemical shifts and chemical shift anisotropy tensors of the component species in the treated and unleached as well as the treated and leached fractions. The

spectra were taken on a 400 MHz Chemagnetics Infinity NMR spectrometer with a 9.4 Tesla magnet corresponding to a ^{31}P NMR frequency of 161.9 MHz. The samples were spun in 7.5 mm (OD) zirconia rotors in a double resonance probe at spin rates between 1 to 7 kHz at a temperature of about 23 ± 2 °C. The magic angle was set by observing the chemical shift of the aromatic resonance of hexamethyl-benzene. The spin rate was measured with a fiberoptic sensor and is accurate to ±2 Hz. All spectra were recorded with proton decoupling while using 10 μs 90° ^{31}P pulses (except where noted); pulse lengths were calibrated by observing the ^{31}P resonance of $NH_4H_2PO_4$ (ammonium dihydrogen phosphate). The recycle delay was set to 10 s based on approximate ^{31}P T_1 measurements of some of the samples. The number of scans acquired ranged from 500 to 4,000. Chemical shifts were referenced to an external standard sample of $NH_4H_2PO_4$.; (δ (^{31}P) = 0 ppm with respect to 85% H_3PO_4.[41]

The analysis of ^{31}P NMR spectra of inorganic phosphates is generally done by a consideration of both the isotropic chemical shift and the individual chemical shift tensor elements (principal axis system). These values are obtained from the ^{31}P NMR spectrum using the graphical method of Herzfeld and Berger[42] or by a Simplex and gradient search method.[43] The latter was used here as it is optimized for multiple component systems.

XPS

A Perkin Elmer Physical Electronics Division 5100 hybrid XPS was used to identify and quantify possible chemical phases as well as to quantify elements in the samples. Detailed methods are provided elsewhere.[38] For energy referencing, the entire system was calibrated to the gold 84.0 $4f_{7/2}$ binding energy. Correction for peak shift due to static charge buildup on the sample was achieved through the adventitious carbon reference method using a C 1s binding energy of 284.8 eV as a conducting reference.[44] Details on full width, half maximum values used for curve fitting[45,46,47] as well as spectral deconvolution are provided elsewhere[38].

Leaching Apparatus

All leaching tests were conducted in leaching apparatus maintained in a laminar flow hood (Envirco, Houston, Texas) with Type 2 HEPA air filters (>0.3 μm). The apparatus is comprised of parallel units; each consisting of a 1000 ml Teflon leaching vessel with a screw cap, a stir plate, a stir bar, and constant temperature bath (25°C). Each vessel was maintained at a constant pH using a Cole-Parmer pH/ORP Controller (Model 5652-10). The controller opens and closes solenoids allowing the introduction of strong acid (3N HNO_3) or base (3N NaOH). The set points on the controller allowed for a ±0.1 pH variation around a target value.

Total Availability Leaching Procedure

The procedure is based on the Dutch Total Availability Leaching test NEN 7341.[48] It was used to quantify the elemental mass fraction available for leaching. The method can assess what fraction of the total concentration of an element is leachable over geologic time (1,000-10,000 years). During the extraction, all readily soluble and marginally soluble minerals will solubilize. Desorption of tightly sorbed species will also occur. Details are provided elsewhere[38].

After filtration the leachates were combined. The sample was then split for metals analysis (graphite furnace and flame atomic absorption spectrophotometry,), anions analysis (ion chromatography), and alkalinity determinations (titration).[49,50,51] Additionally, the weight of the leached residue was determined for mass balance purposes. Residues were dried for 72 hours at 60°C to obtain a dry weight measure.

pH-Dependent Leaching

The pH-dependent leaching procedure is a means of determining the equilibrium leaching behavior over a range of pH values. Each extraction was done at a L/S ratio of 10.0 so as to ensure solid phase control. Eighty grams of sample were placed into the Teflon vessel to which 800 mls of distilled, deionized water was added. 3N HNO_3 was used to control the pH at various set points 4,6,8 for 24 hours. This pH range corresponds to values expected for both regulatory leaching tests and open CO_2(g) leaching systems (e.g. landfills). The leachates were filtered and analyzed as described above. Additionally, Pb^{2+} was determined using isotope dilution procedures and thermal ionization mass spectrometry after ion exchange concentration.[52] PO_4^{3-} was also determined by using a Lachat low level colorimetric assay.[53]

Leaching Modeling

The geochemical equilibrium model MINTEQA2[54] was used to determine which solid phase controlled leachate composition as a function of pH. The thermo.dbs and type6.dbs databases for MINTEQA2 were modified to include a large number of phosphate mineral phases shown in Table 1. Modeling details are provided elsewhere[38].

The likelihood of solid solution formation during dissolution and reprecipitation required further modification to the MINTEQA2 databases to allow for idealized solid solutions to act as possible controlling solids. A simplistic zero heat of mixing and ideal site substitution model was assumed.[59,60] Standard free energies of formation for the solid solutions ($\Delta G^\circ_{f,ij}$) between end members i and j were used to determine theoretical K_{sp} values for the solid solutions using:

$$\Delta G^\circ_{f,ij} = x\Delta G^\circ_{f,i} + (1-x)\Delta G^\circ_{f,j} + nRT\,[x \ln x + (1-x) \ln (1-x)] \quad (1)$$

where x is the mole fraction of end member i, $\Delta G^\circ_{f,i}$ and $\Delta G^\circ_{f,j}$ are the free energies of formation of end members i and j, respectively, n is the number of sites in the mineral undergoing substitution (e.g. 1.0), R is the universal gas constant, and T is degrees Kelvin. K_{sp} values for hypothetical binary ideal solid solutions [e.g. for (Ca,Pb), (Ca,Cu), (Ca, Cd), and (Ca, Zn)] for the minerals $Ca_3(PO_4)_2$, $Ca_5(PO_4)_3OH$, $Ca_5(PO_4)_3Cl$, and $Ca_4O(PO_4)_2$ (Pb and Ca only) were calculated and entered into the MINTEQA2 databases. No attempts were made to evaluate the likelihood of these solid solutions with respect to theoretical (e.g. $K_{sp,i}/K_{sp,j}$) or experimental distribution coefficients.

RESULTS AND DISCUSSION

Total Composition

Table 2 provides information on the total elemental composition of the dry scrubber fabric filter residue as determined by NAA, XRF, and XPS. The major constituents (> 10,000 mg/kg) in the fabric filter residue were O, Ca, Cl, C, Si, Al, S, Na, and Zn. Minor constituents (1,000-10,000 mg/kg) included K, Ti, Fe, Mg, Pb, and Br. Trace constituents (< 1,000 mg/kg) included Cd, Cr, Hg, and many other elements. These concentrations are fairly typical for MSW dry scrubber fabric filter residues.[36] The presence of small quantities of activated carbon as a mercury sorbent may explain the relatively high C concentrations as well as the relatively high Hg concentrations in the residues. The concentrations of S, Pb, Cd, Cu, and Zn are in typical ranges for these wastes.[36] The observed phosphorus concentration, 2,100 mg/kg, is within the range of reported values (1,700 to 4,600 mg/kg) for untreated scrubber residues.

Particle Composition Based on STEM-XRM

Table 3 contains the atomic percent data generated from the analysis of discrete particle assemblages with STEM-XRM. Analyses were conducted on 10 assemblages for both the treated unleached and the treated and leached fractions. Particles were polycrystalline and small (100-5,000 nm). A wide variety of elements were observed in the residues. For the treated and unleached residues, O, Ca and Cl were very common elements. Mg, Al, Si, P, S, and K were also present. No Fe, Zn or Pb was observed. For the treated and leached residues, O, Al, P, S, Ca, Fe and Zn were very common elements. Mg, Si, Cl and K were also observed. Leaching appeared to have increased the relative concentration of many elements, particularly Al, P, Fe and Zn. This occurred because of the relative loss of Cl, K and Ca.

It is very likely that given the very small particle sizes that were interrogated (100 to 5,000 nm) as well as the complex structure of the polycrystalline particles, discrete homogeneous single crystals were not analyzed. The determination of molecular formulas from the data proved tedious and inconclusive.

It is important to note that the elements that were observed are many of the major and minor elements seen in the residues with total compositional analyses. Further, the elemental complexities of the assemblages agrees in principal with the types of phases observed with other methods like XRPD and XPS (see below). Finally, virtually all of the assemblages contained phosphorus; particularly in the leached residues. This is viewed favorably with respect to the availability of the stabilization agent to all particles at the nanometer scale under the mixing regime that was used.

Stabilization Reaction Mechanism Based on SIMS

Figure 2a shows typical depth profiles for the mineral standard $Ca_5(PO_4)_3Cl$ (calcium chloroapatite; Harvard University Mineralogical Museum 107354) which was ground to very small particle sizes (<50 μm). This control sample represents a "homogeneous precipitate". As can be seen in the figure, $^{40}Ca^+$, $^{31}P^+$ and $^{35}Cl^+$ were relatively constant with depth (up to depth less than or equal to 0.5 μm). The background indium foil signal is also relatively constant. As expected, the homogeneous particulate gave a rather uniform depth profile for all of its constituents.

Figure 2b shows typical depth profiles for the treated and unleached fraction (other fraction mass fragment depth profiles are not shown). The profiles are similar to the calcium chloroapatite standard. Elements were uniformly distributed with depth. More $^{31}P^+$ was present in the treated residue than in the chloroapatite. The $^{113}I^+$ and $^{28}Si^+$ profiles did not change significantly with depth (up to less than or equal to 0.5 μm).

The use of ion mass fragment ratios is more illustrative of relative behaviors as a function of depth. $^{40}Ca^+$ is used to normalize the data. As shown in Figure 2c, the $^{31}P^+/^{40}Ca^+$ ratios in the chloroapatite, treated and unleached fraction and the untreated and unleached fraction were similar. The $^{31}P^+/^{40}Ca^+$ ratio was relatively constant with depth. These ratio profiles are similar to ones reported by Fulghum et al.[24] for the coprecipitate. They differ markedly from the adsorbed scenario. This suggests that the stabilization process produced a homogeneous precipitate. Stabilization via surface sorption was not likely. The leached residues showed clear enrichment of P relative to Ca in the particle surface. This is ascribed to preferential loss of Ca and salts during leaching at pH 4.0 in the Total Availability Leaching test. Though resorption of PO_4^{3-} cannot be ruled out at pH 4.0, the other spectroscopic techniques (particularly XPS) also showed clear loss of calcium in the outer particle surfaces during leaching.

The $^{208}Pb^+/^{40}Ca^+$ ratios showed similar, though less dramatic behavior, to the $^{31}P^+/^{40}Ca^+$ ratios as a function of depth. As shown in Figure 2d, the leached samples were surface enriched in $^{208}Pb^+$ while the

unleached samples showed uniform distribution as a function of depth. Contrary to PO_4^{3-} resorption, Pb^{2+} will not readily sorb at pH 4 so the data support the theory that the surface enrichment is an artifact of Ca salt loss during leaching. Similar behaviors were seen with the untreated and leached residues, though heterogenaity at the nm level was less than heterogenaity with depth.

These results strongly suggest that stabilization of Ca^{2+} and Pb^{2+} is largely via PO_4^{3-}- based precipitation and not by surface sorption processes. The former reaction mechanism is more geochemically stable and resistant to leaching than the later mechanism. However, it is also likely that at a smaller spatial scale level, some sorption processes are occurring. There are other techniques that can be employed to verify the presence or absence of sorption processes.[22,25] However, sorption isotherms, desorption assays, and isotopic exchange experiments are problematic with respect to the highly soluble nature of these residues. The use of SIMS is just one spectroscopic technique that was used in elucidating reaction mechanisms.

Phosphate Crystalline Phase Identification Based on XRPD

Table 4 contains possible phosphate crystalline phases that were identified in each of the four fractions using the computerized search-match routine. As stated above, the list is extensive and it is unlikely that all the listed phases are present. In the untreated and unleached residues, a few apatite family minerals (e.g. $Ca_5(P,Si,S)O_{12}(Cl,OH,F)$, chlorellestadite and $Ca_{10}(PO_4)_3(CO_3)_3(OH)_2$, carbonate apatite) and $CaHPO_4$ (monetite) are observed. This is likely given the presence of phosphorus in the untreated residue. These phases are generally absent after leaching. After treatment with the soluble phosphate, a large number of potential phosphate mineral phases are observed, including apatite family minerals (e.g. $Ca_5(P,Si,S)O_{12}(Cl,OH,F)$, $Ca_{10}(PO_4)_3(CO_3)_3(OH)_2$), tertiary metal phosphates (e.g. α- $CaZn_2(PO_4)_2$, $Zn_3(PO_4)_2$), and more complex phosphate minerals. Ca, Al, Zn, Fe, K, Pb, and Cd phosphate minerals are seen. Particularly noteworthy minerals for Pb are $Pb_4O(PO_4)_2$, and two apatite-family minerals: $Pb_5(PO_4)_3OH$ (lead hydroxypyromorphite), and $KPb_4(PO_4)_3$. After leaching, many of the same phosphate minerals remain; indicating their relative stability to aggressive leaching environments.

^{31}P Chemical Environment Based on MAS-NMR

The treated and unleached and treated and leached spectra are found in Figure 3a and 3b, respectively. Table 5 summarizes the data from the Herzfeld-Berger (deGroot program[43]) analysis of the spectra.

The ^{31}P MAS NMR spectrum of the treated and unleached fraction was acquired at 2,4 and 6 kHz spin rates. The faster spin rates enable better detection of small differences in the isotropic chemical shift, while the slower spin rates yield more sidebands and should, in principal, be easier to fit. One problem that can be encountered is an isotropic chemical shift that occurs at the same frequency as the sideband from another resonance. This did not occur (see Table 5), but a fit of the 6 kHz data with a two component model showed a convergence to an isotropic chemical shift at the spinning sideband of a neighboring resonance leading us to discount the two component model for the 6 kHz data. The spectra for the 2 and 4 kHz data were both filled to two component models (see Figure 3a for the 4 kHz data); the quality of the fit was better for the 4 kHz data based on the smaller residual.

The closest match between the 4 kHz major component in the treated and unleached spectrum and likely calcium phosphate minerals[61] appears to be with a mixture of minerals with isotropic chemical shifts near 0 ppm. A mixture containing $CaHPO_4 \cdot 2H_2O$ (brushite), $CaHPO_4$ (monetite), $Ca_5(PO_4)_3OH$ (calcium hydroxyapatite), and α-$CaZn_2(PO_4)_2$ would lead to a good match with the major component with central transitions near 0 ppm and $|\Delta\delta|$ from 27 to 103 ppm. These minerals were detected by both

XRPD and XPS (see below). The three calcium phosphates also belong to the generalized Ca-phosphate precipitation reaction sequence.[28]

The closest match between the 4 kHz minor component in the treated and unleached spectra and likely calcium phosphate minerals[61] is $Ca_2P_2O_7$ or another pyrophosphate (e.g. $Na_4P_2O_7$). The minor component has a very large $|\Delta\delta|$ of 181 ppm. To our knowledge, this is one of the largest ^{31}P chemical shift anisotropies seen, and it indicates a distorted coordination geometry at phosphorus with non-ideal O-P-O bond angles. This conclusion is based on the correlation of $|\Delta\delta|$ with O-P-O bond angle as reported by Oldfield and coworkers.[62]

The ^{31}P MAS NMR spectrum of the treated and leached fraction (Figure 3b) was acquired at 6 kHz. A two component fit was used with some residuals present. Based on the intensity of the ^{31}P signal and the spectral side band intensity; it is obvious that the four likely major components were susceptible to aggressive leaching during the Total Availability Leaching test at pH 4.

The closest match between the 6 kHz major component in the treated and leached spectrum and likely calcium phosphate minerals[61] is $CaHPO_4 \cdot 2H_2O$ (brushite), a mineral also seen by MAS-NMR in the treated and unleached fraction (see Table 5). The closest match between the 6 kHz minor component in the treated and leached spectrum and likely calcium phosphate minerals[61] is $Ca_2P_2O_7$; a mineral also seen by XPS.

Crystalline and Amorphous Surface Phosphate Phases Based on XPS

As shown in Table 6, there are a number of crystalline phosphate phases found in the surface layers of the residues. In the untreated and unleached fraction, only a few phases were identified. After leaching, and with subsequent improvement in detection limit, some small quantities of apatite family (e.g. $Ca_5(PO_4)_3OH$, $Ca_5(PO_4)_3Cl$) and tertiary metal phosphate ($Ca_3(PO_4)_2$, $Pb_3(PO_4)_2$) minerals were seen. However, after treatment with the PO_4^{3-}, significant quantities of numerous Ca and Na phases were seen; including $Ca_5(PO_4)_3OH$, $Ca_5(PO_4)_3Cl$, $Ca_2P_2O_7$, $Ca_8H_2(PO_4)_6 \cdot 5H_2O$, $CaHPO_4$, Na_3PO_4, and $Na_4P_2O_7$. A number of the Ca-phosphates from the generalized Ca-phosphate precipitation reaction sequence[28] were seen (e.g. $Ca_8H_2(PO_4)_6 \cdot 5H_2O$, $CaHPO_4$, and $Ca_5(PO_4)_3OH$). After leaching of the treated residues, these same Ca-phosphate phases were still seen at high levels; suggesting resistance to solubilization at pH of 4. The principal Pb phase that was observed in the treated and leached fraction was chloropyromorphite ($Pb_5(PO_4)_3Cl$).

Total Availability Leaching Behavior

The total availability leaching data for the untreated and treated residues are shown in Table 7. The table contains data on the concentration of the analytes in the leachate (not corrected for added weight of treatment additives) and a calculated stabilization fraction (corrected for added weight of treatment additives). The calculated stabilization fraction examines the percentage of the total available fraction in the untreated residue that was immobilized by the treatment process.

The dose of 1.2 moles of H_3PO_4 per kg of residue reduced the leachability of Al (75.5%), Ba (27.7%), Ca (6.8%), Cd (37.5%), Cl (7.7%), Cu (57.9%), Pb (99.5%) and Zn (28.2%). The larger reduction in Pb leaching agrees with the insoluble phases seen with XRPD and XPS.

The treatment increased the leachability of As (-3.8%), Hg (-3,979%), Mg (-19.9%), Si (-97.5%), and PO_4^{3-} (-2,385%). The Hg data reflect large changes in a very small leachate concentration number. The Mg and As data reflect likely substitution reactions (Ca for Mg, PO_4^{3-} for AsO_4^{3-}). The increased Si

concentrations reflect the dissolution of aluminosilicates by acid attack (H_3PO_4 addition). It is also clear that either not all of the PO_4^{3-} was reacted or that some of the phases that formed were not the most thermodynamically stable ones at the pH of the Total Availability Leaching Test.

The stabilization agent has a clear positive impact on the reduction of leaching of many divalent cations (Pb^{2+}, Cd^{2+}, Cu^{2+}, Zn^{2+}) in general agreement with the formation of insoluble phases which were seen with the various spectroscopic methods. These phases are insoluble and geochemically stable even under aggressive leaching conditions.

pH Dependent Leaching and Geochemical Modeling

Particular attention is given here to the components Ca^{2+} and Pb^{2+}, although similar behaviors were seen for Cd^{2+}, Cu^{2+} and Zn^{2+}. The leaching of $Ca^{2+}$and Pb^{2+} is shown in Figures 4 and 5, respectively. Each of the figures depicts pH-dependent leaching of the untreated and treated residues as well as the leachate concentrations in the modeled leachates when potential controlling solids were individually introduced as infinite solids in the model at each pH. As infinite solids, the candidate mineral dictates the activity of its components in the leachate in response to system pH and to all attendant aqueous phase complexation reactions. Table 8 identifies the top few controlling solids (based on their saturation indices) that were initially identified as well as other solids of interest; some of which were used as candidate infinite solids.

Ca^{2+} shows a clear reduction in leaching over the entire pH range after treatment (Figure 4a). As shown in Table 8, there are a number of phases that were excellent candidates as controlling solids; particularly $CaHPO_4$ (monetite) and $CaHPO_4 \cdot 2H_2O$ (brushite). These were seen with XRPD, MAS-NMR and XPS in the treated residues whereas anhydrite and gypsum were less prevalent. As infinite solids, monetite and brushite each are able to depict Ca^{2+} leaching in the treated residues (Figure 4b). Despite their high saturation indices, $Ca_5(PO_4)_3Cl$ (calcium chloroapatite) and $Ca_5(PO_4)_3OH$ (calcium hydroxyapatite) (Figure 4c) both describe the general shape and pH-trend for Ca^{2+} leaching from the treated residues. While these phases were seen with XRPD, XPS, and MAS-NMR in the treated residues; they may be less suitable, but still plausible candidates for controlling solids.

The pH-dependent leaching of Pb^{2+} shows 1 to 2 log reduction in leaching after treatment (Figure 5a). As with Cu^{2+} and Cd^{2+}, a few candidate phases may control at each of the pH values (Figure 5b). These phases include apatite and tertiary metal phosphates ideal solid solutions (e.g. $(Pb_2,Ca)(PO_4)_2$, $(Pb,Ca_4)(PO_4)_3Cl$). The end member $Pb_5(PO_4)_3Cl$ (chloropyromorphite) is a controlling solid (Figure 5c) and is present in the treated and leached fraction. $PbHPO_4$ is also not a likely candidate.

Stabilization Reaction Pathway Kinetics and Products

The typical "ideal" solution phase reaction sequence when PO_4^{3-} is titrated into a Ca-salt solution involves the sequential formation of $Ca_9(PO_4)_6$ (non-stoichiometric amorphous calcium phosphate), $CaHPO_4 \cdot 2H_2O$ (brushite), $CaHPO_4$ (monetite), $Ca_8H_2(PO_4)_6 \cdot 5H_2O$ (octacalcium phosphate), and then $Ca_5(PO_4)_3OH$ (hydroxyapatite); the thermodynamically most stable reaction product.[28] This sequence of nucleation and crystallite growth from supersaturated solutions is dependent upon system pH, temperature, the presence of "seed" crystals or catalytic surfaces, and reaction kinetics.[26] Intermediates are typically "active", geochemically labile, and dependent upon reaction kinetics. Under ideal conditions, hydroxyapatite is the most thermodynamically stable end product over a fairly wide pH range (e.g. 4 to above 8).[26]

The more complex stabilization system studied here is similar in principal to the one just described. PO_4^{3-} is titrated into a Ca-salt dominated waste. While the L/S ratio is much less than the "ideal" system, there is evidence that the same reaction sequence is observed here. The minerals brushite, monetite and calcium hydroxyapatite were seen in the treated residues with XRPD, MAS-NMR or XPS. Data also suggest that the initial 10 minute mixing scenario at pH values above 12 was not sufficient time to allow for complete conversion of all Ca-phosphates to apatites. Not only were intermediaries seen, but subsequent paragenic transformations occurred during the seven hours of the Total Availability Leaching test at pH 7 and then 4. To optimize the stabilization process, more process water and longer reaction times might be preferred. Nevertheless, despite the short reaction times, significant reductions in metals leachability and formations of more stable reaction products were seen. For instance, the dissolution of calcium hydroxyapatite in the presence of Pb^{2+} and the subsequent formation of "mature" lead chloropyromorphite can take place on the order of minutes to hours provided liquid-to-solid ratios are high and pH is in the neutral region.[17,18,19,20]

The pH-dependent leaching modeling shows that for Cd^{2+}, Cu^{2+},Pb^{2+} and Zn^{2+}; ideal solid solutions of Ca-apatites (both hydroxyapatite and chloroapatite) and whitlockite were found to adequately describe pH-dependent leaching. Neither Ca-apatites nor whitlockite controlled Ca^{2+} leaching; yet these phases were detected with XRPD, XPS, and MAS-NMR; particularly the highly substituted apatite mineral chlorellestadite. It may be reasonable to assume that the solid solutions that were found to control leaching (e.g. $(Cd, Ca_4)(PO_4)_3OH$; $(Cu, Ca_4)(PO_4)_3OH$, $(Pb, Ca_4)(PO_4)_3OH$) were in fact present and controlling leaching but that the degree of isostructural substitution was small enough as to not interfere with their detection using crystallographic or nearest-neighbor spectroscopic signatures.

This is consistent with the premise that major-minor cation solid solutions limit the concentration of the minor component to levels below saturation of the minor cation end member.[63] Formation of these types of solid solutions allows for the "burial" of the minor cation in the Ca-apatites or whitlockite. These solid solutions can be easily formed from saturated solutions[34,35] and it is reasonable to infer that this process occurred here.

The very small particle sizes of the reaction products as seen with STEM (100-5,000 nm) suggests that Ostwald ripening processes must also be considered. Nanometer-sized crystallites are many orders of magnitude more soluble than larger, ripened crystals.[28] Such phenomenon have been theorized[64] and modelled[65,66] for Ca-phosphates. At crystallite sizes less than 500 nm, particle interfacial tensions increase solubilities exponentially.[28,68] It is therefore also possible that some of the positive saturation indices seen for some of the major cation end members could be explained by incomplete ripening and overly "active" small crystal solubilities. If this is the case, then, the allowance for longer reaction times and more process water would ensure crystallite growth, aggregation, and maturation. This would help further decrease equilibrium leachate concentrations of Cd^{2+}, Cu^{2+}, Pb^{2+}, and Zn^{2+} and further increase the fraction stabilized during treatment.

Implications for the Waste-to-Energy Industry

Chemical stabilization of dry scrubber residue using soluble phosphate is an effective means of immobilizing divalent metals in the waste. The treatment process holds promise for the industry. Knowledge about the fundamental immobilization mechanism allows for further optimization of the process. Successful identification of geochemically stable and insoluble reaction products using numerous spectroscopic methods confirms the role of the apatite mineral family as the dominant reaction product. Geochemical modeling also showed the importance of these minerals in controlling leaching of divalent metals. Such modeling techniques can be used as predictive tools for refining treatment

formulations, examining long term disposal behavior of treated residues, and developing management strategies for the treated residues.

CONCLUSIONS

The use of soluble orthophosphate as a heavy metal chemical stabilization agent was evaluated for a calcium-based scrubber residue from the combustion of municipal solid waste. At an experimental dose of 1.2 moles of H_3PO_4 per kg of residue, the reduction in the fraction available for leaching (using the Total Availability Leaching test) is 38% for Cd, 58% for Cu, 99% for Pb and 28% for Zn. pH-dependent leaching (pH 4,6,8) showed that the treatment was able to reduce equilibrium concentrations by 0.5 to 3 log units for many of these metals; particularly Pb. Numerous spectroscopic techniques were used to identify stabilization reaction mechanisms and reaction products both prior to and after Total Availability Leaching. Depth profiling of particles with secondary ion mass spectroscopy (SIMS) suggests that stabilization is by discrete heterogeneous phases precipitation rather than by adsorption. Scanning transmission electron microscopy/x-ray microanalysis (STEM/XRM), x-ray powder diffraction (XRPD), magic angle spinning-nuclear magnetic resonance (MAS-NMR), and x-ray photoelectron spectroscopy (XPS) suggest that the insoluble metal phosphate reaction products are small (nm-sized) crystalline and amorphous precipitates and that calcium phosphates, tertiary metal phosphates, and apatite family minerals are dominant reaction products. Observed phases include $CaHPO_4 \cdot 2H_2O$ (brushite), $CaHPO_4$ (monetite), β-$Ca_3(PO_4)_2$ (whitlockite), $Ca_5(PO_4)_3OH$ (hydroxyapatite); $CaZn_2(PO_4)_2$; and $Pb_5(PO_4)_3Cl$ (lead chloropyromorphite); many of which are geochemically stable. The geochemical thermodynamic equilibrium model MINTEQA2 was modified to include both extensive phosphate minerals and ideal divalent cation binary solid solutions for modeling solid phase control of leaching. Both end members (e.g. $CaHPO_4$, $CaHPO_4 \cdot 2H_2O$) and ideal solid solutions (e.g. $(Pb,Ca_4)(PO_4)_3Cl$, $CaZn_2(PO_4)_2 \cdot 2H_2O$) were seen to act as controlling solids for Ca^{2+}, Zn^{2+}, Pb^{2+}, Cu^{2+}, and Cd^{2+}. The formation of solid solutions is both plausible and highly likely in this system and describes a mechanism whereby minor cation components (e.g. Cd^{2+}, Cu^{2+}, Pb^{2+}, Zn^{2+}) are "buried" in the precipitating calcium phosphate reaction product. However, issues related to Ostwald ripening and small reaction product particle size may also explain some of the observed leaching behavior. Soluble phosphate is an effective stabilization agent for divalent metal cations in waste materials such as scrubber residues.

ACKNOWLEDGEMENTS

This work was supported by a research contract from Wheelabrator Environmental Systems Inc. and Kurita Water Industries Ltd. We thank Nan Collins, Dr. Henri Gaudette and Dr. Ted Loder of UNH; Dr. Milenko Markovic of NIST; George Bruno of AMRAY Inc.; Dr. Sheldon Landsberger and Dr. Wesley Wu of the University of Illinois at Champaign-Urbana; Brian Hart of the University of Western Ontario; Rusty Foster and Bud Berry of Resource Laboratories Inc.; and Tim Wilson of Eastern Analytical Inc. for their assistance in this effort. The financial support for the Analytical Shared Experimental Facility at the Center for Materials Science and Engineering at MIT comes from NSF grant DMR90-22933.

LITERATURE CITED

1. T.T. Eighmy, S.F. Bobowski, T.P. Ballestero, M.R. Collins, in "Theoretical and applied methods of lead and cadmium stabilization in combined ash and scrubber residues," Proceedings of the Second International Conference on Municipal Solid Waste Combustor Ash Utilization, W.H. Chesner, T.T. Eighmy, Eds., UNH Press, Durham, N.H., 1990, pp 275-314.

2. T.T. Eighmy, B.S. Crannell, J.R. Krzanowski, J.D. Eusden, L.G. Butler, F.K. Cartledge, E. Emery, E.L. Shaw, C.A. Francis, "Fundamental mechanisms of phosphate stabilization in granular waste materials," Abstract ANYL 186, 211th ACS National Meeting, New Orleans, Louis., March 24-28, 1996.

3. T.T. Eighmy, B.S. Crannell, J.R. Krzanowski, J.D. Eusden, L.G. Butler, F.K. Cartledge, E. Emery, E.L. Shaw, C.A. Francis, "The use of surface analysis and geochemical modeling to describe leaching behavior in chemically-stabilized particulate waste residues," Abstract 169, 70th Colloid and Surface Science Symposium, Clarkson University, Postdam, N.Y., June 16-19, 1996.

4. V. Laperche, P. Gaddam, S.J. Traina, "Immobilization of lead by apatite," Abstract GEOC 087, 211th ACS National Meeting, New Orleans, Louis., March 24-28, 1996.

5. J. Wright, J. Conca, T. Moody, X. Chen, "Immobilization of metals using apatite minerals: precipitation or sorption?," Abstract GEOC 088, 211th ACS National Meeting, New Orleans, Louis., March 24-28, 1996.

6. W.L. Lindsay, and P.L. Vlek, Minerals in Soil Environments; J.B. Dixon, Ed. Soil Science Society of America, Madison, Wisconsin, 1977. pp 639-672.

7. J.O. Nriagu, Phosphate Minerals; J.O. Nriagu, P.B. Moore, Eds. Springer-Verlag: Berlin, 1984, pp 318-329.

8. W.L. Lindsay and E.C. Moreno, "Phosphate phase equilibria in soils," Soil Sci. Soc. Amer. Proc., 24: 177-182 (1960).

9. J.J. Jurniak and T.S. Inouye, "Some aspects of zinc and copper phosphate formation in aqueous systems," Soil Sci. Soc. Amer. Proc., 26: 144-147 (1962).

10. J.O. Nriagu, "Lead orthophosphates. IV: formation and stability in the environment," Geochim. Cosmochim. Acta., 38: 887-898 (1974).

11. J. Santillan-Medrano and J.J. Jurinak, "The chemistry of lead and cadmium in soil: solid phase formation," Soil Sci. Soc. Amer. Proc., 39: 851-856 (1975).

12. J.J. Street, W.L. Lindsay and B.R. Sabey, "Solubility and plant uptake of cadmium is soils amended with cadmium and sewage sludge," J. Environ. Qual., 6: 72-77 (1977).

13. M.V. Ruby, A. Davis and A. Nicholson, "In situ formation of lead phosphates in soils as a method to immobilize lead," Environ. Sci. Technol., 28: 646-654 (1994).

14. J.O. Nriagu, "Lead orthophosphates.II: stability of chloropyromorphite at 25°C," Geochim. Cosmochim. Acta., 37: 367-377 (1973).

15. Y. Takeuchi and H. Arai, "Removal of coexisting Pb^{2+}, Cu^{2+} and Cd^{2+} ions from water by addition of hydroxyapatite powder," J. Chem. Eng. Japan, 23: 75-80 (1990).

16. V. Laperche, S.J. Traina, P. Gaddam and T.J. Logan, "Chemical and mineralogical characterizations of Pb in a contaminated soil: reactions with synthetic apatite," Environ. Sci. Technol., 30: 3321-3326 (1996).

17. Q.Y. Ma, S.J. Traina, T.J. Logan and J.A. Ryan, "In situ lead immobilization by apatite," Environ. Sci. Technol., 27: 1803-1810 (1993).

18. Q.Y. Ma, T.J. Logan, S.J. Traina and J.A. Ryan, "Effects of NO_3^-, Cl^-, F^-, SO_4^{2-}, and CO_3^{2-} on Pb^{2+} immobilization by hydroxyapatite," Environ. Sci. Technol., 28: 408-418 (1994).

19. Q.Y. Ma, S.J. Traina, T.J. Logan and J.A. Ryan, "Effects of aqueous Al, Cd, Cu, Fe(II), Ni and Zn on Pb immobilization by hydroxyapatite," Environ. Sci. Technol., 28: 1219-1228 (1994).

20. Q.Y. Ma, T.J. Logan and S.J. Traina, "Lead immobilization from aqueous solutions and contaminated soils using phosphate rocks," Environ. Sci. Technol., 29: 1118-1126 (1995).

21. M.B. McBride, Environmental Chemistry of Soils, Oxford University Press, New York, 1990.

22. R.B. Corey, Adsorption of Inorganics at Solid-Liquid Interfaces, M.A. Anderson, A.J. Rubin, Eds. Ann Arbor Science, Ann Arbor, Michigan, 1981, pp 161-182.

23. K.J Farley, D.A. Dzombak and F.M.M. Morel, "A surface precipitation model for the sorption of cations on metal oxides," J. Colloid Interface Sci., 106: 226-242 (1985).

24. J.E. Fulghum, S.R. Bryan, R.W. Linton, C.F. Bauer and D.P. Griffis, "Discrimination between adsorption and coprecipitation in aquatic particle standards by surface analysis techniques: lead distributions in calcium carbonates," Environ. Sci. Tech., 22: 463-467 (1988).

25. G. Sposito, Geochemical Processes at Mineral Surfaces; J.A. Davis, K.F. Hayes, Eds. ACS, Washington, D.C., 1986, pp 217-228.

26. G.H. Nancollas, Phosphate Minerals; J.O. Nriagu, P.B. Moore, Eds. Springer-Verlag, Berlin, 1984, pp 137-154.

27. P. van Cappellen, and R.A. Bernier, Water-Rock Interaction; D. Miles Ed. Rotterdam, the Netherlands, 1989, pp 707-710.

28. J.W. Morse and W.N. Casey, "Ostwald processes and mineral paragenesis in sediments," Am. J. Sci., 288: 537-560 (1988).

29. J. Cristofferson, M.R. Christoffersen, W. Kibalczyc and F.A. Andersen, "A contribution to the understanding of the formation of calcium phosphates," Crys. Growth, 94: 767-777 (1989).

30. J.J. Middleburg and R.N.J. Comans, "Sorption of cadmium on hydroxyapatite," Chem. Geol., 90: 45-53 (1991).

31. D.N. Misra, R.L. Bowen and B.M. Wallace, "Adhesive bonding of various materials to hard tooth tissues. VII Nickel and copper ions on hydroxyapatite; role of ion exchange and surface nucleation," J. Colloid Interface Sci., 51: 36-43 (1975).

32. D.N. Misra and R.L. Bowen, Adsorption and Surface Chemistry of Hydroxyapatite; D.N. Misra, Ed. Plenum Press, New York, N.Y, 1984, pp 169-175.

33. Y. Xu, F.W. Schwartz and S.J. Traina, "Sorption of Zn^{2+} and Cd^{2+} on hydroxyapatite surfaces," Environ. Sci. Technol., 28: 1472-1480 (1994).

34. A. Panda, B. Sahu, P.N. Patel and B. Mishra, "Hydroxylapatite solid solutions: preparation, infrared and lattice constant measurements," Transition Met. Chem., 16: 476-477 (1991).

35. M. Pujari and P.N. Patel, "Strontium-copper-Calcium hydroxyapatite solid solutions: preparation, infrared, and lattice constant measurements," Solid State Chem., 83: 100-104 (1989).

36. International Ash Working Group (IAWG), Municipal Solid Waste Incinerator Residues. An International Perspective on Their Characteristics, Disposal, Treatment and Utilization, Summary Report, Netherlands Energy Research Foundation: Petten, the Netherlands, 1994.

37. T.T. Eighmy, J. Krzanowski, D. Domingo, D. Stämpfli, J.D. Eusden, Jr., K. Marsella, K. Killeen, H. Gardenier and J. Hogan, The Nature of Lead, Cadmium and Other Elements in Incineration Residues and Their Stabilized Products, U.S. EPA Final Report, U.S. Environmental Protection Agency, Washington, D.C. (in press).

38. T.T. Eighmy, J.D. Eusden, Jr., J.E. Krzanowski, D.S. Domingo, D. Stämpfli, J.R. Martin and P.M. Erickson, "A comprehensive approach towards understanding element speciation and leaching behavior in municipal solid waste incineration electrostatic precipitator ash," Environ. Sci. Technol., 29: 629- 646 (1995).

39. B.A. Buchholz and S. Landsberger, "Trace metal analysis of size-fractionated municipal solid waste incineration fly ash and its leachates," J. Environ. Sci. Health, A28: 423-441 (1993).

40. S. Landsberger, B.A. Buchholz, M. Kaminski and M. Plewa, "Trace Elements in Municipal Solid Waste Incineration Fly Ash," J. Radioanal. Nucl. Chem., 167: 331-340 (1993).

41. I.L. Mudrakovskii, V.P. Shmachkova, N.S. Kotsarenko and V.M. Mastikhin, "Phosphorus-31 NMR study of polycrystalline phosphates of group I-IV elements," J. Phys. Chem. Solids, 47: 335-339 (1986).

42. J. Herzfeld and A.E. Berger, "Sideband intensities in NMR spectra of samples spinning at the magic angle," J. Chem. Phys., 73: 6021-6030 (1980).

43. H.J.M. de Groot, S.O. Smith, A.C. Kolbert, M.M.L. Courtin, C. Winkel, J. Lugtenberg, J. Herzfeld and P.G. Griffin, "Iterative fitting of magic angle spinning NMR spectra," J. Magn. Reson., 91: 30-38 (1991).

44. T.L. Barr and S. Seal, "Nature of the use of adventitious carbon as a binding energy standard," J. Vac. Sci. Tech., A13: 1239-1246 (1995).

45. D. Briggs and M.P. Seah, Practical Surface Analysis, J. Wiley & Sons, Chichester, U.K., 1990.

46. J.F. Moulder, W.F. Stickle, P.E. Sobol, et al., Handbook of X-ray Photoelectron Spectroscopy, Perkin Elmer Corp., Eden Prairie, Minn, 1992.

47. C.J. Powell and M.P. Seah, "Precision, accuracy, and uncertainty in quantitative surface analyses by Auger-electron spectroscopy and x-ray photoelectron spectroscopy," J. Vac. Sci. Tech., A8: 735-763 (1990).

48. H.A. van der Sloot, D. Hoede and P. Bonouvrie, Comparison of Different Regulatory Leaching Test Procedures for Waste Materials and Constuction Materials, ECN-C-91-082, Netherlands Energy Research Foundation: Petten, the Netherlands, 1991.

49. U.S. EPA, Methods for Chemical Analysis of Water and Wastes, EPA-600/4-79-020, U.S. Environmental Protection Agency, Washington, D.C., 1979.

50. U.S. EPA, Test Methods for Evaluating Solid Waste-Physical/Chemical Methods, U.S. EPA SW846; U.S. Environmental Protection Agency, Washington, D.C., 1984.

51. American Public Health Association, Standard Methods for the Examination of Waters and Wastewaters, 16th ed., APHA, Washington, D.C., 1989.

52. G. Faure, Principles of Isotope Geology, John Wiley & Sons, New York, N.Y., 1986.

53. Lachat Instruments, Phosphate in Brackish Seawater, QuikChem Method 31-115-01-3-a, Lachat Instruments, Milwaukee, Wisconsin, 1994.

54. J.D. Allison, D.S. Brown and K.K. Novo-Gradac, MINTEQA2/PRODEFA2, A Geochemical Assessment Model for Environmental Systems: Version 3.0 User's Manual, Environmental Research Laboratory, U.S. Environmental Protection Agency, Athens, Georgia, 1990.

55. J.O. Nriagu, "Phosphate-clay mineral relations in soils and sediments," Can. J. Earth Sci., 13: 717-736 (1976).

56. P. Viellard and Y. Tardy, Phosphate Minerals; J.O. Nriagu and P.B. Moore, Eds. Springer-Verlag, Berlin, 1984, pp 171-198.

57. D.T. Rickard and J.O. Nriagu, The Biochemistry of Lead in the Environment; J.O. Nriagu, Ed. Elsevier/North-Holland Biomedical Press, Amsterdam, 1978, pp 219-284.

58. D.D. Wagman, W.H. Evans, V.P. Parker, R.H. Schumm, I. Halow, S.M. Bailey, K.L. Churney and R.L. Nuttall, "The NBS tables of chemical thermodynamic properties: selected values for inorganic and C_1 and C_2 organic substances in SI units," J. Phys. Chem. Ref. Data, 11(2): 2-1 - 2-392 (1982).

59. A. Davis, M.V. Ruby, M. Bloom, R. Schoof, G. Freeman and P.D. Bergstrom, "Mineralogical constraints on the bioavailability of arsenic in smelter-impacted soils," Environ. Sci. Technol., 30: 392-399 (1996).

60. H.J. Greenwood, Short Course in Application of Thermodynamics to Petrology and Ore Deposits; H.J. Greenwood, Ed. Mineralogical Association of Canada, Toronto, 1977, pp 38-46.

61. T.M. Duncan, A Compilation of Chemical Shift Anisotropies, Farragut Press, Madison, Wisconsin, 1990.

62. G.L. Turner, K.A. Smith, R.J. Kirkpatrick and E. Oldfield, "Structure and cation effects on phosphorus-31 NMR chemical shifts and chemical shift anisotropies of orthophosphates," J. Magn. Reson., 70: 408-415 (1986).

63. D. Langmuir, Aqueous Environmental Geochemistry, Prentice Hall, Upper Saddle River, New Jersey, 1997.

64. F.C. Smales, Tooth Enamel II, its composition, properties and fundamental structure; R.W. Fernhead and M.V. Stack, Eds. John Wright & Sons, Bristol, England, 1971, pp 187-191.

65. T.P. Feenstra and P.L. De Bruyn, "The Ostwald rules of stages in precipitation from highly supersaturated solutions: a model and its application to the formation of nonstoichiometric amorphous calcium phosphate precursor phase," J. Colloid Inter. Sci., 84: 66-72 (1981).

66. C.I. Steefel and P. van Cappellen, "A new kinetic approach to modeling water-rock interaction: the role of nucleation, precursors, and Ostwald ripening," Geochim. Cosmochim. Acta, 54: 2657-2677 (1990).

Table 1. Some Divalent Metal Phosphate Minerals and Their Solubility Products

Mineral Name	Dissolution Reaction		-Log K_{sp}	ΔG_f°	Reference
Apatites					
Hydroxyapatite	$Ca_5(PO_4)_3OH + H^+$	<=> $5Ca^{2+} + 3PO_4^{3-} + H_2O$	38.15	-6,279.0	(a)
Chloroapatite	$Ca_5(PO_4)_3Cl$	<=> $5Ca^{2+} + 3PO_4^{3-} + Cl^-$	46.89	-6,223.0	(b)
Hydroxypyromorphite	$Pb_5(PO_4)_3OH + H^+$	<=> $5Pb^{2+} + 3PO_4^{3-} + H_2O$	62.80	-3,774.0	(b)
Chloropyromorphite	$Pb_5(PO_4)_3Cl$	<=> $5Pb^{2+} + 3PO_4^{3-} + Cl^-$	84.43	-3,791.5	(b)
$Cd_5(PO_4)_3OH$	$Cd_5(PO_4)_3OH + H^+$	<=> $5Cd^{2+} + 3PO_4^{3-} + H_2O$	42.49	-3,924.0	(a)
$Cd_5(PO_4)3Cl$	$Cd_5(PO_4)_3Cl$	<=> $5Cd^{2+} + 3PO_4^{3-} + Cl^-$	49.66	-3,859.0	(b)
$Zn_5(PO_4)3$ OH	$Zn_5(PO_4)_3OH + H^+$	<=> $5Zn^{2+} + 3PO_4^{3-} + H_2O$	49.10	-4,309.0	(c)
$Zn_5(PO_4)_3Cl$	$Zn_5(PO_4)_3Cl$	<=> $5Zn^{2+} + 3PO_4^{3-} + Cl^-$	37.53	-4,137.0	(a)
$Cu_5(PO_4)_3OH$	$Cu_5(PO_4)_3OH + H^+$	<=> $5Cu^{2+} + 3PO_4^{3-} + H_2O$	51.62	-6,279.0	(c)
$Cu_5(PO_4)_3Cl$	$Cu_5(PO_4)_3Cl$	<=> $5Cu^{2+} + 3PO_4^{3-} + Cl^-$	53.96	-3,168.0	(a)
Tertiary Metal Phosphates					
Low Whitlockite	β-$Ca_3(PO4)_2$	<=> $3Ca^{2+} + 2PO_4^{3-}$	32.69	-3,884.8	(b)
$Pb_3(PO_4)_2$	$Pb_3(PO4)_2$	<=> $3Pb^{2+} + 2PO_4^{3-}$	44.36	-2,364.0	(d)
$Zn_3(PO_4)_2$	$Zn_3(PO4)_2$	<=> $3Zn^{2+} + 2PO_4^{3-}$	27.11	-2,633.4	(b)
$Cu_3(PO4)_2$	$Cu_3(PO4)_2$	<=> $3Cu^{2+} + 2PO_4^{3-}$	36.85	-2,051.6	(b)
$Cd_3(PO4)_2$	$Cd_3(PO4)_2$	<=> $3Cd^{2+} + 2PO_4^{3-}$	32.60	-2,456.3	(b)
$Mg_3(PO4)_2$	$Mg_3(PO4)_2$	<=> $3Mg^{2+} + 2PO_4^{3-}$	24.38	-3,538.8	(b)
Tetra Metal Phosphates					
Hilgenstockite	$Ca_4O(PO_4)_2 + 2H^+$	<=> $4Ca^{2+} + 2PO_4^{3-} + H_2O$	17.36	-4,588.0	(b)
$Pb_4O(PO_4)_2$	$Pb_4O(PO_4)_2 + 2H^+$	<=> $4Pb^{2+} + 2PO_4^{3-} + H_2O$	36.86	-2,582.8	(b)
Other Phosphate Minerals					
$AlPO_4$	$AlPO_4$	<=> $Al^{3+} + PO_4^{3-}$	17.00	-1,601.2	(b)
Monetite	$CaHPO_4$	<=> $Ca^{2+} + PO_4^{3-} + H^+$	19.09	-1,681.2	(e)
Brushite	$CaHPO_4 \cdot 2H_2O$	<=> $Ca^{2+} + PO_4^{3-} + 2H_2O + H^+$	18.93	-2,154.8	(b)
Cornetite	$Cu_3PO_4(OH)_3 + 3H^+$	<=> $3Cu^{2+} + PO_4^{3-} + 3H_2O$	5.94	-1,567.7	(c)
Libethenite	$Cu_2PO_4OH + H^+$	<=> $2Cu^{2+} + PO_4^{3-} + H_2O$	14.00	-1,204.9	(c)
Pseudomalachite	$Cu_5(PO_4)_2(OH)_4 + 4H^+$	<=> $5Cu^{2+} + 2PO_4^{3-} + 4H_2O$	19.83	-2,771.9	(c)
Corkite	$PbFe_3(PO_4)(OH)_6SO_4 + 6H^+$	<=> $Pb^{2+} + 3Fe^{3+} + PO_4^{3-} + SO_4^{2-} + 6H_2O$	28.66	-3,388.2	(c)
Spencerite	$Zn_4(PO_4)_2(OH)_2AlPO_4 \cdot 3H_2O + 2H^+$	<=> $4Zn^{2+} + 2PO_4^{3-} + 5H_2O$	24.77	-3,953.0	(c)
Zn Rockbridgite	$ZnFe_4(PO_4)_3(OH)_5 + 5H^+$	<=> $Zn^{2+} + 4Fe^{3+} + 3PO_4^{3-} + 5H_2O$	68.55	-4,799.0	(c)
Scholzite	$CaZn_2(PO_4)_2 \cdot 2H_2O$	<=> $Ca^{2+} + 2Zn^{2+} + 2PO_4^{3-} + 2H_2O$	34.10	-3,553.5	(c)
Tarbuttite	$Zn_2(PO_4)OH + H^+$	<=> $2Zn^{2+} + PO_4^{3-} + H_2O$	12.55	-1,621.7	(c)
Faustite	$ZnAl_6(PO_4)_4(OH)_8 \cdot 4H_2O + 8H^+$	<=> $Zn^{2+} + 6Al^{3+} + 4PO_4^{3-} + 12H_2O$	65.70	10,355.4	(c)
Plumbogummite	$PbAl_3(PO_4)_2(OH)_5 \cdot H2O + 5H^+$	<=> $Pb^{2+} + 3Al^{3+} + 2PO_4^{3-} + 6H_2O$	29.36	-5,108.7	(c)
Hinsdalite	$PbAl_3(PO_4)(SO_4)(OH)_6 + 6H^+$	<=> $Pb^{2+} + 3Al^{3+} + PO_4^{3-} + SO_4^{2-} + 6H_2O$	15.10	-4,753.0	(d)
Tsumebite	$CuPb_2(PO_4)(OH)_3 \cdot 3H_2O + 3H^+$	<=> $Cu^{2+} + 3Pb^{2+} + PO_4^{3-} + 6H_2O$	9.36	-2,478.6	(d)

[a] Estimated by method of Nriagu[55]
[b] Veillard and Tardy[56]
[c] Nriagu[7]
[d] Rickard and Nriagu[57]
[e] Wagman et al.[58]

Table 2. Total Elemental Composition for Dry Scrubber Residue

Element	Concentration mg/kg error	Element	Concentration mg/kg error
Ag	19.6 ± 0.3	Mn	385.9 ± 19.0
Al	29,600 ± 2,100	Mo	29.2 ± 3.5
As	46.0 ± 4.8	Na	14,500 ± 900
Au	0.25 ± 0.01	Nd	5.55 ± 0.79
Ba	449.3 ± 95	Ni	49.5 ± 8.4
Br	1,550 ± 130	O	~300,000
C	~70,000	P	2,100 ± 200
Ca	354,400 ± 11,400	Pb	1,990 ± 6
Cd	99.3 ± 6.8	Rb	26.9 ± 1.8
Ce	12.8 ± 0.4	S	19,800 ± 1,000
Cl	118,400 ± 6,000	Sb	473.5 ± 28.1
Co	9.43 ± 0.13	Sc	1.88 ± 0.02
Cr	131.8 ± 1.3	Se	3.07 ± 0.52
Cs	1.42 ± 0.08	Si	42,100 ± 4,900
Cu	362.1 ± 2.5	Sm	0.91 ± 0.09
Dy	1.53 ± 0.52	Sr	< 538
Eu	0.25 ± 0.04	Ta	0.36 ± 0.05
Fe	6,570 ± 107	Tb	< 0.13
Hf	2.26 ± 0.07	Th	1.93 ± 0.06
Hg	31.4 ± 0.3	Ti	6,090 ± 400
In	0.79 ± 0.07	U	< 1.80
I	25.6 ± 13.1	V	< 12.3
K	< 7,500	W	5.78 ± 0.72
La	6.83 ± 0.77	Yb	< 0.41
Mg	5,200 ± 1,700	Zn	11,770 ± 70
		Zr	125.5 ± 28.1

Table 3. Particle Atomic Concentrations (%) Based on STEM-XRM Analyses

Fraction	Particle Number	O	Mg	Al	Si	P	S	Cl	K	Ca	Fe	Zn	Pb
Treated and Unleached	1	39.1	-	13.1	-	-	-	30.2	-	17.6	-	-	-
	2	59.7	-	5.1	-	-	-	10.8	-	24.0	-	-	-
	3	78.3	-	-	-	-	9.9	0.3	-	11.5	-	-	-
	4	31.9	-	-	0.8	7.2	5.8	12.2	-	42.8	-	-	-
	5	42.0	2.4	3.3	6.3	4.2	2.3	13.5	1.1	19.2	-	-	-
	6	45.7	0.8	0.9	1.3	2.1	15.5	4.8	0.8	27 3	-	-	-
	7	32.0	0.6	5.6	0.5	0.8	1.9	-	-	58.0	-	-	-
	8	54.6	-	-	-	-	-	22.6	0.6	22.0	-	-	-
	9	55.9	-	-	-	-	-	21.6	-	22.6	-	-	-
	10	14.6	5.3	2.9	4.4	7.0	6.1	16.5	0.8	42.4	-	-	-
Treated and Leached	1	71.2	0.9	9.8	1.9	4.9	2.8	-	-	6.1	0.7	0.7	-
	2	40.1	0.8	-	-	19.9	3.6	-	-	31.3	1.5	2.2	-
	3	17.7	-	5.2	-	28.1	1.8	1.6	-	41.1	1.3	2.4	-
	4	40.2	-	14.8	16.9	13.8	-	-	-	7.9	1.4	3.0	-
	5	73.4	-	3.0	-	10.1	1.0	-	-	10.7	-	0.7	-
	6	62.3	-	9.5	0.5	13.9	1.0	-	-	7.1	1.3	1.6	-
	7	64.3	0.8	7.4	2.6	10.0	0.6	-	-	5.7	2.2	1.9	-
	8	51.8	-	12.5	-	19.5	0.9	-	-	5.6	7.2	1.4	-
	9	67.5	0.6	3.9	-	12.4	0.9	-	-	12.2	-	0.7	-
	10	54.1	-	19.0	18.3	-	-	-	1.5	-	-	-	-

Table 4. Possible Phosphate Crystalline Phases [and Range in FOM] in the Scrubber Residue Fractions Based on XRPD[a]

Element	Fraction			
	Untreated and Unleached	Untreated and Leached	Treated and Unleached	Treated and Leached
Ca	$Ca_5(P,Si,S)_3O_{12}(Cl,OH,F)$ [11.4-19.3] $Ca_5(PO_4)_3OH$ [16.6-17.6] $Ca_{10}(PO_4)_3(CO_3)(OH)_2$ [17.6-18.3] $CaHPO_4$ [17.5-22.9]	—	$Ca_5(P,Si,S)_3O_{12}(Cl,OH,F)$ [17.6] α-$CaZn_2(PO_4)_2$ [13.6-14.0] $Ca_{10}(PO_4)_3(CO_3)_3(OH)_2$ [14.1] $CaFe_{12}(PO_4)_8(OH)_{12} \cdot 4H_2O$ [13.3-13.4]	$Ca_3Mg_2(PO_4)_4$ [19.2-19.6] $Ca_3(PO_4)_2 \cdot xH_2O$ [14.4-16.6] α-$CaZn_2(PO_4)_2$ [12.7] $Ca_5(P,Si,S)_3O_{12}(Cl,OH,F)$ [15.5]
Al	—	$Al_2(PO_4)(OH)_3$ [16.3-17.2]	$AlPO_4$ [20.7-21.3]	$AlPO_4$ [15.0-21.1] $AlPO_4 \cdot xH_2O$ [11.0] $Al_2(PO_4)(OH)_3 \cdot H_2O$ [15.0]
Na	$NaAl_3(PO_4)_2(OH)_4 \cdot 2H_2O$ [11.8-17.4]	—	—	$NaAl_3(PO_4)_2(OH)_4 \cdot 2H_2O$ [11.3-16.9] χ-Na_3PO_4 [16.8-21.0] $NaCaPO_4$ [15.6-19.7] α-$NaMgPO_4$ [16.8-23.1]
Zn	—	—	$Zn_3(PO_4)_2 \cdot 2H_2O$ [17.5] $ZnHPO_4 \cdot H_2O$ [14.5-16.1]	$Zn_3(PO_4)_2$ [22.6]
Fe	—	—	$Fe_5(PO_4)_3(OH)_5 \cdot H_2O$ [21.1] $FePO_4 \cdot H_2O$ [15.5-17.4] $FePO_4$ [18.2-19.3] $(Fe,Mn)PO_4$ [17.1-18.9]	$Fe_5(PO_4)_4(OH)_2 \cdot 2H_2O$ [21.3] $Fe_3(PO_4)_2(OH)_2$ [18.2]
K	—	—	$KPb_4(PO_4)_3$ [16.0-18.4] $KPb_3(PO_4)_2(OH)_5 \cdot H_2O$ [13.2-16.4]	$KPb_4(PO_4)_3$ [11.7] $KPb_3PO_4(SO_4)_2$ [17.1]
Mg	—	$(Mg,Fe)_3(PO_4)_2(OH)_{1.5} \cdot 1.5H_2O$ [14.3-22.6]	—	—
Cu	—	—	—	$CuFe_2(PO_4)_2(OH)_2$ [14.9-17.5] $Cu_3(PO_4)(OH)_3$ [14.6-24.4]
Cd	$Cd_5(PO_4)_3Cl$ [11.0]	—	$Cd_3(PO_4)_2$ [17.9]	$Cd_5(PO_4)_3Cl$ [15.5] $Cd_3(PO_4)_2$ [22.1]

[a]Within any one element and fraction category, the possible mineral phases are listed vertically by decreasing likelihood of presence (based on average FOM).

Table 5. ^{31}P MAS NMR Data and Analysis

Fraction	Component	δ_{iso}	δ_{11}	δ_{22}	δ_{33}	$\lvert\Delta\delta\rvert$	% Comp	Probable Phases	Notes
Treated, Unleached	1	-0.30	-27.3	-1.5	27.9	42	45.8	-	2kHz[a]
	2	-1.43	-57.1	-9.8	62.6	96	54.2	-	
	1	-0.67	-36.5	-6.8	41.2	63	60.1	$CaHPO_4 \cdot 2H_2O$, $CaHPO_4$, $Ca_5(PO_4)_3OH$, α-$CaZn_2(PO_4)_2$	4kHz[a]
	2	-0.98	-104.4	-18.4	119.9	181	39.9	$Ca_2P_2O_7$	
	1	-0.8	-49.5	-10.8	57.9	88	100	-	6kHz[a]
Treated, Leached	1	-0.95	-62.1	-2.3	61.6	94	72.9	$CaHPO_4 \cdot 2H_2O$	6kHz[b]
	2	-9.16	-55.5	-55.4	83.5	139	27.1	$Ca_2P_2O_7$	

[a]Spectra acquired with 10 μs, 90° ^{31}P pulse
[b]Spectra acquired with 4 μs, 90° ^{31}P pulse

Table 6. Possible Phosphate Mineral Phases in the Scrubber Residue Fractions Based on XPS

Element	Fraction			
	Untreated and Unleached	Untreated and Leached	Treated and Unleached	Treated and Leached
Al[b]	(89,800 mg/Kg)	(178,700 mg/Kg)	(67,600 mg/Kg)	(106,500 mg/Kg)
	NA[c]	$AlPO_4$	$AlPO_4$	ND
Ca	(250,200 mg/Kg)	(42,700 mg/Kg)	(270,900 mg/Kg)	(135,100 mg/Kg)
	NA	$Ca_5(PO_4)_3OH$	$Ca_5(PO_4)_3OH$	$Ca(PO_4)_3OH$
		$Ca_5(PO_4)_3Cl$	$Ca_5(PO_4)_3Cl$	$Ca_5(PO_4)_3Cl$
		β-$Ca_3(PO_4)_2$	$Ca_2P_2O_7$	$Ca_2P_2O_7$
			$Ca_8H_2(PO_4)_6 \cdot 5H_2O$	β-$Ca_3(PO_4)_2$
			$CaHPO_4$	
Na	(57,700 mg/Kg)	(ND)[d]	(54,400 mg/Kg)	(ND)
	$Na_4P_2O_7$	-	Na_3PO_4	-
			$Na_4P_2O_7$	
O	(239,300 mg/Kg)	(502,100 mg/Kg)	(309,600 mg/Kg)	(398,000 mg/Kg)
	$Na_4P_2O_7$	NA	$Ca_5(PO_4)_3OH$	$Ca_5(PO_4)_3OH$
			$Ca_2P_2O_7$	$Ca_5(PO_4)_3Cl$
			$Na_4P_2O_7$	$Ca_2P_2O_7$
				$Pb_5(PO_4)_3Cl$
P	(ND)	(29,600 mg/Kg)	(34,900 mg/Kg)	(130,900 mg/Kg)
	NA	$AlPO_4$	$AlPO_4$	$Ca_5(PO_4)_3OH$
		$Ca_5(PO_4)_3OH$	$Ca_5(PO_4)_3OH$	$Ca_5(PO_4)_3Cl$
		$Ca_5(PO_4)_3Cl$	$Ca_5(PO_4)_3Cl$	$Ca_2P_2O_7$
		β-$Ca_3(PO_4)_2$	$Ca_2P_2O_7$	β-$Ca_3(PO_4)_2$
		$Pb_3(PO_4)_2$	$Ca_8H_2(PO_4)_6 \cdot 5H_2O$	$Pb_5(PO_4)_3Cl$
			$CaHPO_4$	
			Na_3PO_4	
			$Na_4P_2O_7$	
Pb	(16,000 mg/Kg)	66,600 mg/Kg)	(ND)	17,500 mg/Kg)
	NA	$Pb_3(PO_4)_2$	-	$Pb_5(PO_4)_3Cl$

[a] Phases are listed alphabetically by first element.

[b] Surficial concentrations of the element in the indicated fraction are shown; concentrations based on XPS analysis and standard sensitivity factors.

[c] NA; no phosphate species assigned.

[d] ND; element not detected.

Table 7. Total Availability Leaching Data

Constituent	Leachate Concentration, mg/L		% of Available Fraction Stabilized Because of Treatment[a]
	Untreated	Treated	
Al	5.0	1.1	75.5
As	0.030	0.028	-3.8
Ba	2.0	1.3	27.7
Ca	1,540	1,290	6.8
Cd	0.600	0.337	37.5
Cl	522	433	7.7
Cr	<0.04	<0.04	0.0
Cu	0.66	0.25	57.9
Fe	<0.04	0.26	-
Hg	0.0012	0.044	-3,979
K	42	39	-
Mg	21.9	23.6	-19.9
Na	51.5	46	0.6
Pb	2.3	0.01	99.5
PO_4^{3-}	0.05	20.9	-2,385
Si	40	71	-97.5
SO_4^{3-}	113	100	1.8
Zn	41.5	26.8	28.2
Mass	-	-	2.9

[a]Corrected for weight of H_3PO_4 added.

Table 8. Possible Controlling Solids and Their Saturation Indices

Component			pH		
			4	6	8
Ca^{2+}	Ranked	$CaSO_4$	0.11	-0.07	-0.04
		$CaHPO_4$	-0.03	-0.04	-0.49
		$CaSO_4 \cdot 2H_2O$	0.30	0.13	0.17
		$CaHPO_4 \cdot 2H_2O$	-0.21	-0.21	-0.66
	Other	$Ca_8H_2(PO_4)_6 \cdot 5H_2O$	-28.07	-10.38	-4.60
		β-$Ca_3(PO_4)_2$	-5.37	1.77	4.98
		$Ca_5(PO_4)_3OH$	-15.09	-2.48	4.26
		$Ca_5(PO_4)_3Cl$	-10.81	-0.31	4.41
Pb^{2+}	Ranked	$(Pb,Ca_4)(PO_4)_3Cl$	0.28	5.09	9.20
		$(Pb,Ca_4(PO_4)_3OH$	-6.40	0.46	6.52
		$(Pb_2,Ca)(PO_4)_2$	-3.74	-0.84	0.95
		$(Pb,Ca_2)(PO_4)_2$	-0.90	2.35	4.82
		$(Pb_3,Ca_2)(PO_4)_3OH$	-8.12	-1.62	3.77
	Other	$Pb_5(PO_4)_3OH$	-13.80	-8.37	-5.00
		$Pb_5(PO_4)_3Cl$	3.15	6.53	7.95
		$Pb_3(PO_4)_2$	-6.72	-4.19	-3.06
		$PbHPO_4$	-1.95	-2.31	-3.43

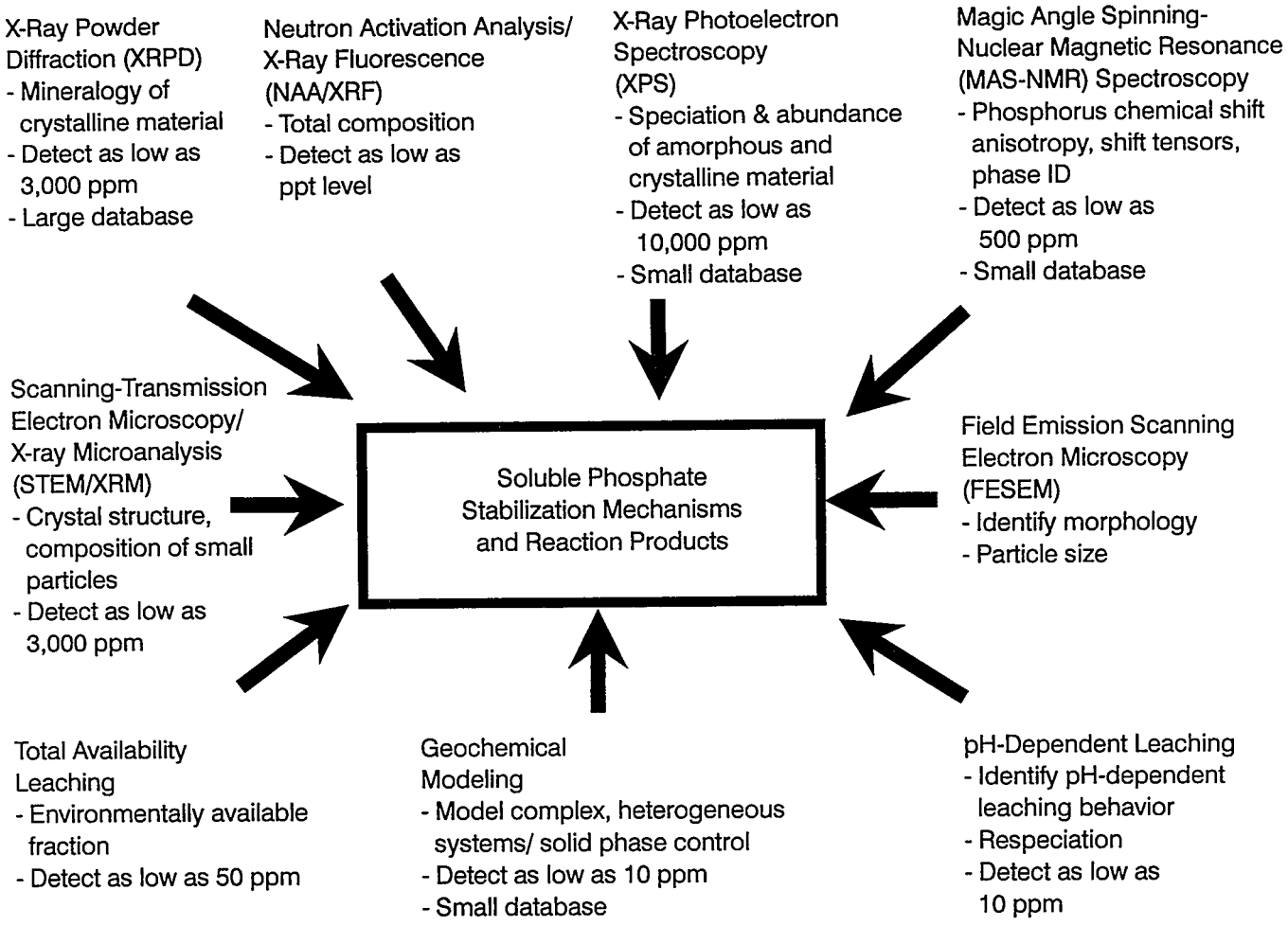

Figure 1. Schematic depicting approach used to identify stabilization reaction mechanisms and reaction products.

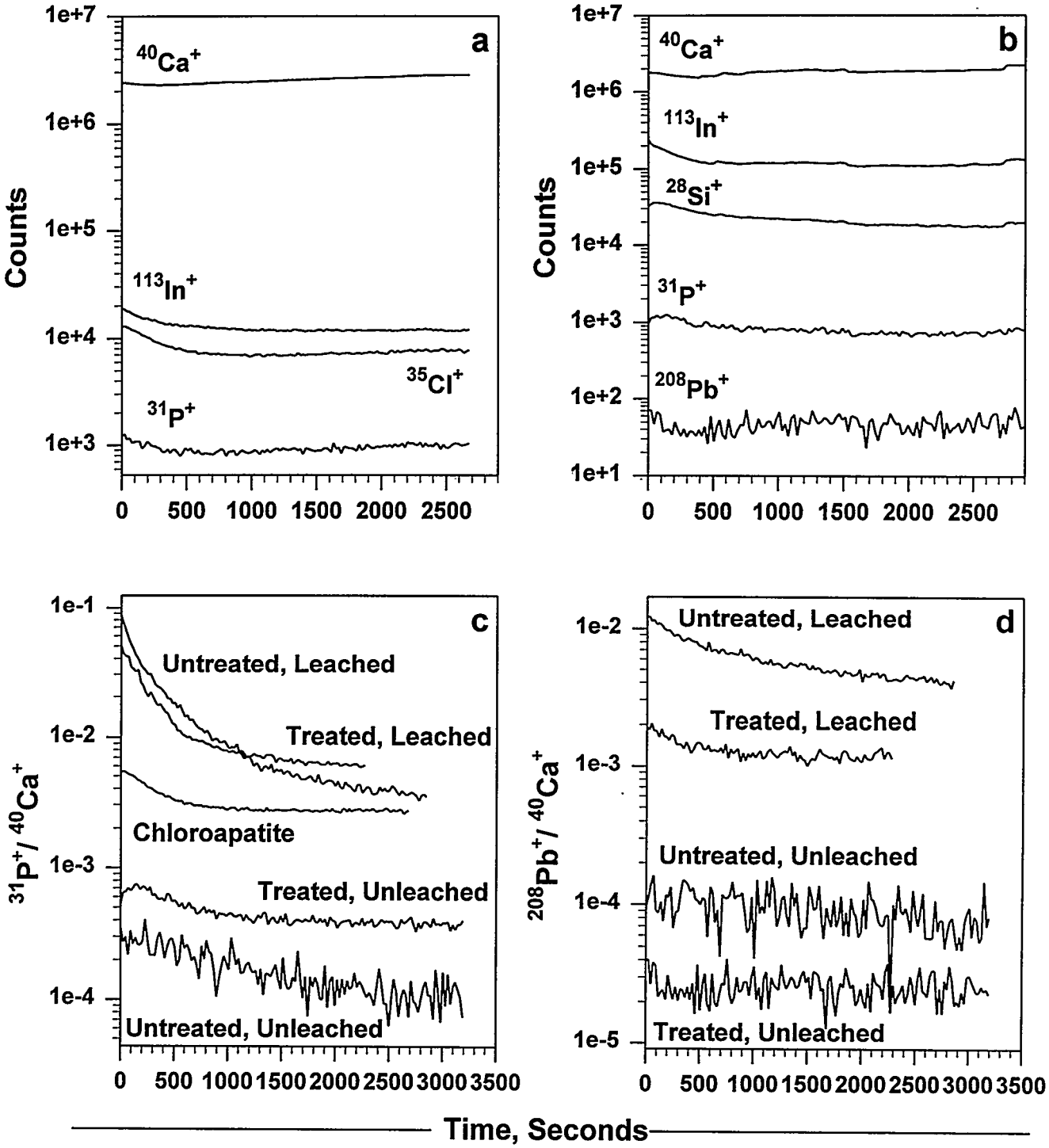

Figure 2. SIMS ion fragment depth profiles and ion fragment ratio depth profiles. (a) depth profiles for chloroapatite powder standard, (b) depth profiles for treated and leached fraction, (c) $^{31}P^+/^{40}Ca^+$ depth profiles, and (d) $^{208}Pb^+/^{40}Ca^+$ depth profiles.

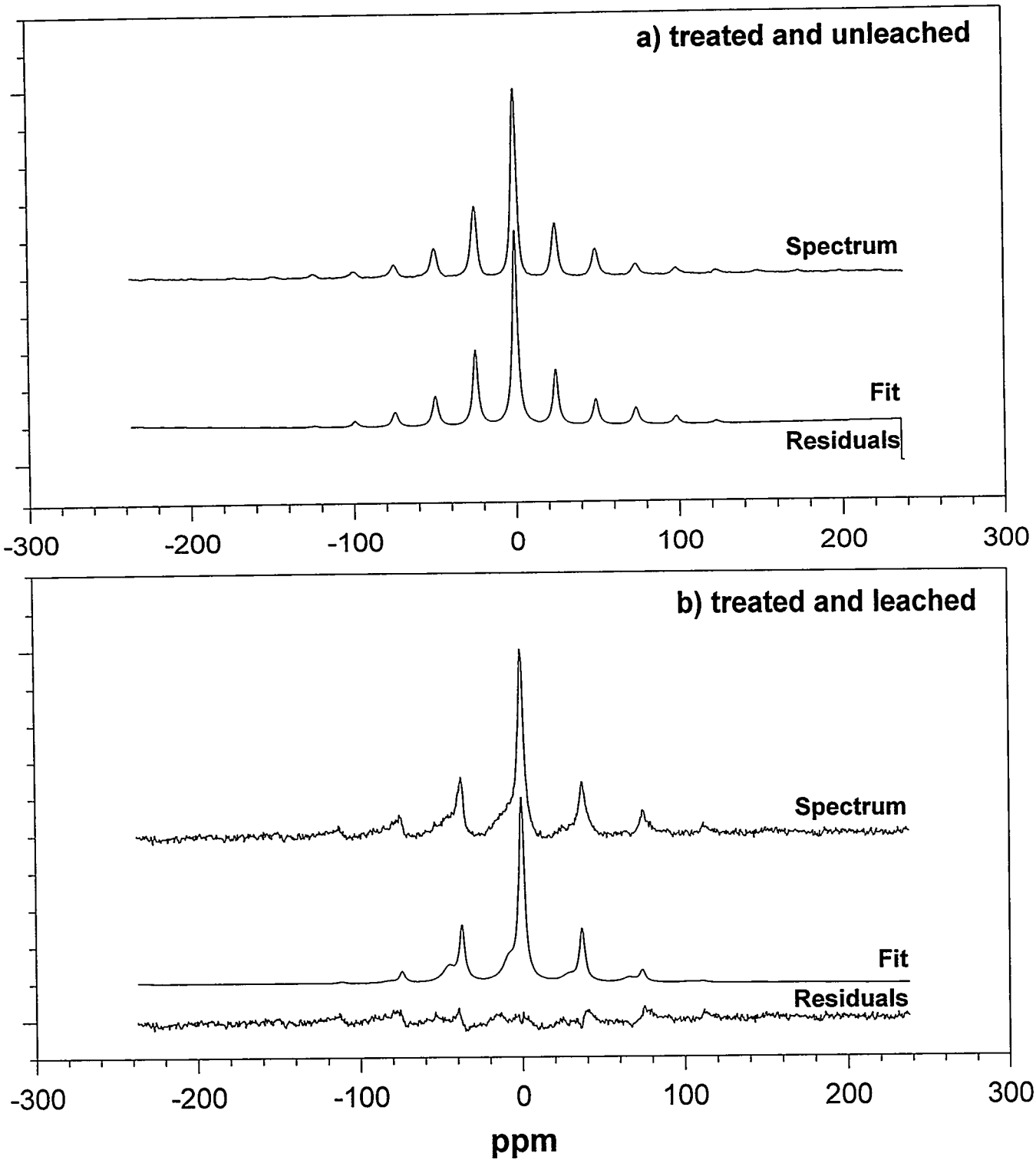

Figure 3. MAS-NMR spectra for (a) treated and unleached fraction and (b) treated and leached fraction.

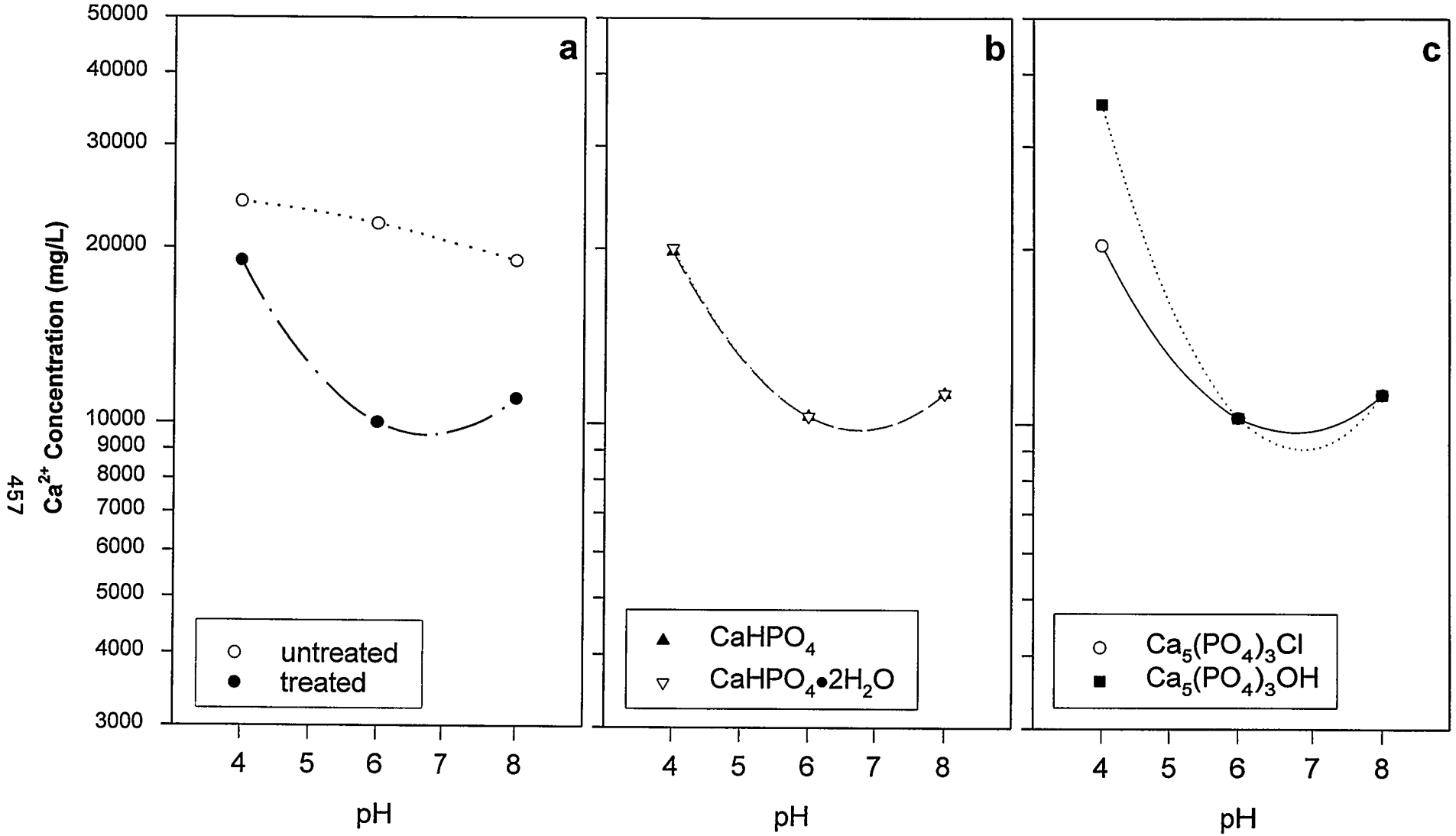

Figure 4. pH-dependent leaching plots for Ca^{2+}, (a) untreated and treated plots, (b),(c) selected infinite solids plots.

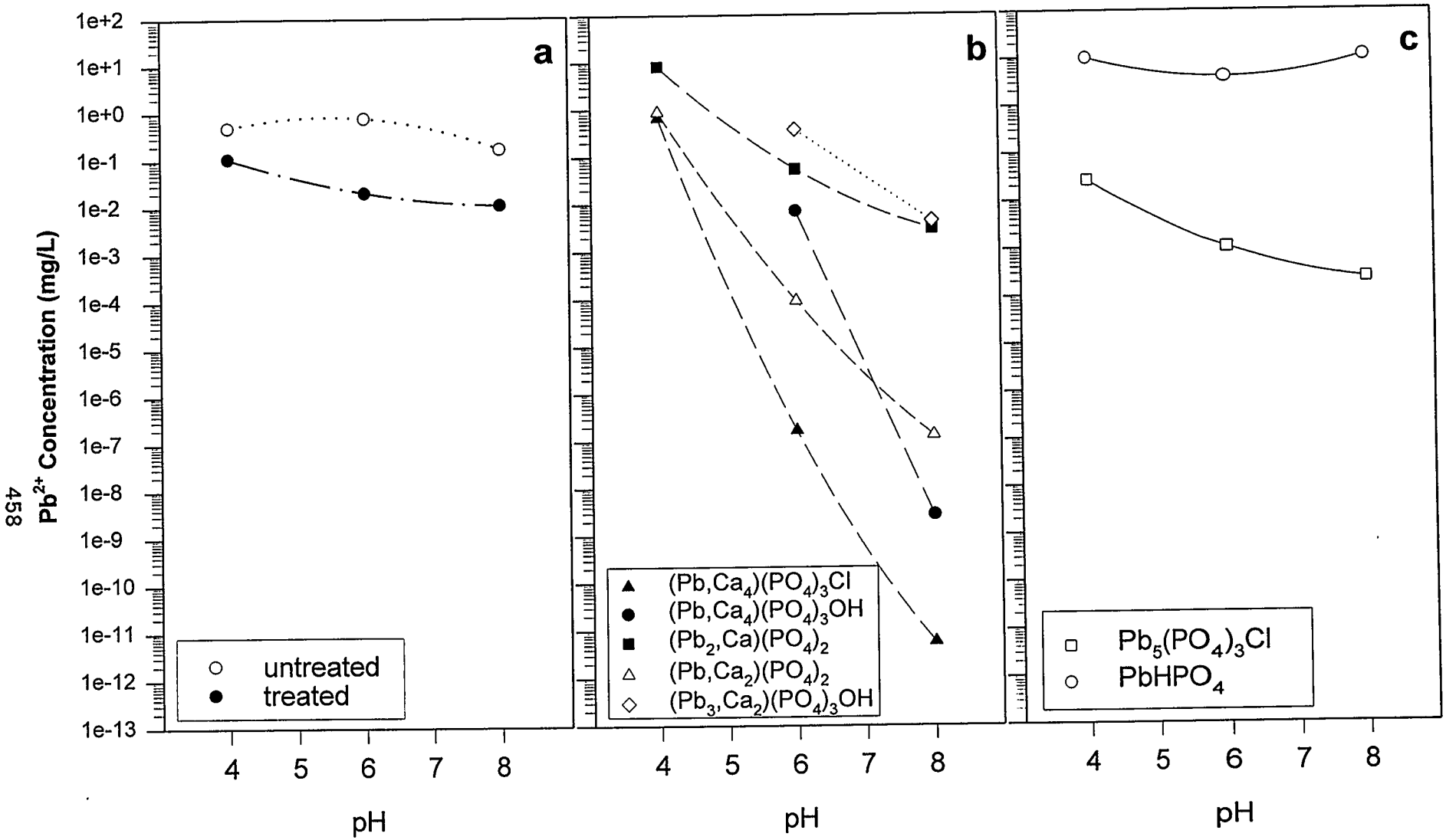

Figure 5. pH-dependent leaching plots for Pb^{2+}, (a) untreated and treated plots, (b),(c) selected infinite solids plot.

Fifth Annual North American Waste-To-Energy Conference (NAWTEC V)
April 22-25, 1997, Research Triangle Park, North Carolina, USA

A process for treatment of APC residues from municipal solid waste incinerators: Preliminary results

Ole Hjelmar and Henrik Birch
VKI
Agern Allé 11
DK-2970 Hørsholm
Denmark

INTRODUCTION

The problem of environmentally safe management of the residues from air pollution control (APC) systems at municipal solid waste (MSW) incinerators, particularly the residues from the semidry/dry acid gas cleaning processes (dry scrubber residues), has not yet been solved in a satisfactory and sustainable manner. These residues are in many cases simply stored indefinitely in big bags or they are landfilled under conditions that in the long term may not be able to prevent potentially harmful constituents from leaching and leaking into the environment. The APC residues, including fly ash, are in many countries classified as hazardous or special waste due to their high contents of soluble salts (particularly calcium chloride) and trace elements/heavy metals. The semidry/dry APC residues are strongly alkaline due to a content of excess lime, and the high pH favours the leaching of several contaminants, particularly lead.

This paper presents preliminary results of a study of a process for treatment of semidry/dry APC residues and fly ash from MSW incinerators. In the process the contaminants are partly removed, partly immobilized thus improving the above mentioned situation and allowing for subsequent safe management (i.e. utilization or landfilling) of the treated residues.

DESCRIPTION OF THE PROCESS

The primary objective of the study was to establish a treatment process which would render dry scrubber residue and fly ash from MSW incinerators acceptable for landfilling under sustainable conditions, i.e. without requiring total encapsulation or extended operation, management and aftercare. Another requirement was that any wastewater produced by the process should be treated in such a manner that it can be accepted for discharge into the sewer system or directly into a surface water body.

Numerous studies[1,2,3,4] have demonstrated that it is virtually impossible to achieve the above mentioned objectives at a reasonable cost through direct solidification/stabilization or thermal treatment of raw scrubber residue. One of the major reasons for this is that the dry scrubber residues typically contain 25 to 50 percent of readily soluble salts (mainly calcium chloride) which will leach relatively fast from the solid matrix resulting from many solidification/stabilization processes. Cement-based solidification/stabilization techniques generally create highly alkaline porewater which tends to mobilize amphoteric components such as lead and zinc that are present in significant amounts in raw scrubber residues. In many thermal treatment processes partial (re)evaporation of both the chlorides and some of the trace elements will cause problems. It has also been demonstrated that chemical stabilization of raw dry scrubber residue alone or as a component of combined ash may immobilize lead, cadmium and certain other constituents of the scrubber residues rather effectively[5,6,7]. One such example is the phosphate based WES-PHix ash stabilization process developed by Wheelabrator Environmental Systems Inc.[8] Since these processes focus only on immobilization of the trace elements/heavy metals, the salts are relatively unaffected by the treatment and will leach unhindered from the stabilized products after landfilling. The process described in this paper is also, in part, based on phosphate fixation of some of the trace elements, but it differs significantly from those mentioned above beacuse the additives are applied to an aqueous suspension of a washed product from which most of the soluble salts have been removed.

From an environmental perspective, a well buffered residue with a neutral to slightly alkaline pH in contact with water and a low content of soluble salts and leachable trace elements will often be preferable. The study described in this paper has been aimed at establishing a treatment process which is able to produce treated APC residues with such properties.

Since the presence of large amounts of readily soluble material in the dry scrubber residue is a major obstacle to the achievement of an acceptable result, the basic principle of the process developed in this study is removal of most of the soluble salts in an initial aqueous extraction of the residue followed by chemical stabilization of the extracted residue. The extraction and stabilization may be carried out simultaneously or in two (or more) separate stages. The latter is preferable since it ensures the most effective removal of salts from the product. Various extraction and treatment schemes have been investigated in laboratory and pilot scale. A pilot scale extraction unit was installed at an incinerator plant (KARA in Roskilde, Denmark) and used to test and partially optimize extraction and dewatering conditions (e.g. L/S, contact time, number of extraction steps, pH control vs. no control, addition of carbon dioxide). Trace elements were successfully removed from the extract by conventional methods (pH adjustment and TMT polishing). The salt containing treated extract may be discharged into a marine recipient or the salts (mainly calcium chloride) may be recovered. The solid remnant from the extraction was treated with various additives designed to immobilize specific trace elements, especially under conditions similar to those the treated residues may be expected to be subjected to in the future. The stabilization efficiency was tested and optimized using pH-static leaching procedures supported by hydrogeochemical modelling. The best performing stabilized residues were subjected to a more comprehensive test programme.

One of the most promising process configurations was a two-stage process in which the residue from a semidry APC process without precollection of fly ash was first extracted with water at a liquid to solid ratio (L/S) of approximately 3 l/kg in a continuously stirred tank. The slurry was then

passed through a filter press and the remnant collected on the filter was subsequently washed with an amount of water corresponding to L/S = 4.6 l/kg. The remnant was resuspended in an amount of water corresponding to L/S = 3.1 l/kg in a stirred tank, and an amount of phosphoric acid corresponding to approximately 35 kg H_3PO_4/ton of raw scrubber residue (dry weight basis) was added. Carbon dioxide was then added to the stirred suspension by means of a diffusor placed at the bottom of the tank and used to maintain a pH of 9.0 in the suspension for 2 hours. The suspension was then transferred to the filter press, washed with an amount of water corresponding to L/S = 3.2 l/kg and subsequently dewatered by compression in the filterpress. On a dry weight basis, the amount of washed residue from the first stage of the process corresponds to approximately 720 kg/ton of raw scrubber residue and the amount of final product corresponds to 746 kg/ton of raw scrubber residue. The initial raw scrubber residue, the washed filter cake from the first extraction and the final product were subjected to leaching tests in order to assess and compare their quality.

The primary purpose of adding carbon dioxide to the suspension is to lower the pH of the suspension and the final product without loosing alkalinity. The carbon dioxide reacts with the excess lime in the residue (relatively high in this particular scrubber residue = 15 percent, calculated as hydrated lime) to form calcium carbonate. The lower pH will lower the solubility of the amphoteric trace elements. Some of the trace elements may also form carbonates with low solubility. The addition of carbon dioxide alone (without phosphoric acid) produces a remnant with low leachability of many trace elements. If a full scale scrubber residue tretment facility is located at an incinerator plant, the carbon dioxide could be supplied by dispersing a sidestream of the flue gas through the suspended residue.

Although some test runs with recycling of washwater were performed, the water consumption has not been optimized. The total water consumption which corresponds to approximately 13.9 l/kg is too high and could probably be reduced to less than half that amount without significant changing the product quality. This is particularly important if there is a desire to recover the calcium chloride from the wastewater. The wastewater treatment process is comparable to the treatment processes normally used at wet scrubber systems. The sludge produced by the treatment of the wastewater from the process has relatively favourable landfilling properties.

PRELIMINARY RESULTS

The quality of the untreated scrubber residue, the washed residue and the treated scrubber residues was evaluated and compared in terms of leachability by subjecting each of the products to pH-static leaching tests at L/S = approximately 5 l/kg and 100 l/kg, respectively. Some of the residues were also subjected to a two-step serial batch leaching test at L/S = 0-2 l/kg and 2-10 l/kg, respectively.

The pH-static leaching tests were carried out by contacting the residues with the appropriate amounts of demineralized water in covered (but not sealed) vessels for 24 hours. A constant pH of 5, 6, 7, 8, 9, 10 and 11, respectively, was maintained automatically in 7 parallel tests at each L/S value by feedback control and addition of the necessary amounts of HNO_3 and NaOH. The material was kept in suspension by continuous stirring with a paddle. At the end of the contact period the suspensions were filtered through 0.45 μm filters and subjected to chemical analysis (most elements

were determined by ICP-MS or ICP-AES). The tests carried out at L/S = 5 l/kg provide information about the leching as a function of pH under conditions where several saturation phenomena are likely to occur, whereas the tests carried out at L/S = 100 l/kg represent the behaviour of the system when the conditions approach an availability controlled situation for many components.

The serial batch leaching test was carried out in accordance with the proposed European Standard compliance batch leaching test for leaching of granular waste materials and sludges, Procedure C (Draft European Standard prEN 12457[9]). The materials were leached with demineralized water in a closed bottle for 6 hours by end over end rotation at 10 rpm at L/S = 2 l/kg, the eluate was separated off by filtration through a 0.45 µm filter, new water was added to L/S = 8 l/kg and the leaching procedure was repeated for a period of 18 hours after which the second eluate was filtered. Both eluates were subsequently analyzed for the same parameters as the extracts from the pH-static tests. It is a requirement that the granular material to be tested must be < 10 mm and 90 % (w/w) must be < 4 mm. This requirement is of no concern in this case since all the residues consist of very fine particles (65 to 85 percent < 0.125 mm). This test in which the pH is controlled by the solid phase represents a more "natural" situation than the pH-static leaching tests. The results may with some caution be interpreted as two points on a curve describing the leaching from a landfill containing the tested material in terms of leachate composition or accumulated leached amounts of various components as a function of L/S (or, for a specific physical scenario, as a function of time).

Four residues were subjected to the pH-static leaching tests: The untreated scrubber residue (marked 57a), the washed residue (marked 51), a residue from a two-stage process in which the washed residue has been stabilized with carbon dioxide, but not with phosphoric acid (marked 69), and a residue from the previously described two-stage process in which the washed residue has been treated both with carbon dioxide and phosphoric acid (marked 70).

The results of the pH-static leaching at L/S = 5 l/kg are shown in figures 1a, 1b and 1c. The results of the pH-static leaching at L/S = 100 (data for the washed residue missing) are shown in tables 2a, 2b and 2c. The results of the serial batch leaching test are shown in table 3a and 3b for the untreated residue, the washed residue and the stabilized washed residue (CO_2 + H_3PO_4).

The results demonstrate the effect of the treatment on most contaminants, most notably lead, cadmium, chloride, sodium and potassium. Good results were obtained both with carbon dioxide alone and carbon dioxide and phosphoric acid. The phosphate is needed to minimize the leaching of lead at lower pH values. Only a few contaminants, particularly chromium, are mobilized by the treatment with phosphoric acid.

CONCLUSION

A process for treatment of dry scrubber residues from MSW incinerators have been developed and tested in pilot scale. The process involves an initial aqueous extraction followed by a resuspension and treatment of the filtercake with phosphoric acid and carbon dioxide to reach a stabilized product with highly improved leaching properties. The wastewater from the process may be discharged after treatment (pH adjustment and TMT polishing). Preliminary results of leaching tests performed on

untreated and treated residues are presented to demonstrate the effectiveness of the treatment process. Good results were obtained both with carbon dioxide alone and carbon dioxide and phosphoric acid. The phopshate is needed to minimize the leaching of lead at lower pH values.

ACKNOWLEDGEMENT

The work described in this paper was funded by the Danish Ministry of Energy, the Danish Ministry of Industry, KARA Roskilde, FLS Miljø A/S and VKI. The project was carried out by VKI, FLS Miljø A/S and KARA.

REFERENCES

1. D.S. Kosson, T.T. Kosson and H.A. van der Sloot, Evaluation of solidification/stabilization treatment processes for municipal waste combustion residues, CR 818178-01-0, U.S. Environmental Protection Agency, Risk Reduction Laboratory, Cincinnati, Ohio, USA,1993.

2. O. Hjelmar, "Municipal solid waste incinerator flue gas cleaning in Denmark: Residue properties and residue management options" in Proceedings of ISWA Pecialized conference on Incineration and biological Treatment, Amsterdam, The Netherlands, ISWA, 1992.

3. A.J. Chandler, T.T. Eighmy, J. Hartlén, O. Hjelmar, D.S. Kosson, S.E. Sawell, H.A. van der Sloot and J. Vehlow, Municipal solid waste incinerator residues, The International Ash Working Group (IAWG), Studies in Environmental Science 67, Elsevier, 1997.

4. S. Kullberg and A.-M. Fällman, "Leaching properties of natural and stabilized flue gas cleaning residues from waste incineration", in Proceedings of the International Conference on Municipal Waste Combustion, US EPA and Environment Canada, Hollywood, Florida, USA,1989.

5. T.T. Eighmy, S.F. Bobowski, T.P. Ballestero and M.R. Collins, "Theoretical and applied methods of lead and cadmium stabilization in combined ash and scrubber residues," in (W.H. Chesner and T.T. Eighmy, eds.) Proceedings of the Second International Conference on Municipal Solid Waste Combustor Ash Utilization, UNH Press, Durham, New Hampshire, USA, 1990, pp. 275-314.

6. T.T. Eighmy, B.S. Crannell, J.R. Krzanowski, J.D. Eusden, L.G. Butler, F.K. Kartledge, E. Emery, E.L. Shaw and C.A. Francis, Fundamental research on the mechanisms of the WES-PHix process. I: Studies on the Wheelabrator dry scrubber residue, UNH, Durham, New Hampshire, USA, 1996.

7. K.E. Forrester and M.Lyons, "The WES-PHix field experience" in Municipal Waste Combustion, Proceedings of an International Specialty Conference, Williamsburg, Virginia, March 1993, Air and Waste Management Association, Pittsburg, Pennsylvania, USA, 1993, pp.
371-378.

8. M.R. Lyons, The WES-PHix ash treatment process, Wheelabrator Environmental Systems Inc., NH, USA, 1995.

9. CEN-European Standardization Organisation, Characterization of waste. Leaching. Compliance test for leaching of granular waste materials. Determination of the leaching properties of constituents from granular waste materials and sludges. Draft European Standard prEN 12457, CEN/TC 292, CEN, Bruxelles, 1996.

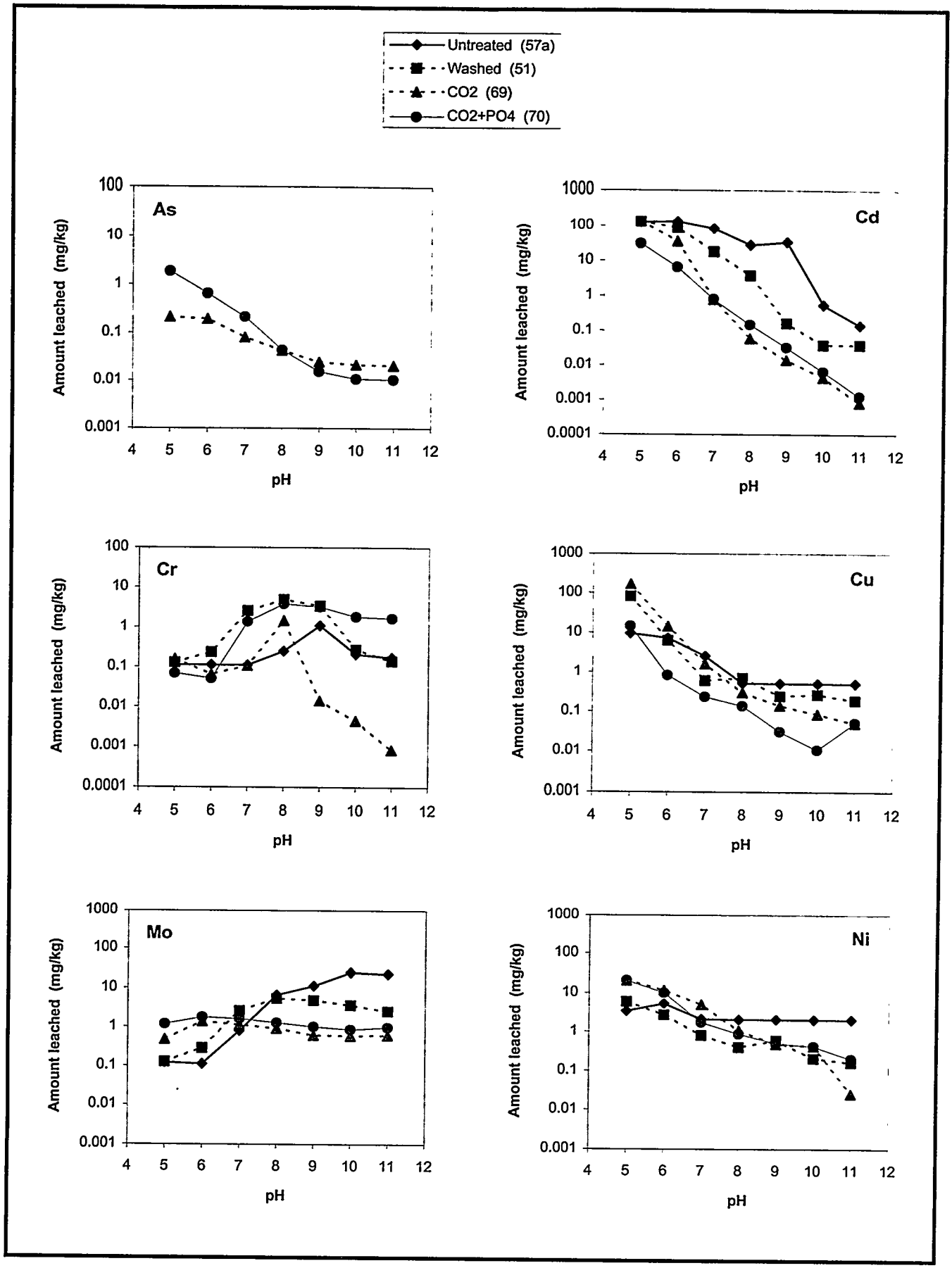

Figure 1a: Results of pH-static leaching tests at L/S = 5 l/kg

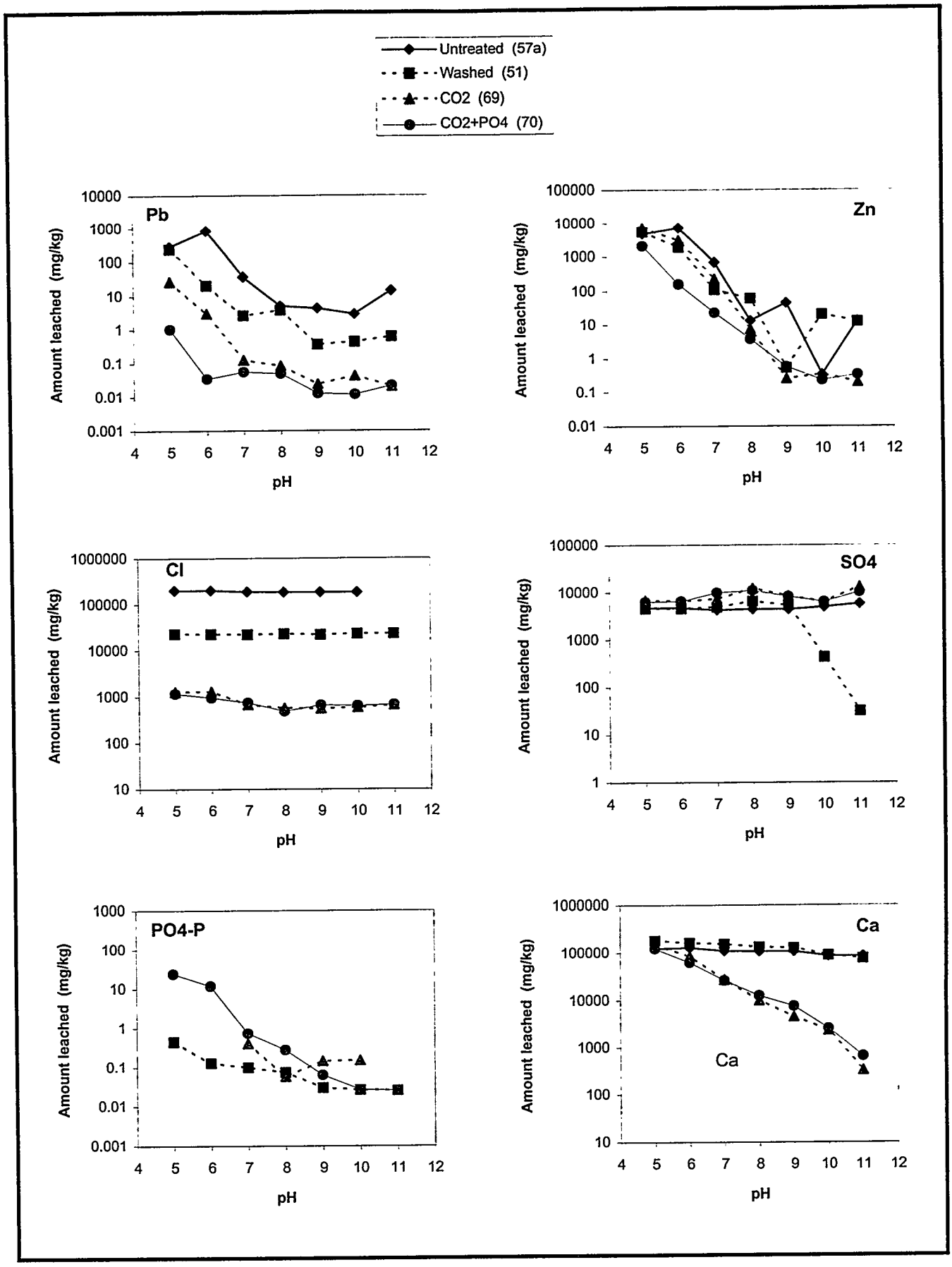

Figure 1b: Results of pH-static leaching tests at L/S = 5 l/kg.

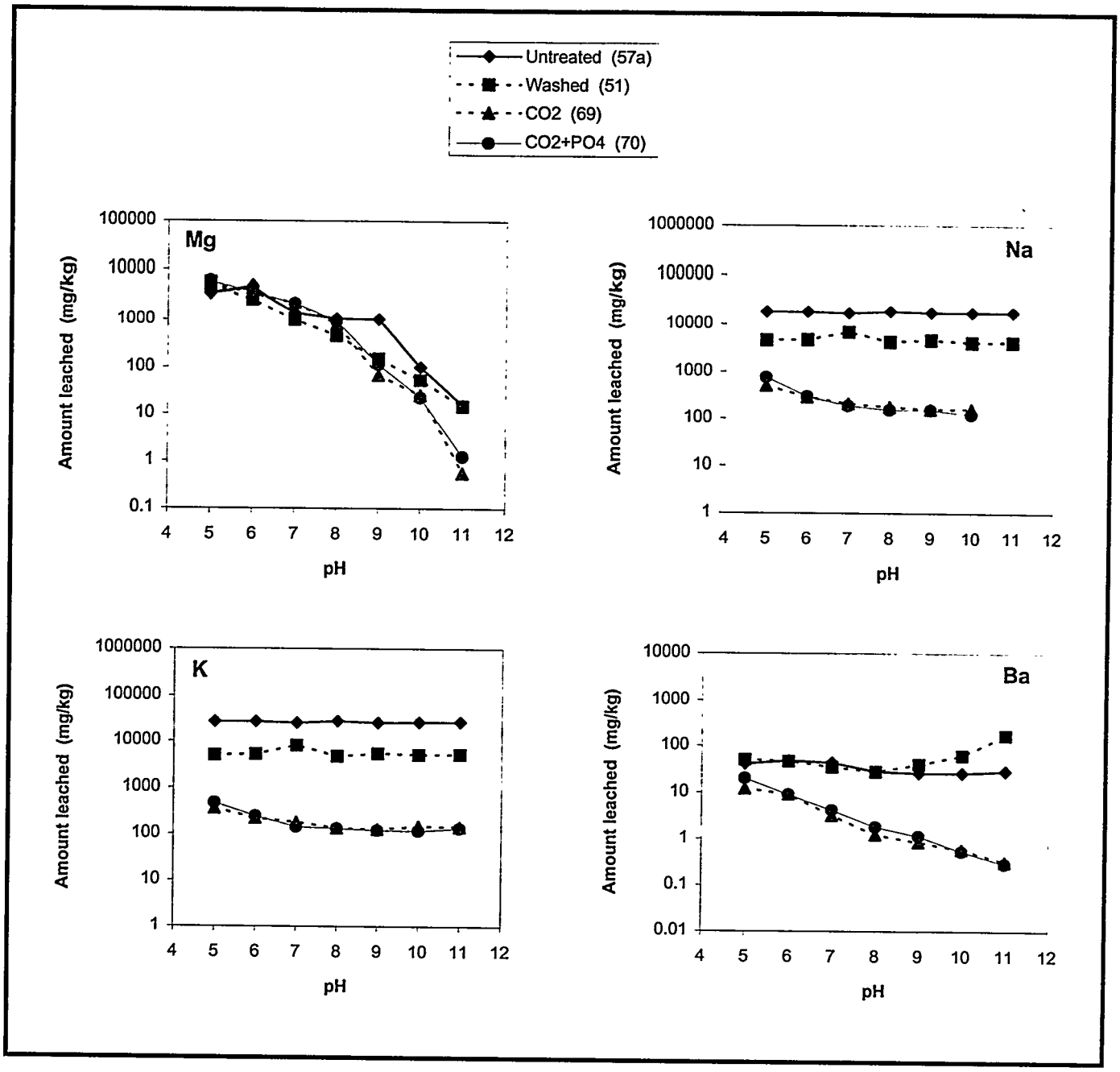

Figure 1c: Results of pH-static leaching tests at L/S = 5 l/kg.

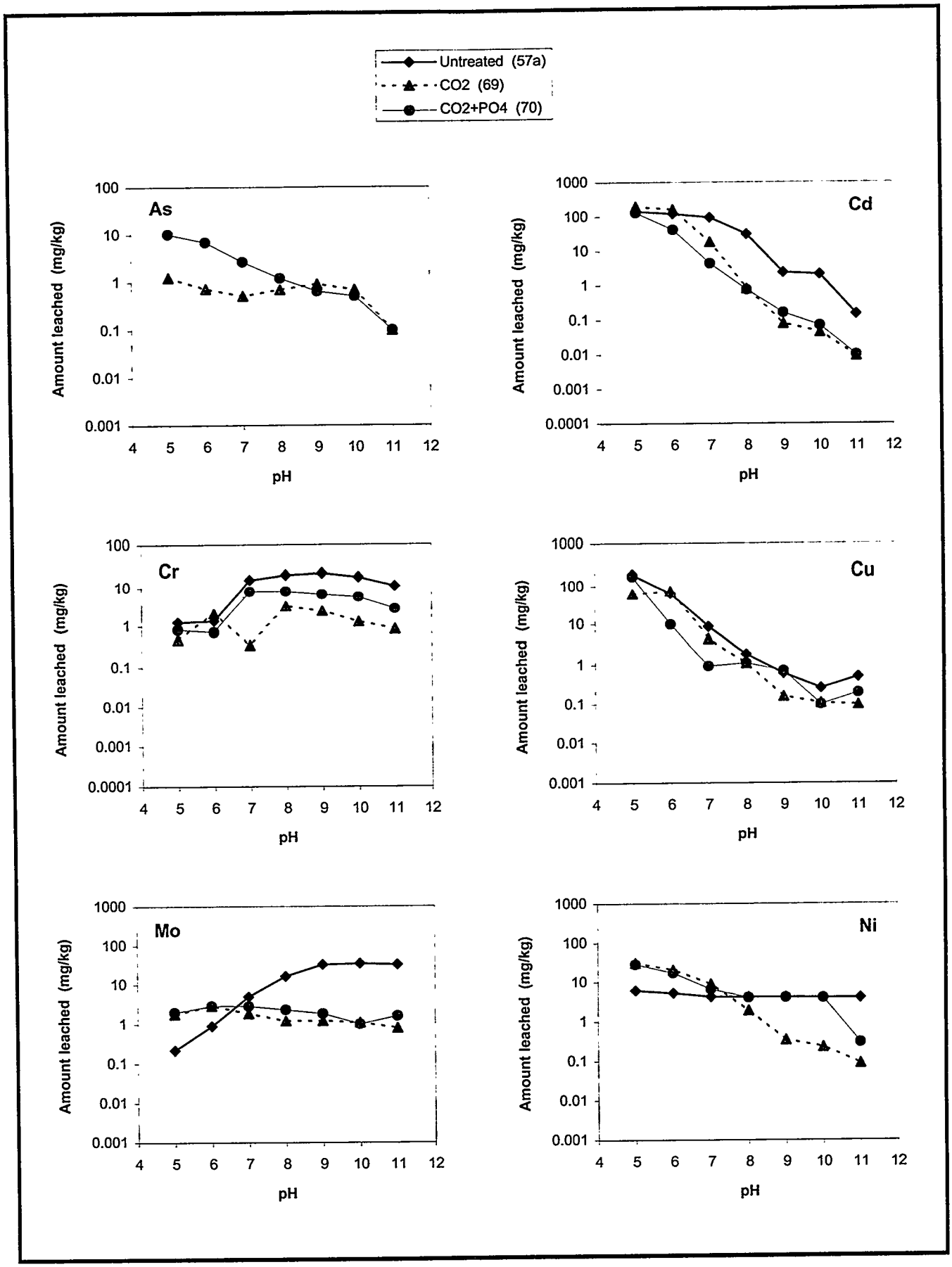

Figure 2a: Results of pH-static leaching tests at L/S = 100 l/kg.

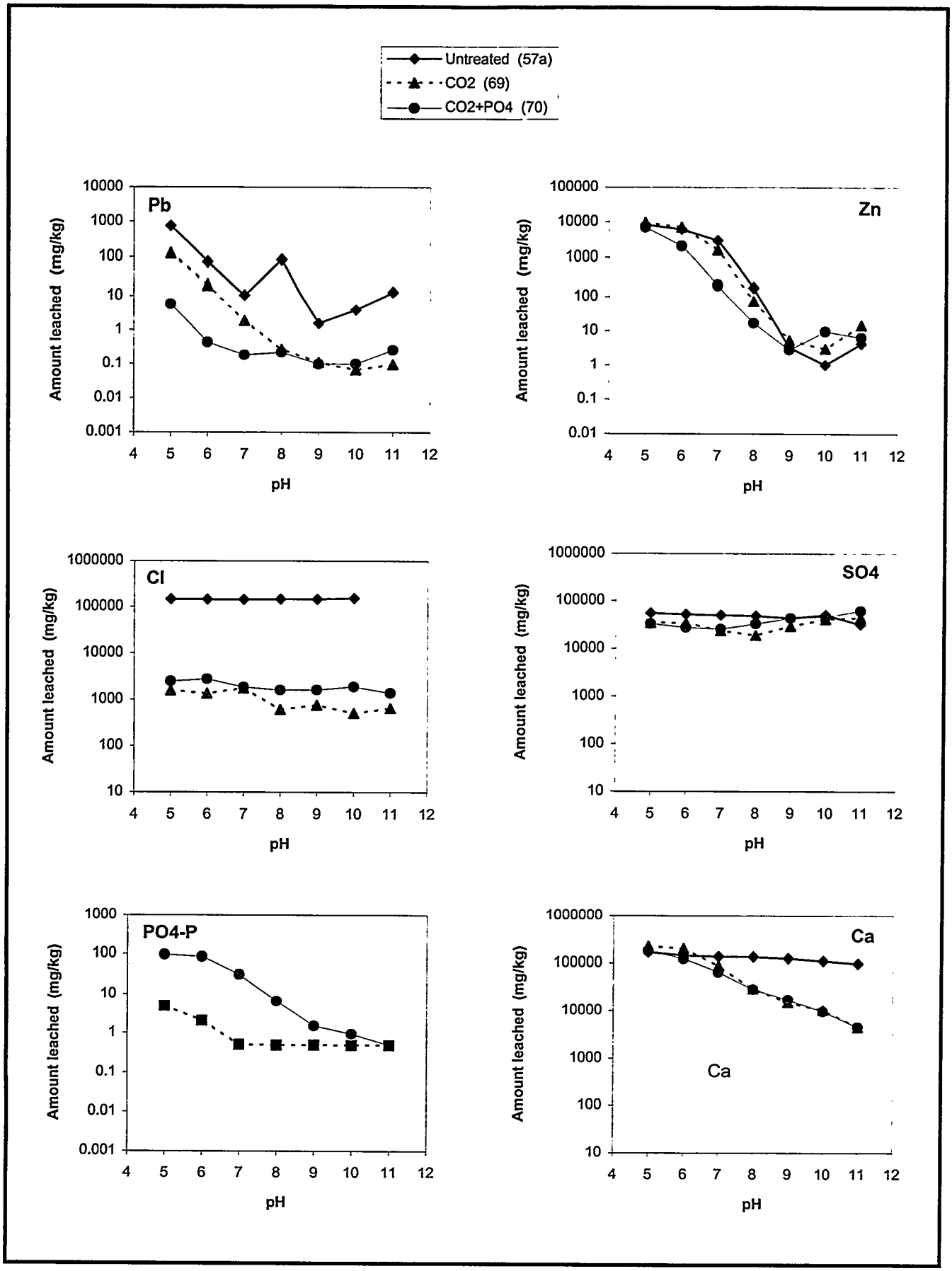

Figure 2b: Results of pH-static leaching tests at L/S = 100 l/kg.

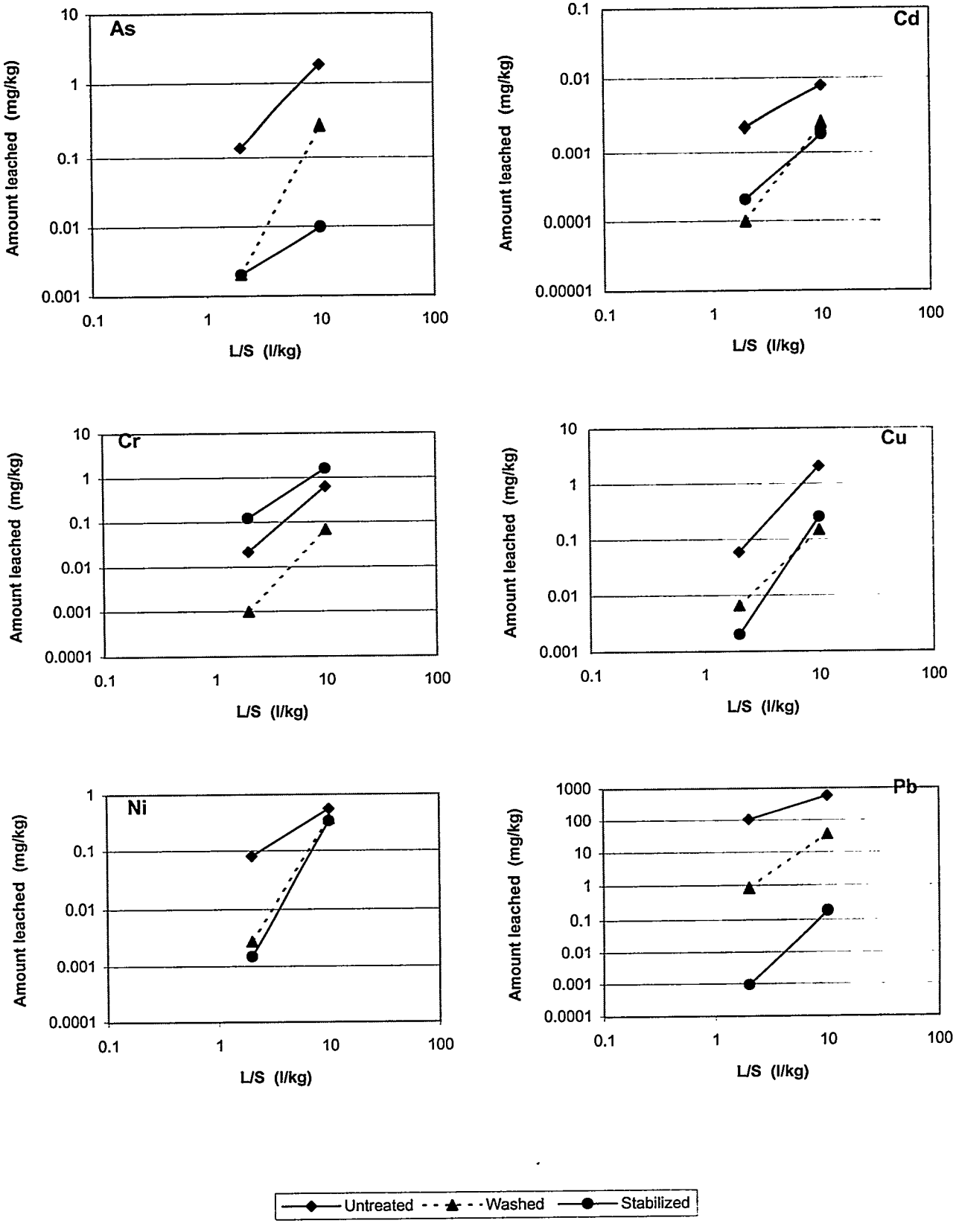

Figure 3a: Results of serial batch leaching test (two steps).

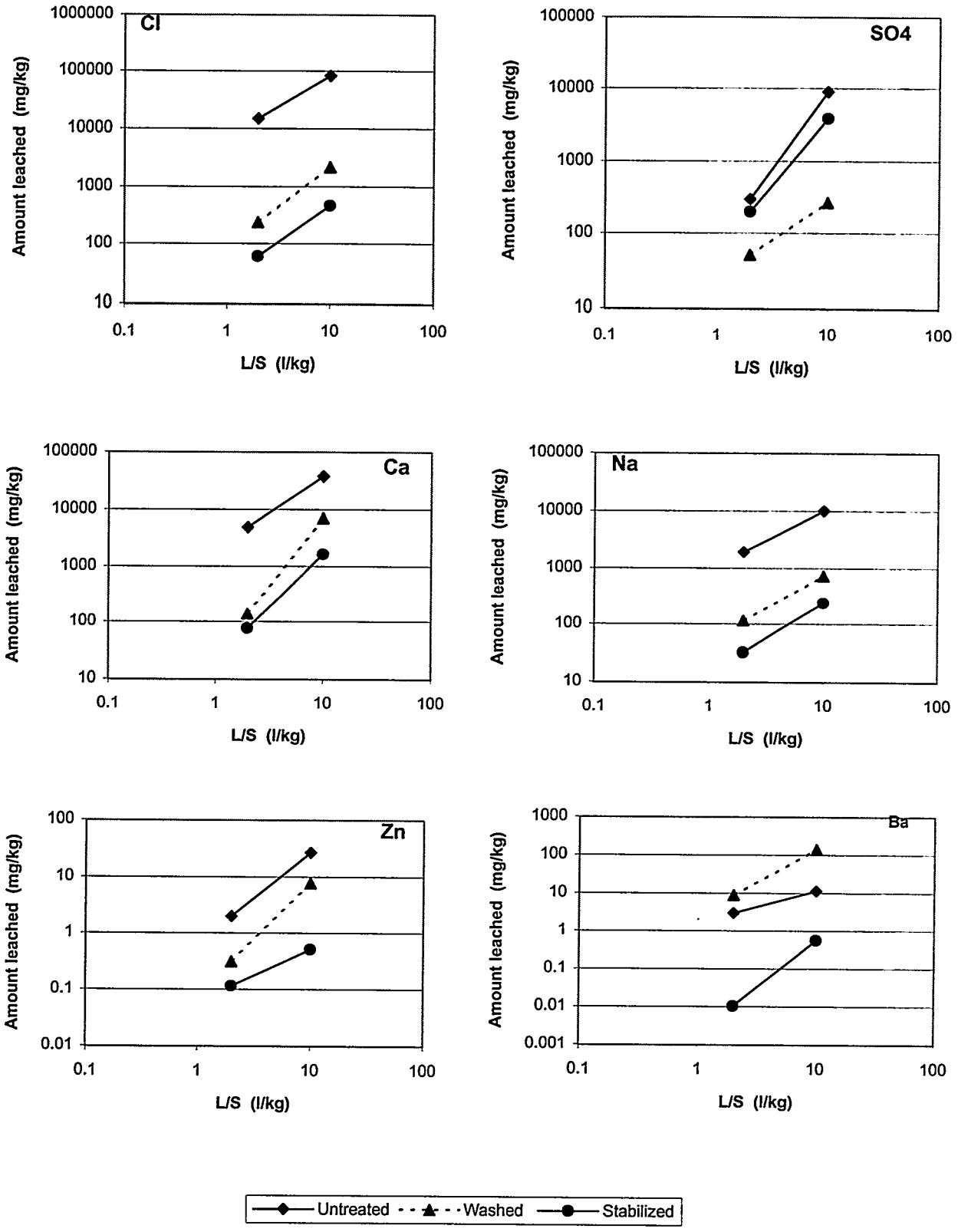

Figure 3b: Results of serial batch leaching test (two steps).